

2023-05-01

## **An Approach For Verification Of Traffic Speed Deflectometer Measurements**

Mahsa Beizaei  
*University of Texas at El Paso*

Follow this and additional works at: [https://scholarworks.utep.edu/open\\_etd](https://scholarworks.utep.edu/open_etd)



Part of the [Civil Engineering Commons](#)

---

### **Recommended Citation**

Beizaei, Mahsa, "An Approach For Verification Of Traffic Speed Deflectometer Measurements" (2023).  
*Open Access Theses & Dissertations*. 3766.  
[https://scholarworks.utep.edu/open\\_etd/3766](https://scholarworks.utep.edu/open_etd/3766)

This is brought to you for free and open access by ScholarWorks@UTEP. It has been accepted for inclusion in Open Access Theses & Dissertations by an authorized administrator of ScholarWorks@UTEP. For more information, please contact [lweber@utep.edu](mailto:lweber@utep.edu).

AN APPROACH FOR VERIFICATION OF TRAFFIC SPEED DEFLECTOMETER  
MEASUREMENTS

MAHSA BEIZAEI

Doctoral Program in Civil Engineering

APPROVED:

---

Soheil Nazarian, Ph.D., P.E, DGE.

---

Cesar Tirado, Ph.D.

---

Michael Pokojovy, Ph.D.

---

Gonzalo R. Rada, Ph.D., P.E.

---

Gerardo Flintsch, Ph.D., P.E.

---

Stephen L. Crites, Jr., Ph.D.  
Dean of the Graduate School

## **DEDICATION**

This dissertation is dedicated to my parents for their sacrifice and indulgence to make education a priority for me. Their presence was always the source of my energy and motivation even from a long distance.

I would like to dedicate this dissertation to my beloved husband and best friend, Ali, who has encouraged and supported me on this journey. His tolerance, adamant devotion, and love were worth more than I can express on paper.

AN APPROACH FOR VERIFICATION OF TRAFFIC SPEED DEFLECTOMETER  
MEASUREMENTS

by

MAHSA BEIZAEI, MSCE

DISSERTATION

Presented to the Faculty of the Graduate School of  
The University of Texas at El Paso  
in Partial Fulfillment  
of the Requirements  
for the Degree of

DOCTOR OF PHILOSOPHY

Department of Civil Engineering  
THE UNIVERSITY OF TEXAS AT EL PASO

May 2023

## ACKNOWLEDGEMENTS

This study was funded through the National Cooperative Highway Research Program (NCHRP) 10-106 project, and the support is gratefully acknowledged.

I would like to express my deepest gratitude to my advisor, Dr. Soheil Nazarian, for all his support, practical advice, and instructions during my Ph.D., which enabled me to successfully finish the research. His continuing encouragement has been my invaluable source of support during this process.

I would especially like to thank Dr. Tirado for his immense assistance and support in completing this study. This research has certainly benefited from his insightful suggestions. I also would like to thank Mr. Rocha for being a valuable part of this research and for his guidance in experimental field testing.

I would like to thank my dissertation committee members: Dr. Rada, Dr. Flintsch, and Dr. Pokojovy who provided me with perspicacious comments and kind support, without which the successful outcome of the research would not have been possible.

I would like to extend my gratitude to the department faculty, staff, and Center for Transportation Infrastructure Systems (CTIS) for their assistance throughout my study at UTEP.

Last but not least, I would like to express my deepest appreciation to my parents, my beloved husband, Ali, my sister, Mojgan, and my brothers Alireza and Amir for their unconditional love, support, and encouragement throughout my Ph.D. journey.

## **ABSTRACT**

Recent research studies have shown the usefulness and applicability of Traffic Speed Deflectometers (TSD) in support of the network-level pavement management process. There are, however, no accepted procedures for verification and validation of the TSD measurements to be utilized by practitioners. To address this need, TSD measurements may be verified with the data obtained by widely accepted road-testing equipment, Falling Weight Deflectometer (FWD). In this study, TSD and FWD operations on pavement sections were simulated employing the finite layer approach which resulted in the development of a comprehensive database of pavement responses. Using the established numerical simulation database, theoretical relationships between FWD and TSD data were developed by applying machine learning techniques which served as the basis for a robust verification procedure for the TSD measurements. To assure the reliability of the numerical simulations and presented relationships, the results were validated using the data obtained from extensive field testing conducted in various operational and structural conditions.

# TABLE OF CONTENTS

DEDICATION .....	II
ACKNOWLEDGEMENTS .....	IV
ABSTRACT .....	V
LIST OF TABLES .....	X
LIST OF FIGURES .....	XI
CHAPTER 1. INTRODUCTION .....	1
Background .....	1
Objective .....	2
Dissertation organization .....	3
CHAPTER 2. LITERATURE REVIEW .....	5
Traffic-Speed Deflection Devices .....	5
TSD Measurement Principle .....	7
Factors Affecting TSD Measurements .....	9
Pavement Factors .....	9
Environmental Factors .....	10
Operating Conditions Factors .....	11
TSD Accuracy and Precision .....	12

Verification of TSD Measurements .....	14
Numerical Simulation of Traffic Speed Deflectometer Testing .....	16
References .....	19
<b>CHAPTER 3. NUMERICAL SIMULATION OF TRAFFIC SPEED DEFLECTOMETER TESTING.....</b>	
Abstract .....	25
Introduction.....	26
Objective.....	29
Methodology .....	29
Field TSD Tests .....	30
Numerical Simulation Characteristics .....	31
Geometry of Tire Contact Area .....	31
Time History vs. Instantaneous Pavement Surface Response .....	36
Numerical Simulation Validation .....	39
Conclusion .....	40
References .....	43
<b>CHAPTER 4. IMPACT OF PAVEMENT STIFFNESS ON PERFORMANCE OF TRAFFIC SPEED DEFLECTION MEASUREMENTS.....</b>	
Abstract .....	47
Introduction.....	47
Objective.....	50
Methodology .....	50
Field Data Collection .....	50
Instrumentation .....	52
TSD Tests.....	53
Results and Discussion .....	56
Accuracy .....	57
Precision.....	58

Conclusion .....	64
References .....	65
CHAPTER 5. QUALITATIVE ASSESSMENT OF TRAFFIC SPEED DEFLECTOMETER DATA COLLECTION PRACTICE .....	67
Abstract .....	67
Introduction.....	67
Objective .....	70
Methodology .....	70
Field TSD Testing.....	70
Parametric Analysis .....	73
Results and Discussion .....	73
Effect of the Pavement Type on the Variability of the TSD Measurements .....	73
Effect of Spatial Averaging of Data (Data Intervals) .....	78
Effect of Vehicle Speed on the TDS Data .....	83
Conclusion .....	83
References .....	85
CHAPTER 6. PRACTICAL PROCESS FOR VERIFICATION OF TRAFFIC SPEED DEFLECTOMETER MEASUREMENTS.....	87
Abstract .....	87
Introduction.....	88
Objective .....	92
Methodology .....	92
Field Data Collection .....	94
Numerical Simulation Modeling.....	96
FWD and TSD Simulation.....	97
Approach to Validate Numerical Simulations .....	98
ANN Models Development .....	99
Results and Discussion .....	102
Validation of Numerical Simulations .....	102

Verification of Field TSD Data.....	104
Conclusion .....	106
References.....	108
CHAPTER 7. CONCLUSIONS AND RECOMMENDATIONS FOR FUTURE WORK .....	112
Summary.....	112
Conclusions.....	113
• Numerical Simulation of Traffic Speed Deflectometer Testing .....	113
• Impact of Pavement Stiffness on Performance of Traffic Speed Deflection Measurements .....	114
• Qualitative assessment of Traffic Speed deflectometer data collection .....	114
• Practical Process for Verification of Traffic Speed Deflectometer Measurements...	115
Recommendations for Future Studies.....	115
VITA.....	117

## LIST OF TABLES

Table 3.1: Pavement Test Sections properties. ....	30
Table 3.2: Range of Layer Thicknesses and Material Properties Considered in Numerical Modeling. ....	35
Table 4.1: MnROAD Test Sections Properties. ....	51
Table 5.1: MnROAD Pavement Test Sections. ....	71
Table 6.1: MnROAD Pavement Test Sections. ....	95
Table 6.2: Range of Layer Thicknesses and Material Properties for Numerical Modeling. ....	97

## LIST OF FIGURES

Figure 2.1: Photograph of TSD available in the United States. ....	7
Figure 2.2: Illustration of the Doppler effect after Hildebrand et al (1998). ....	8
Figure 2.3: Schematic of the measurement principle of the TSD (Katicha et al. 2017). ....	9
Figure 3.1: TSD axle load configuration, and arrangement of the Doppler laser sensors. ....	32
Figure 3.2: Finite element model of TSD moving tire on pavement section. ....	32
Figure 3.3: Footprint of TSD tire in finite element model. ....	33
Figure 3.4: Comparison of deflection velocity obtained from finite element simulation of the pavement test sections under TSD and the measured values in the field at 30 mph. ....	33
Figure 3.5: TSD tire footprint dimensions considered in 3D-Move models; a) rectangular and b) circular. ....	34
Figure 3.6: Comparison of deflection parameters induced by TSD with rectangular and circular tire contact area at different sensor positions; (a) vertical deflections and (b) deflection velocities. ....	35
Figure 3.7: Vertical stress variations for time history and instantaneous response conditions. ...	37
Figure 3.8: Comparison of vertical stress variations from 3D-Move instantaneous response case and finite element simulation. ....	37
Figure 3.9: Critical strain variations for time history and instantaneous response conditions, a) tensile strain at the bottom of asphalt, and b) compressive strain at top of the subgrade. ....	38
Figure 3.10: Vertical deflection variations for time history and instantaneous response conditions. ....	39
Figure 3.11: Comparison of deflection velocity obtained from 3D-Move simulation of the pavement test sections under TSD and the measured values in the field. ....	42

Figure 4.1: Schematic of geophone installed in pavement surface and installing geophone in the field. ....	52
Figure 4.2: Arrangement of the three geophones embedded at each section.....	53
Figure 4.3: Australian Road Research Board (ARRB) TSD truck. ....	54
Figure 4.4: TSD instrumented rear axle dual tires with Doppler laser sensor configuration. ....	54
Figure 4.5: Image frame of the best-aligned TSD pass at Section 1 at a speed of 30 mph. ....	55
Figure 4.6: TSD collected data vs. geophones obtained data averaged at each TSD sensor position for Section 1 at 30 mph (48 km/hr).....	56
Figure 4.7: Comparison of average TSD deflection velocity and embedded geophone deflection velocity at the best-aligned pass for each section. ....	59
Figure 4.8: TSD deflection measurements in MnROAD test sections. ....	60
Figure 4.9: Variability of TSD deflection measurements in MnROAD test sections. ....	61
Figure 4.10: Variations of COV with the magnitude of deflection velocity. ....	63
Figure 4.11: Variations of COV with the magnitude of deflection slope.....	63
Figure 5.1: TSD axle configuration and loads, and instrumented rear axle with Doppler laser sensor configuration.....	72
Figure 5.2: TSD deflection measurements in MnROAD test sections. ....	76
Figure 5.3: Variability of TSD deflection measurements in MnROAD test sections for 2 in. (50 mm) data interval. ....	77
Figure 5.4: Variations of COV with the magnitude of a) TSD deflection velocity and b) TSD deflection slope, for 2 in (50 mm) data interval.....	78
Figure 5.5: TSD deflection measurements in Low Volume Road and Main-Line sections for 3.3 ft (1 m) data interval. ....	80

Figure 5.6: Variability of TSD deflection measurements in MnROAD test sections for 3.3 ft (1 m) data interval. ....	81
Figure 5.7: Variations of COV with the magnitude of a) TSD deflection velocity and b) TSD deflection slope, for 3.3 ft (1 m) data interval. ....	82
Figure 5.8: Deflection slopes obtained by TSD at different operating speeds vs. deflection slopes at 30 mph (48 km/hr). ....	83
Figure 6.1: TSD load and laser configuration, (a) Schematic of loading by rear axle right dual tires and deflection velocity curve provided by lasers (Hasanuzzaman and Ives 2016), (b) laser beam between the dual tires and Doppler lasers (Katicha et al. 2017), and (c) Doppler laser reflection on pavement surface. ....	89
Figure 6.2: Flowchart of research methodology. ....	93
Figure 6.3: TSD collected data vs. geophones obtained data averaged at each TSD sensor position for Section 1 at 45 mph (72 km/hr). ....	96
Figure 6.4: TSD axle configuration and instrumented rear axle with Doppler laser sensor configuration. ....	98
Figure 6.5: Flowchart for 3D-Move models validation. ....	99
Figure 6.6: Architecture of multi-layer ANN model used to relate FWD and TSD data. ....	100
Figure 6.7: ANN estimated VS. numerical analysis calculated TSD deflection velocities for vehicle speed of 30 mph (48 km/hr). ....	101
Figure 6.8: Estimated vs. measured FWD deflections at three MnROAD test sections. ....	103
Figure 6.9: Estimated vs. measured TSD deflection velocity at three MnROAD test sections. ....	104
.....	106

Figure 6.10: ANN estimated vs. measured TSD deflection velocity at three MnROAD test sections at speed of a) 30 mph, and b) 45 mph..... 106

# CHAPTER 1. INTRODUCTION

## Background

Pavement surface conditions (e.g., ride and distresses) were traditionally relied on by State Highway Agencies (SHAs) for characterization and surveying of the overall condition of the pavement networks and consequently determination of the maintenance and rehabilitation (M&R) strategies to be adopted. However, the structural condition of the pavement networks is an important driver of deterioration (Katicha et al. 2017) that is not completely reflected by the surface condition of the pavements. Hence, the optimal rehabilitation strategy cannot be identified if the pavement structural condition is ignored at the network level. In other words, incorporating the structural condition along with the surface condition into the pavement management decision-making process can lead to better-informed and more cost-effective decisions (Ferne et al. 2013, Steele 2015).

To characterize the structural condition of the pavement networks, Falling Weight Deflectometer (FWD) measurements have been widely used by several SHAs in their pavement management processes at the network level (Flintsch and McGhee 2009, Katicha et al. 2013). Although FWD allows the measurement of deflections with acceptable accuracy, it has significant limitations which makes it a deflection-measuring device that is not practical for network-level testing. FWD testing disrupts traffic flow and requires lane closures which causes safety issues, traffic delays, and potential costs. In addition, the FWD production rates are lower than those associated with a continuous testing operation. Therefore, to characterize the network-level structural condition, traffic speed deflection devices (TSDDs) have been investigated by many researchers such as Rada and Nazarian (2011), Flintsch et al. (2013), Rada et al. (2016), and

Katicha et al. (2017). One popular TSDD, the Traffic Speed Deflectometer (TSD), is a device that has been used worldwide. Although the referenced research efforts have shown the usefulness and applicability of TSDs, SHAs have reservations about fully implementing TSDs in their network-level pavement management efforts since there are no accepted procedures for verification of the TSD measurements. This leads to a need for developing TSD verification procedures so that agencies can identify reliable data within acceptable levels of accuracy and precision.

One pragmatic method of verifying the TSDs' measurements can be through comparison with widely accepted FWD measurements. The underlying differences between TSD and FWD in terms of the type of loading, load contact area, pavement response measurement technology, and the method to estimate pavement deflections, should be rigorously considered in this comparison. Since the responses measured by the two devices are not the same, it would be difficult to obtain a "straightforward universal" relationship between the TSD and FWD measurements (Saremi 2018). Hence, a method is needed to post-process the FWD data obtained in the field in a way that can be comparable to TSD measurements. In this study, relationships between TSD and FWD measurements were developed which are the basis of the verification procedure of the TSD-obtained data.

### **Objective**

The dissertation's goal is to develop a robust procedure for verification of the measurements obtained by the TSD in the field. To that end, the following objectives have been pursued:

- Simulate the TSD moving load on the pavement surface with realistic specifications of the tire contact area and the pavement response using finite layer analytical tool.

- Evaluate the performance of the deflection velocities collected by TSD Doppler laser sensors by assessing the accuracy and precision of the TSD data acquired at roadway sections.
- Assess the impact of different factors on the changes and variability of the data collected by TSD on different pavement sections.
- Devise a robust and rapid verification procedure of TSD measurements by comparing the TSD deflection-based measurements with those estimated from FWD using machine-learning techniques.

### **Dissertation organization**

This journal paper-based dissertation is organized in the following manner:

- Chapter 1 includes a summary of the background, research objectives, and dissertation organization.
- Chapter 2 provides a state-of-the-art annotated bibliography, including a thorough literature review on traffic speed deflection devices, verification of TSD measurements, and numerical simulation of TSD testing.
- Chapter 3 contains the first journal article entitled “**Numerical Simulation of Traffic Speed Deflectometer Testing**” that discusses the simulation of the TSD operation on the pavement sections with different structural properties using a finite-layer program. This article also defines the numerical models that can realistically simulate TSD testing on the pavement surface.
- Chapter 4 presents the second journal article entitled “**Impact of Pavement Stiffness on Performance of Traffic Speed Deflection Measurements**” that discusses the evaluation of the performance of the TSD measurements using the data from instrumented pavement

test sections. The article also explains the effect of the pavement structural condition, i.e., pavement stiffness, on the accuracy and precision of the TSD data.

- Chapter 5 presents the third journal article entitled “**Qualitative Assessment of Traffic Speed Deflectometer Data Collection Practice**” that describes the impact of several parameters such as data collection intervals, vehicle operational speed, pavement section structural strength, and deflection velocity magnitudes on the TSD data recorded at pavement sections with different types and characteristics.
- Chapter 6 presents the fourth journal article entitled “**Practical Process for Verification of Traffic Speed Deflectometer Measurements**” that presents relationships for the verification and interpretation of the TSD data. The article describes artificial neural network (ANN) models for different pavement types and properties, and vehicle speeds, which were developed to relate TSD and FWD results.
- Chapter 7 provides a summary along with conclusions and recommendations for future studies.

## **CHAPTER 2. LITERATURE REVIEW**

This chapter provides a state-of-the-art annotated bibliography, including a thorough literature review on traffic-speed deflection devices, different factors affecting TSD measurements and their accuracy and precision as well as verification of TSD measurements. This chapter also includes an extended literature review on the numerical simulation of TSD testing.

### **Traffic-Speed Deflection Devices**

Nondestructive devices that collect pavement deflections induced under the device's loads as it travels over a length of pavement are known as continuous deflection devices (CDDs) (Flintsch et al. 2013) or moving measurement platforms (MMP, Andersen et al. 2017, Madsen and Pedersen 2019). The purpose of the development of the continuous deflection measurement devices was mainly network-level pavement structural evaluation since traditional stop-and-go devices, like the widely used FWDs, were not a practical option to meet this need. TSDDs are CDDs that can obtain pavement surface deflection measurements while traveling at traffic speeds of 35 mph (55 km/h) or greater with no need for disrupting the normal flow of traffic (Flintsch et al. 2013). They can survey pavement stretches of up to 400 miles/day (640 km/day) (Steele et al. 2020).

The first working prototypes of TSDDs were released in the late 1990s (Arora et al. 2006). Several research efforts assessed the performance of different devices and proposed methods to interpret properly the collected data in pavement structural evaluation for project-level pavement engineering and network-level asset management (Rada and Nazarian 2011, Flintsch et al. 2013, Rada et al. 2016, Elseifi and Elbagalati 2017). The following devices are examples of TSDDs:

- Road Deflection Tester (RDT) developed in Sweden by the Swedish National Road and Transport Research Institute (VTI) (Andrén 1999)
- Traffic Speed Deflectometer (TSD), originally called High-Speed Deflectograph, developed in Denmark by Greenwood Engineering in collaboration with the Danish Road Institute (Hildebrand and Rasmussen 2002)
- Rolling Wheel Deflectometer (RWD) developed in the United States by Applied Research Associates (ARA) in collaboration with the Federal Highway Administration (FHWA) (Steel et al. 2002),
- Rapid Pavement Tester (RAPTOR) developed in Denmark by Dynatest (Andersen et al. 2017).

TSD and RWD have been extensively tested in the United States (Rada et al. 2016), while the RAPTOR is a relatively new device that first arrived in the United States in 2019. RDT, RWD, and RAPTOR rely on distance-measuring lasers to estimate the pavement deflection that wheel load induces whereas the TSD relies on velocity-measuring lasers (Doppler lasers) to measure the pavement deflection velocity. All devices use a beam on which the measuring lasers are mounted. As this dissertation specifically studies the TSD, more information about this device is provided in this section.

The TSD, shown in Figure 2.1, is a truck with a rear-axle load between 13 kips to 29 kips (60 kN to 130 kN). Up to a dozen Doppler lasers can be mounted on a servo-hydraulic beam to measure the pavement deflection velocity. In addition to the deflection velocity measuring lasers, an extra sensor is positioned 11.5 ft (3.5 m) in front of the rear axle, largely outside the deflection bowl, to act as a reference laser. To keep the lasers at a constant height from the road surface, the laser beam moves up and down in opposition to the movement of the trailer. To prevent thermal

distortion of the steel measurement beam, a climate control system maintains the trailer temperature at 68°F (20°C). Data are recorded at a survey speed of up to 60 mph (96 km/h) at a sampling rate of 1000 Hz (250 kHz in newer devices).



Figure 2.1: Photograph of TSD available in the United States.

### TSD MEASUREMENT PRINCIPLE

TSD Doppler lasers measure velocities rather than deflections which are the time derivatives of deflection. The Doppler lasers rely on the Doppler effect as shown in Figure 2.2 (Hildebrand et al 1998). Doppler laser sends a wave to the pavement surface which is reflected to a receiver within the Doppler laser. As an object moves toward the Doppler laser, each successive wave peak reaches the object at a time smaller than the original time interval between the two peaks. The reflected wave will therefore exhibit an increased frequency (shorter wavelength) compared to the original wave (see Figure 2.2). In the case where an object is moving away from the Doppler laser, the effect is reversed and the reflected wave will exhibit a decreased frequency, which can be calculated according to the following equation:

$$F_{Doppler} = - F_{source} \frac{v}{c}$$

where  $F_{Doppler}$  is the change in frequency at the receiver,  $F_{source}$  is the transmitted frequency,  $v$  is the relative velocity between source and receiver, and  $c$  is the speed at which the transmitted

wave propagates. Since the wave speed is known, the change in the frequency is used to determine the velocity at which the object is moving.

The TSD Doppler lasers are mounted at a small angle to the vertical to measure the vertical pavement deflection velocity with components of the horizontal vehicle speed and the vertical and horizontal vehicle suspension velocities. The vertical angle of a Doppler laser is an important calibration parameter that affects the measured pavement response.

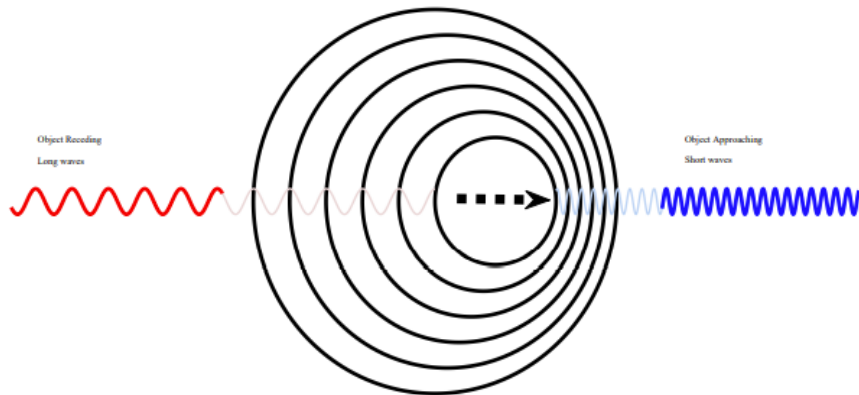


Figure 2.2: Illustration of the Doppler effect after Hildebrand et al (1998).

To remove the dependence of deflection velocity on the speed of the vehicle, the deflection velocity,  $V_v$ , is divided by the instantaneous vehicle speed,  $V_h$ , to obtain the deflection slope, as illustrated in Figure 2.3. Therefore, the deflection slope,  $S$ , is calculated from:

$$S = \frac{V_v}{V_h}$$

Typically, the deflection velocity is reported at a 3.3-ft (1-m) and 33-ft (10-m) intervals.

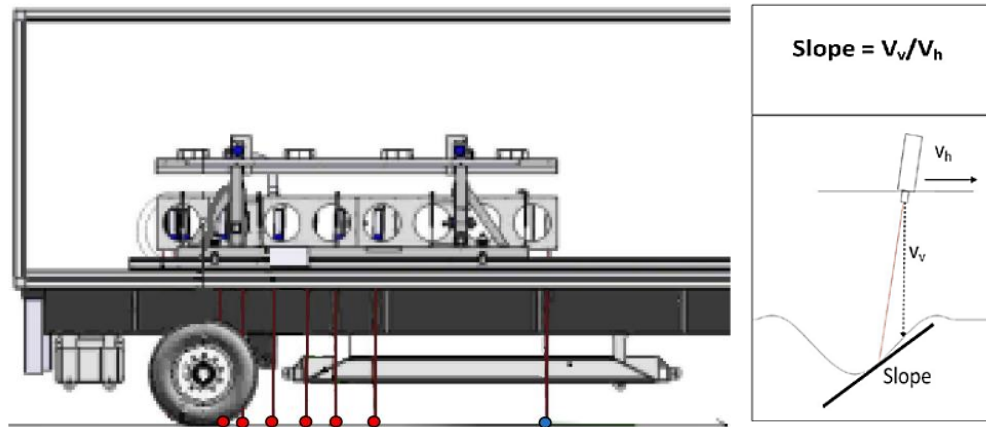


Figure 2.3: Schematic of the measurement principle of the TSD (Katicha et al. 2017).

The commercially available TSD spans three generations of the TSD, with the first-generation device limited to four Doppler lasers and the latest third-generation device equipped with as many as 10 Doppler lasers. An important difference between the different generations is the calibration procedure for the Doppler laser vertical angles and the Doppler laser sampling frequency (from 1 kHz (first and second generation) to up to 250 kHz).

## FACTORS AFFECTING TSD MEASUREMENTS

The factors affecting the TSD measurements include pavement factors, environmental factors, and operational factors. The details about how each factor impacts the pavement responses under TSDs are presented in this section.

### Pavement Factors

The pavement characteristics such as pavement type, pavement smoothness in terms of the International Roughness Index (IRI), gradient, and curvature can significantly affect the deflection measurements. Flintsch et al. (2013) studied the effect of the pavement surface on laser capabilities. They reported that binder-rich surfaces caused faulty operation of the TSD Doppler

lasers. Rada et al. (2016) concluded that the accuracy of the TSD is affected by the pavement stiffness but not affected by IRI. Elseifi and Zihan (2018) concluded that higher pavement roughness resulted in a higher coefficient of variation of the TSD data.

### **Environmental Factors**

Temperature is an environmental factor that can significantly influence the material characteristics of the pavement layers, which in turn affects the pavement responses. Additionally, the temperature has a significant effect on the TSD laser beams. Therefore, all devices incorporate a climate control system that maintains a trailer temperature of 68°F (20°C) (Flintsch et al. 2013). Assessment of continuous deflection devices performed by Flintsch et al. (2013) showed that the laser beam was sensitive to temperature variations in the trailer which, if not properly controlled, can significantly affect the measurements. Rada et al. (2016) reported that the precision of the measurements decreased with an increase in temperature. The coefficient of variations for the afternoon tests' data were 32 percent higher than for the morning tests. A high correlation was observed in the precision from the morning and afternoon tests with an  $R^2$  of 0.87.

Rain also has a detrimental effect on the capability of TSD devices to perform appropriately. As TSD works based on laser technology, it can fail to report accurate measurements in the presence of moisture on the pavement surface (Elseifi et al. 2011). Flintsch et al. (2013) stated that TSD failed to measure deflection parameters correctly when the road was damp or wet. Rada et al. (2016) also recommended that testing should not be performed if the pavement surface was wet or during precipitation.

Crosswind perpendicular to the side of the trailer is another environmental factor causing asymmetric loads between the two sides of the vehicle. A theoretical evaluation of the effect of wind on the load distribution between the two sides of the trailer was performed by Zofka et al.

(2015). They found that wind load resulted in asymmetric loading which would affect the measured pavement response. Rada et al. (2016) proposed that testing should not be performed under strong crosswind conditions, especially if the applied load on each side of the trailer was not measured using strain gauges.

### **Operating Conditions Factors**

In terms of the effect of vehicle speed on TSD measurements, Elseifi and Zihan (2018) performed a theoretical investigation using 3D-Move simulations of TSD loading configuration. They suggested a small effect of speed, although increasing speed slightly reduced the deflection. Rada et al. (2016) reported similar trends on the impact of vehicle speed on the accuracy and precision of the TSD. They reported that the TSD truck speed seemed to inversely affect the measured deflection slope precision. Based on an analytical study, Saremi (2018) demonstrated that as long as the hot mix asphalt (HMA) layer is less than 4 in. (100 mm), the impact of the viscoelasticity is within the uncertainty of the TSDs' measurements.

Horizontal curves and vertical gradients of the roads are potential parameters that could affect the measurements obtained from TSDs. Flintsch et al. (2013) did not observe an obvious relationship among the longitudinal profiles, gradient, transverse slope, or curvature on TSD measurements. Rada et al. (2016) did not notice a clear correlation between the vertical gradient and coefficient of variation of the TSD measurements. The study also reported that although most of the high coefficient of variations corresponded to sharp horizontal turns, quantitatively no clear correlation was present between the horizontal curvature and coefficient of variation (COV) from TSD.

## **TSD ACCURACY AND PRECISION**

Several research efforts have been undertaken to assess the accuracy and repeatability of TSDs. Ferne et al. (2009) evaluated short-term repeatability for six runs on a test track recorded on the same day. For the long-term repeatability, an investigation of possible causes linked temperature variation to variations in the data. Detailed measurements of the temperature at various points on the measurement beam were collected during surveys. The short-term repeatability of TSD was good. Comparison of the temperature measurements with the survey results showed that the repeatability at beam temperatures below 59°F (15°C) was poor. Rada and Nazarian (2011) assessed the TSD raw data repeatability and accuracy of the devices, and hence, to determine the suitability of those devices for various possible pavement applications. They concluded that depending on the TSD data application, an optimized level of repeatability should be achieved over a reasonable spatial averaging of the data. Bryce et al. (2012) evaluated the repeatability of TSD measurements in terms of the mean square error of deflection slope measurements, which was decomposed into variance and bias. A method for determining standard deviations was presented and applied to analyze the repeatability of the TSD. The repeatability of TSD could be considered constant over a range of measurements. The bias was generally not significant, meaning that the level of accuracy of the data was acceptable.

Flintsch et al. (2013) analyzed the TSD repeatability for measurements averaged over 1-m, 10-m, and 100-m intervals. Five runs were obtained for each section resulting in five sets of slope measures at each location. The repeatability of TSD could be considered adequate for network-level pavement management applications. Katicha and Flintsch (2015) estimated the standard deviation and repeatability of TSD measurement in the state of New York using a single run and the methodology was validated using repeated TSD runs. The two sets of measurements

agreed reasonably. This suggested that the TSD is repeatable and that most variations in the measurements were due to the structural condition. Muller and Roberts (2013) assessed the accuracy of TSD data by field-validating deflection bowl predictions. TSD surface velocity measurements for seven Queensland test sites were re-analyzed by the authors and compared with the corresponding FWD measurements. TSD showed the potential to be used to collect measurements of pavement deflection bowls at highway speeds that were comparable with FWD deflection bowls. Kannemeyer et al. (2014) conducted verification of TSD measurements by instrumenting an experimental section near Pretoria. TSD measurements were repeatable in terms of speed, roughness, and deflection.

Muller and Wix (2014) carried out a series of field trials at three locations for field validating the TSD device. TSD measurements and the resulting calculation of maximum deflections were both relatively repeatable as quantified by  $R^2 = 0.879$ . Rada et al. (2016) evaluated the precision and accuracy of the TSDs at different speeds and at different times of the day in Minnesota. The results showed that TSD could provide reasonably accurate and precise pavement response measurements. The results from the accuracy and precision analyses were used to recommend optimum operational conditions and device limitations. Katicha et al. (2017) evaluated the short-term and long-term repeatability of TSD and compared TSD measurements with data from a PMS. The short- and long-term repeatability was generally good. Repeated measurements of consecutive days (short-term) or two different years (long-term) followed similar trends. There could still be improvements in repeatability in terms of temperature correction of measurements. Lee et al. (2019) conducted multiple TSD testing to confirm the repeatability of the measurements. The results did not support the statement that the pavement response is

significantly affected by the speed of testing. Although the results did not exactly match, it demonstrated that TSD was repeatable.

### **Verification of TSD Measurements**

Various studies have compared TSD measurements to measurements with other deflection-based testing devices, in particular with the FWD. Measurements from both devices were used to calculate deflection-based indices, e.g. Surface Curvature Index (SCI) and Base Distress Index (BDI), as means to evaluate the comparability between the TSD and the FWD. Employing numerical analyses, different studies have developed relationships to estimate FWD deflections from TSD measurements utilizing genetic programming based on a symbolic regression approach (Saremi 2018) or using an artificial neural network (Elbagalati et al. 2018).

Flintsch et al. (2013) conducted TSD and FWD surveys along flexible, rigid, and composite site sections. The comparability of the TSD with FWD measurements was assessed by using two surface indices, the SCI and BDI. The TSD deflection measurements or indices were comparable to those collected by FWD. Strains at the bottom of the asphalt layer estimated using the FWD and TSD yielded an approximately one-to-one relationship. Rada et al. (2016) evaluated the comparability of the TSD with FWD. Measurements from each device were used to calculate the SCI and BDI. The relationships between the indices measured by TSD and FWD were reasonably close to the equality line. Katicha et al. (2017) reported that the TSD measurements were comparable to FWD measurements. Measurements from both devices followed similar trends and changes in the structural condition were reflected in the TSD measurements.

Elbagalati et al. (2018) developed a methodology to incorporate TSD measurements in the backcalculation analysis. TSD and FWD measurements were used to train and validate an artificial neural network model that would convert TSD deflection measurements to FWD deflection

measurements. Acceptable accuracy and good agreement between the backcalculated moduli from FWD and TSD measurements were achieved. Saremi (2018) used numerical analyses to relate the FWD and TSD deflection parameters. 10,000 three-layer flexible pavement sections with different randomly distributed layer thicknesses and moduli were considered. 3D-Move software was used to simulate the responses of TSD and FWD. Strong relationships among the deflection parameters from the two devices were developed. Relationships were developed for estimating FWD deflections from TSD deflections. A relationship between the deflections from the two devices at the same distance from the load was developed by the symbolic regression approach.

Muller and Roberts (2013) compared more than 1500 TSD deflection bowls with approximately 600 9-kips and 11.2-kips (40-kN and 50-kN) FWD deflection bowl profiles. Correlations between the shape and magnitude of deflection bowls, maximum deflections, and SCI300 (Surface Curvature Index at 300 mm from load), obtained by the two methods were observed. Chai et al. (2016) stated that the FWD and TSD data were highly correlated. The theoretical deflections were in good agreement with the actual deflections obtained from the FWD test. Lee et al. (2019) assessed how TSD measurements compare with FWD measurements using an instrumentation array that was installed and validated using FWD. Then instrumentation outputs during TSD pass-by and FWD testing were monitored. TSD and FWD deflection data at 0 in. to 24 in. (0 mm to 600 mm) offset from load matched well and there was a good correlation between the curvature data collected from the two devices.

Kannemeyer et al. (2014) conducted verification of TSD measurements by instrumenting an experimental section. The authors concluded that TSD and FWD had similar patterns but did not exactly match. Muller and Wix (2014) carried out a series of field trials during their long-term pavement performance annual surveyed by FWD. While the similarity between TSD and FWD

maximum deflections was observed, it was difficult to draw further conclusions. Jansen (2017) based his study on TSD measurements obtained on 300 km of different road classifications. On some tracks, the TSD results were compared with FWD measurements. A consistent correlation was not found between TSD and FWD measurements. However, the same deflection levels were witnessed.

### **Numerical Simulation of Traffic Speed Deflectometer Testing**

Reliable simulation techniques and numerical models are considered necessary to analyze the parameters obtained by TSD and its performance in the structural analysis of pavement sections (Nasimifar 2015). In various research efforts, TSD application was simulated using different approaches such as the finite element method, nonlinear spectral element model (Sun et al. 2022), and finite layer approach. As the latter was used in the majority of the studies, this section provides simulation efforts made by different researchers using the 3D-Move analysis tool which is based on the finite layer method. 3D-Move analysis tool undertakes the pavement response computations using a continuum-based finite-layer approach and accounts for important factors such as any shape of the traffic-induced 3D contact stress distributions, vehicle speed, and viscoelastic material characterization for the pavement layers. This approach treats each pavement layer as a continuum and uses the Fourier transform technique; therefore, it can handle complex surface loadings such as multiple loads and non-uniform tire pavement contact stress distribution (Siddharthan et al. 1998; 2002).

3D-Move was utilized for a wide range of applications such as layer moduli or structural number estimation, developing relationships between FWD and TSD measurements, and assessing the effect of different operational and model parameters on the pavement responses. Nasimifar et al. (2017) used 3D-Move to simulate the TSD loading configuration and concluded that the

dynamic analytical model provided a good match based on a variety of independent pavement responses from field testing. Rada et al. (2016) also applied 3D-Move for the simulation of TSD in the development of procedures for incorporating TSD measurements into network-level PMS applications.

Rada et al. (2016) found that the layers moduli estimated from the TSD deflection velocity calculated by the 3D-Move were close to those from the FWD deflection. Nasimifar et al. (2017) showed that the 3D-Move program was an efficient analytical tool to backcalculate layer moduli by directly using TSD-measured deflection velocities. To develop a new approach to determine the structural number with TSD measurements by modifying the AASHTO method, Zhang et al. (2022) relied on 3D-Move to provide a comprehensive TSD database containing various pavement structures.

An application of the 3D-Move was to calculate different pavement responses to be used in the development of the relationships between TSD and FWD data. Saremi (2018) employed 3D-Move to simulate the deflection bowls under FWD and TSD loading to be used in symbolic regression approach for developing FWD-TSD relationships. Abohamer et al. (2021) validated the 3D-Move model to calculate theoretical FWD and TSD deflection basins for 162 pavement sections which were later used to train an ANN model to predict FWD deflections. 3D-Move was also employed to consider the effect of operational parameters on the models' responses. Zihan (2019) assessed the effect of TSD speed variation on surface deflections using 3D-Move simulation as a reliable analysis tool. In Huang et al. (2022) research study, to understand the impact of the TSD testing characteristics on pavement responses and to find out the underlying differing mechanism between the TSD and FWD, mechanistic simulation models were developed based on the 3D-Move program.

Different characteristics of the 3D-Move models to simulate TSD loading are also crucial to be studied as they could affect the responses calculated by the program. One of these characteristics is the considered shape of the tire contact area and pressure distribution on the pavement surface (Siddharthan et al. 1998). The data generated in Siddharthan et al. (2002) study revealed that there is a significant difference between the responses computed with uniform and nonuniform contact tire-pavement stress distributions. Except in the case of tensile strain at the bottom of the asphalt concrete layer, the responses computed with the nonuniform stress distribution were lower. Different research efforts have been undertaken considering different TSD tire contact areas and pressure distributions. Nasimifar et al. (2015) used a nonuniform pressure distribution in 3D-Move to simulate the TSD loading configuration and concluded that the dynamic analytical model provided a good match with data from field testing. Rada et al. (2016), Saremi (2018), and Zhang et al. (2022) considered uniformly distributed dual circular load in 3D-Move analysis to simulate the loading mechanisms of TSD. Elseifi et al. (2019) utilized the non-uniform contact pressure distribution of tires and non-circular loaded area in their 3D-Move simulations to be used in the backcalculation analysis. Modeling vehicles with a circular area could be somewhat questionable since the tire loading area does not perfectly resemble a circular-shaped area (Elseifi et al. 2019). As a result, it is worthwhile to study the effect of the tire pressure distribution and contact area on the obtained TSD responses.

## References

- Abohamer, H., Elseifi, M. A., Zihan, Z. U., Wu, Z., Kebede, N., & Zhang, Z. (2021). Development of an artificial neural network-based procedure for the verification of traffic speed deflectometer measurements. *Transportation research record*, 2675(9), 1076-1088.
- Andersen, S., Levenberg, E., & Andersen, M. B. (2017). Inferring pavement layer properties from a moving measurement platform. In 10th International Conference on the Bearing Capacity of Roads, Railways and Airfields (pp. 675-682). Taylor & Francis.
- Andr n, P. (1999, January). High-speed rolling deflectometer data evaluation. In *Nondestructive Evaluation of Aging Aircraft, Airports, and Aerospace Hardware III* (Vol. 3586, pp. 137-147). International Society for Optics and Photonics.
- Arora, J., Tandon, V., and Nazarian, S. (2006). Continuous Deflection Testing of Highways at Traffic Speeds, Report No. FHWA/TX-06/0-4380, Texas Department of Transportation, Austin, TX.
- Bryce, J., Katicha, S., Flintsch, G. W., & Ferne, B. (2012). Analyzing repeatability of continuous deflectometer measurements, Transportation Research Board Meeting (paper No. 12-1732).
- Chai, G., Manoharan, S., Golding, A., Kelly, G., & Chowdhury, S. (2016). Evaluation of the Traffic Speed Deflectometer data using simplified deflection model. *Transportation Research Procedia*, 14, 3031-3039.
- Elbagalati, O., Mousa, M., Elseifi, M. A., Gaspard, K., & Zhang, Z. (2018). Development of a methodology to backcalculate pavement layer moduli using the traffic speed deflectometer. *Canadian Journal of Civil Engineering*, 45(5), 377-385.

- Elseifi, M. A., & Elbagalati, O. (2017). Assessment of continuous deflection measurement devices in Louisiana-rolling wheel deflectometer: final report 581 (No. FHWA/LA. 17/581). Louisiana Transportation Research Center.
- Elseifi, M. A., & Zihan, Z. U. (2018). Assessment of the Traffic Speed Deflectometer in Louisiana for Pavement Structural Evaluation (No. FHWA/LA. 18/590). Louisiana Transportation Research Center.
- Elseifi, M. A., Abdel-Khalek, A., Gaspard, K., Zhang, Z. D., & Ismail, S. (2011). Evaluation of the rolling wheel deflectometer as a structural pavement assessment tool in Louisiana. In Transportation and Development Institute Congress 2011: Integrated Transportation and Development for a Better Tomorrow (pp. 628-637).
- Elseifi, M. A., Zihan, Z. U., & Icenogle, P. (2019). A Mechanistic Approach to Utilize Traffic Speed Deflectometer (TSD) Measurements into Backcalculation Analysis (No. FHWA/LA. 17/612).
- Ferne, B. W., Langdale, P., Round, N., and Fairclough, R. (2009). Development of a Calibration Procedure for the UK Highways Agency Traffic-Speed Deflectometer. Transportation Research Record, 2093(1), 111-117.
- Ferne, B. W., Langdale, P., Wright, M. A., Fairclough, R., & Sinhal, R. (2013). Developing and implementing traffic-speed network level structural condition pavement surveys. In *Proceedings of the international conferences on the bearing capacity of roads, railways and airfields* (pp. 181-190).

- Ferne, B. W., Drusin, S., Baltzer, S., Langdale, P., & Meitei, B. (2015). UK trial to compare 1st and 2nd generation traffic speed deflectometers. In *Proc., Int. Symp. Non-Destructive Testing in Civil Engineering (NDT-CE)*.
- Flintsch, G., & McGhee, K. (2009). Managing the quality of pavement data collection. *Transportation Research Board of the National Academies, Washington, DC*.
- Flintsch, G., Katicha, S., Bryce, J., Ferne, B., Nell, S., & Diefenderfer, B. (2013). Assessment of continuous pavement deflection measuring technologies (No. SHRP 2 Report S2-R06F-RW-1).
- Hildebrand, G; Rasmussen, S.& Andrés, R. (1999): Development of a Laser-Based High Speed Deflectograph. (Report 97). Danish Road Institute.
- Hildebrand, G; Rasmussen, S. (2002): Development of a High Speed Deflectograph. (Report 177) Danish Road Institute.
- Huang, B., Zhang, M., Gong, H., & Polaczyk, P. (2022). *Evaluation of Traffic Speed Deflectometer for Collecting Network Level Pavement Structural Data in Tennessee* (No. RES2020-08). Tennessee. Department of Transportation.
- Jansen, D. (2017). TSD evaluation in Germany. In Proceedings of the International Symposium Non-Destructive Testing in Civil Engineering (pp. 700-708).
- Kannemeyer, L., Lategan, W., and McKellar, A. (2014). Verification of Traffic Speed Deflectometer Measurements using Instrumented Pavements in South Africa. Pavement Evaluation 2014, Blacksburg, VA.
- Katicha, S. W., & Flintsch, G. W. (2015). Field demonstration of the traffic speed deflectometer in New York (No. 15-4630).

- Katicha, S. W., Flintsch, G. W., & Ferne, B. (2013). Optimal averaging and localized weak spot identification of traffic speed deflectometer measurements. *Transportation research record*, 2367(1), 43-52.
- Katicha, S., Flintsch, G., Shrestha, S., and Thyagarajan, S. (2017). Demonstration of Network Level Structural Evaluation with Traffic Speed Deflectometer: Final Report. FHWA.
- Lee, J., Duschlbauer, D. and Chai, G. (2019). Ground Instrumentation for Traffic Speed Deflectometer (TSD). ARRB Report PRP17037-02, Australian Road Research Board (ARRB), Main Road Western Australia (MRWA).
- Madsen, S. S., & Pedersen, N. L. (2019). Backcalculation of Raptor (RWD) Measurements and Forward Prediction of FWD Deflections Compared with FWD Measurements. In *Airfield and Highway Pavements 2019: Design, Construction, Condition Evaluation, and Management of Pavements* (pp. 382-391). Reston, VA: American Society of Civil Engineers.
- Muller, W. B., & Roberts, J. (2013). Revised approach to assessing traffic speed deflectometer data and field validation of deflection bowl predictions. *International journal of pavement engineering*, 14(4), 388-402.
- Muller, W., and Wix, R. (2014). Preliminary field validation of the updated Traffic Speed Deflectometer (TSD) device. In ARRB Conference, 26th October 2014, Sydney, New South Wales, Australia (No. 4.2).
- Nasimifar, S. (2015). *3D-move simulation of TSDDs for pavement characterizations*. University of Nevada, Reno.

- Nasimifar, M., Thyagarajan, S., & Sivaneswaran, N. (2017). Backcalculation of flexible pavement layer moduli from traffic speed deflectometer data. *Transportation Research Record*, 2641(1), 66-74.
- Rada, G.R. and Nazarian, S. (2011). The State-of-the-Technology of Moving Pavement Deflection Testing, Report No. FHWA-HIF-11-013, Federal Highway Administration (FHWA), Washington, DC.
- Rada, G. R., Nazarian, S., Visintine, B. A., Siddharthan, R., & Thyagarajan, S. (2016). Pavement structural evaluation at the network level: final report. Washington, DC: US Federal Highway Administration Report FHWA-HRT-15-074.
- Saremi, S. (2018). Practical models for Interpreting Traffic Speed Deflectometer Data. M.S. Thesis. The University of Texas at El Paso, El Paso, TX.
- Siddharthan, R. V., Yao, J., & Sebaaly, P. E. (1998). Pavement strain from moving dynamic 3 D load distribution. *Journal of Transportation Engineering*, 124(6), 557-566.
- Siddharthan, R. V., Krishnamenon, N., El-Mously, M., & Sebaaly, P. E. (2002). Validation of a pavement response model using full-scale field tests. *International Journal of Pavement Engineering*, 3(2), 85-93.
- Steele, D., Hall, J., Stubstad, R., Peekna, A., & Walker, R. (2002). Development of a high-speed rolling wheel deflectometer. In Pavement Evaluation Conference, 2002, Roanoke, Virginia, USA.
- Steele, D. A., Beckemeyer, C. A., & Van, T. P. (2015, June). Optimizing Highway Funds by Integrating RWD Data into Pavement Management Decision Making. In 9th International Conference on Managing Pavement Assets.

- Steele, D. A., Lee, H., & Beckemeyer, C. A. (2020). Development of the Rolling Wheel Deflectometer (RWD) (No. FHWA-DTFH-61-14-H00019). United States. Federal Highway Administration.
- Sun, Z., Kasbergen, C., Skarpas, A., van Dalen, K. N., Anupam, K., & Erkens, S. M. (2022). A nonlinear spectral element model for the simulation of traffic speed deflectometer tests of asphalt pavements. *International Journal of Pavement Engineering*, 23(4), 1186-1197.
- Zhang, M., Gong, H., Jia, X., Jiang, X., Feng, N., & Huang, B. (2022). Determining pavement structural number with traffic speed deflectometer measurements. *Transportation Geotechnics*, 35, 100774.
- Zihan, Z. U. A. (2019). *Evaluation of Traffic Speed Deflectometer for Pavement Structural Evaluation in Louisiana*. Louisiana State University and Agricultural & Mechanical College.
- Zofka, A., Graczyk, M., & Rafa, J. (2015). Qualitative evaluation of stochastic factors affecting the Traffic Speed Deflectometer results. In *Transportation Research Board 94th Annual Meeting Washington DC*.

## **CHAPTER 3. NUMERICAL SIMULATION OF TRAFFIC SPEED DEFLECTOMETER TESTING**

### **Abstract**

In the last decade, the limitations of the stationary nondestructive tests for pavement structural evaluation at the network level have led to the development of moving deflection devices such as the Traffic Speed Deflectometer (TSD) that can conduct continuous measurements at traffic speeds. The analysis of the parameters obtained by TSD and its performance in the roadway systems needs robust simulation techniques and models. In this study, the operation of the TSD on the pavement sections was simulated with different pavement structural properties using the finite-layer program, 3D-Move. 3D-Move is capable of modeling moving loads with non-uniform stress distributions at the tire-pavement interface and estimating dynamic pavement responses. The specifications of the numerical models that can realistically simulate TSD testing on the pavement surface are presented in this paper. Different characteristics of the finite layer models were verified with the responses obtained from the simulations carried out using a finite element model. The results of the numerical simulations were then validated with the TSD data collected at three full-scale instrumented pavement test sections. The finite layer approach could accurately model the TSD operation on the flexible pavements using the studied loading characteristics and response calculation method.

**KEYWORDS:** Numerical Simulation, Traffic Speed Deflectometer, 3D-Move, Finite Layer Model.

## Introduction

Traffic speed deflection devices (TSDDs) are moving measurement devices collecting pavement surface responses at traffic speeds over 400 miles/day (650 km/day) without disrupting the normal flow of traffic (Steele et al. 2020). In the last three decades, various studies have been conducted to evaluate the performance of different TSDDs and interpret the data collected by them so that they can effectively be deployed as survey tools for pavement structural evaluation at the project- and network-level (Rada et al. 2016, Elseifi and Elbagalati 2017). The TSD has been employed around the world to evaluate the condition of roadway pavements.

An analytical tool is essential to estimate the pavement responses under TSD to incorporate the device's collected data in a pavement management system (Nasimifar 2015). In this study, a numerical modeling tool that undertakes pavement response computations using a continuum-based finite-layer approach (3D-Move) was used for simulating the TSD moving load on pavement sections. The 3D-Move model formulation accounts for important factors such as any shape of the traffic-induced 3D contact stress distributions, vehicle speed, and viscoelastic material characterization for the pavement layers. This approach treats each pavement layer as a continuum using the Fourier transform technique in order to handle complex surface loadings such as multiple loads and non-uniform tire pavement contact stress distribution (Siddharthan et al. 1998; 2002).

Several researchers have evaluated the applicability of 3D-Move in pavement response analysis (e.g., Siddharthan et al. 2002, Sivaneswaran 2014, Leiva-Villacorta and Timm 2013, Nasimifar et al. 2015, Rada et al. 2016, Saremi 2018, Elseifi et al. 2019). 3D-Move was utilized for a wide range of applications from backcalculation of layer moduli to developing relationships between Falling Weight Deflectometer (FWD) and TSD measurements and assessing the effect of different operational parameters on the pavement responses. Nasimifar et al. (2015) used 3D-Move

to simulate the TSD loading configuration and concluded that the model provided a good match based on a variety of independent pavement responses from field testing. Rada et al. (2016) also applied 3D-Move for the simulation of TSD in the development of procedures for incorporating TSD measurements into network-level PMS applications. Rada et al. (2016) found that the layers moduli estimated from the TSD deflection velocity calculated by the 3D-Move were close to those from the FWD deflection. Nasimifar et al. (2017) showed that the 3D-Move program was an efficient analytical tool to backcalculate layer moduli by directly using TSD-measured deflection velocities. Saremi (2018) employed 3D-Move to simulate the deflection bowls under FWD and TSD loading to be used in symbolic regression approach for developing FWD-TSD relationships. Zihan (2019) also assessed the effect of TSD speed variation on surface deflections using 3D-Move simulation as a reliable analysis tool. Abohamer et al. (2021) calculated theoretical FWD and TSD deflection basins for 162 pavement sections with 3D-Move to train an ANN model to predict FWD deflections. To develop a new approach to determine the structural number with TSD measurements by modifying the AASHTO method, Zhang et al. (2022) relied on 3D-Move to provide a comprehensive TSD database containing various pavement structures.

Although the validation of 3D-Move analysis for moving load simulation was sought in a few studies, different characteristics of the 3D-Move models to simulate TSD loading are also crucial to be studied as they could affect the responses calculated by the program. One of these characteristics is the shape of the tire contact area and pressure distribution on the pavement surface (Siddharthan et al. 1998). Different research efforts have been undertaken considering different TSD tire contact areas and pressure distributions. Nasimifar et al. (2015) used a nonuniform pressure distribution in 3D-Move to simulate the TSD loading configuration and concluded that the dynamic analytical model provided a good match with a variety of independent

pavement responses from field testing. Rada et al. (2016), Saremi (2018), and Zhang et al. (2022) considered uniformly distributed dual circular load in 3D-Move analysis to simulate the loading mechanisms of TSD. Elseifi et al. (2019) utilized nonuniform contact pressure distribution of tires and non-circular loaded area in their 3D-Move simulations in backcalculation analysis.

Modeling a circular tire contact area could be somewhat questionable since tire contact does not perfectly resemble a circular area (Elseifi et al. 2019). Additionally, Siddharthan et al. (2002) indicated that there was a significant difference between the responses computed with uniform and nonuniform contact tire-pavement stress distributions. Except in the case of tensile strain at the bottom of the asphalt concrete layer, the responses computed with the nonuniform stress distribution were lower. In a few studies in which nonuniform contact pressure distribution was considered, there was no discussion on the effect of considering different shapes of tire contact on the theoretical pavement responses. Therefore, in this study circular and rectangular tire contact areas were considered in simulation of hundreds of pavement sections to document the effect of conversion from circular to rectangular footprint.

Another important characteristic of the models is the approach employed to extract the pavement responses as the result of simulations. There are only a few studies that clearly define the response points considered in the numerical simulation. Zihan et al. (2020) defined only one response point to obtain the deflection measurements at different distances from the applied load as dynamic analysis with 3D-Move produces a time-deflection history as an output. They extracted the far-distant deflections from the load from the time-deflection history at the specified points of deflection measurements. Nasimifar (2015) defined a point (observation point) on the midline between the tires as the response point of 3D-Move simulations to calculate the deflections at various locations along the midline between the rear tires using time-space superposition from the

vertical deflection time history. An investigation was conducted on the method to consider response points that realistically reflect the nature of TSD lasers data collection was explained. Ultimately, the investigated models were validated using the measured TSD data in the field.

### **Objective**

The objective of this study is to simulate the TSD moving load on the pavement surface with realistic tire contact area and a rigorous approach to obtaining pavement responses using a finite layer analytical tool such as 3D-Move. The representative models were validated using finite element analysis results and collected TSD data in the field.

### **Methodology**

In the approach adopted in this study to achieve the objectives, first, a pavement structure subjected to TSD rolling tire was simulated employing finite element models and validated using the experimental TSD data. Following by identification of the contact area's shape under the moving tire in the finite element model that resembled the actual tire contact area, hundreds of pavement structure scenarios were simulated by the 3D-Move analysis tool using different shapes of the tire contact area. The contact area included the proposed shape by finite element models and the traditional circular shape. The responses obtained by TSD simulation under circular and non-circular tire footprints were then compared. Furthermore, different response point layouts were considered in the numerical simulation and the corresponding results were compared with finite element models' outputs to identify a realistic arrangement of the response points. Ultimately, field pavement test sections were simulated subjected to TSD dynamic load using the recommended loading contact area and set of response points. To verify the results of the 3D-Move simulation of TSD on the pavement test sections, the numerically calculated responses were compared with the measured ones in the field.

## FIELD TSD TESTS

Data from TSD tests in the field were needed to assess the numerical model’s performance. TSD tests were conducted at three pavement sections located at the MnROAD facility in Minnesota. The pavement sections included three-layer flexible pavements with different structural parameters to account for the potential effect of the pavement properties on the measurements. The properties of the pavement test sections are provided in Table 3.1. All sections were instrumented with geophones to validate the measurements obtained by TSD. At each test section, multiple runs of TSD at operational speeds of 30 mph (48 km/hr) and 45 mph (72 km/hr) were conducted. TSD data were nominally recorded at every 3.3 ft (1 m) over a distance of 40 ft (12 m). Beside TSD tests, FWD tests were conducted to provide deflection basins needed for backcalculation of the layers moduli which were needed as input parameters in the numerical simulations of the TSD loading. The measurements collected by TSD in the field were further incorporated into the analysis process to validate the numerical simulation results obtained from 3D-Move software.

Table 3.1: Pavement Test Sections properties.

Pavement Section	Thickness (in.)		Backcalculated Modulus (ksi)		
	Asphalt	Base	Asphalt	Base	Subgrade
1	4.0	16	120	10	8
2	3.5	15	700	18	12
3	3.5	12	500	100	25

## NUMERICAL SIMULATION CHARACTERISTICS

### Geometry of Tire Contact Area

The axle load and dimensions shown in Figure 3.1 reflect the axle load and configuration and sensor arrangement associated with the currently available TSDs in the United States. The TSD truck modeled consisted of three axles, whose rear axle's right dual tires, spaced 13 in. (330 mm) apart, are equipped with 11 Doppler laser sensors to acquire the surface particle velocity (a.k.a. deflection velocity) profile of the pavement. The laser beam was equipped with three sensors behind the dual tires as well as eight sensors ahead of the tires with no sensor at the center of the tires. These values were used to set the model inputs for numerical simulation. A nominal load of 5200 lbs (2350 kg) per tire and tire pressure of 120 psi (830 kPa) were measured in the field.

The contact shape and area of a 275/70 R22.5 tire used in TSD vehicle were simulated on top of a typical pavement structure in the commercial finite element analysis suite ABAQUS. As the loading was symmetric under the rear right two tires of the TSD, a half model was used. To ensure desirable spatial resolution, around 60,000 tetrahedral elements were simulated consisting of one tire rolling on a section of the pavement with finer mesh at the tire path. Figure 3.2 shows the pavement half model and a closer view of the stresses induced under the moving tire. According to the pressure distribution shown in Figure 3.3, the footprint of the TSD tire was closer to the rectangular shape with a nonuniform distribution of pressure rather than a circular uniform pressure distribution.

To validate the results of the finite element simulation of the TSD tire dynamic load on the pavement, the experimental TSD data that was collected at three full-scale test sections at the MnROAD facility in Minnesota was used. The experimental TSD data and finite element

simulation of the TSD at each of the three test sections are compared in Figure 3.4. For this purpose, the values of deflection velocity collected by each TSD sensor at each test section were averaged and compared with the calculated deflection velocities of TSD sensors by the finite element analysis tool. Since the finite element models on average predicted the results from the field experiments with an uncertainty of about 10% at all sensor locations, the models were considered able to capture field responses adequately. Hence, they were used as a reference for validation for forthcoming finite layer simulation model results.

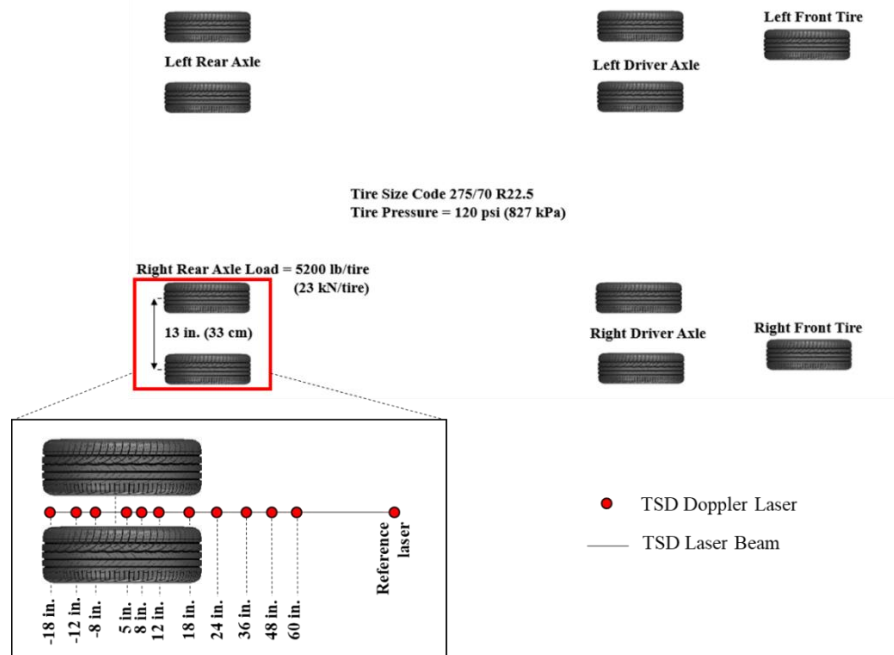


Figure 3.1: TSD axle load configuration, and arrangement of the Doppler laser sensors.

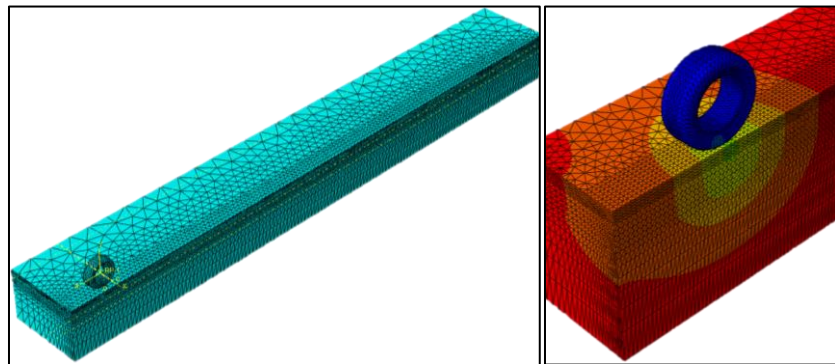


Figure 3.2: Finite element model of TSD moving tire on pavement section.

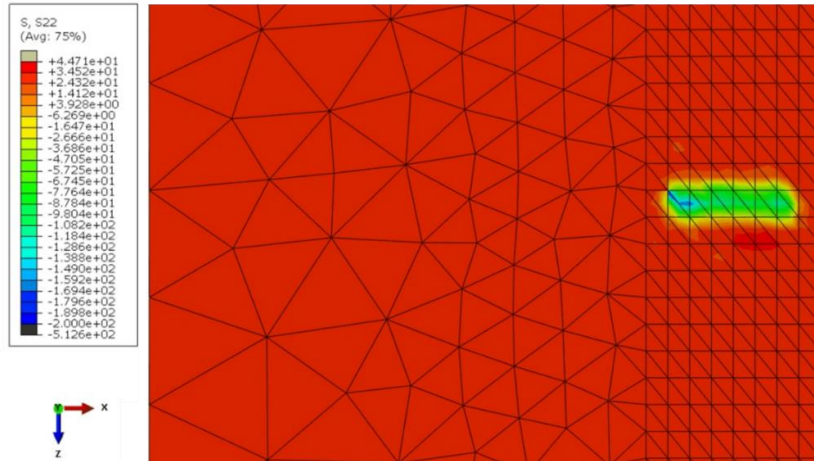


Figure 3.3: Footprint of TSD tire in finite element model.

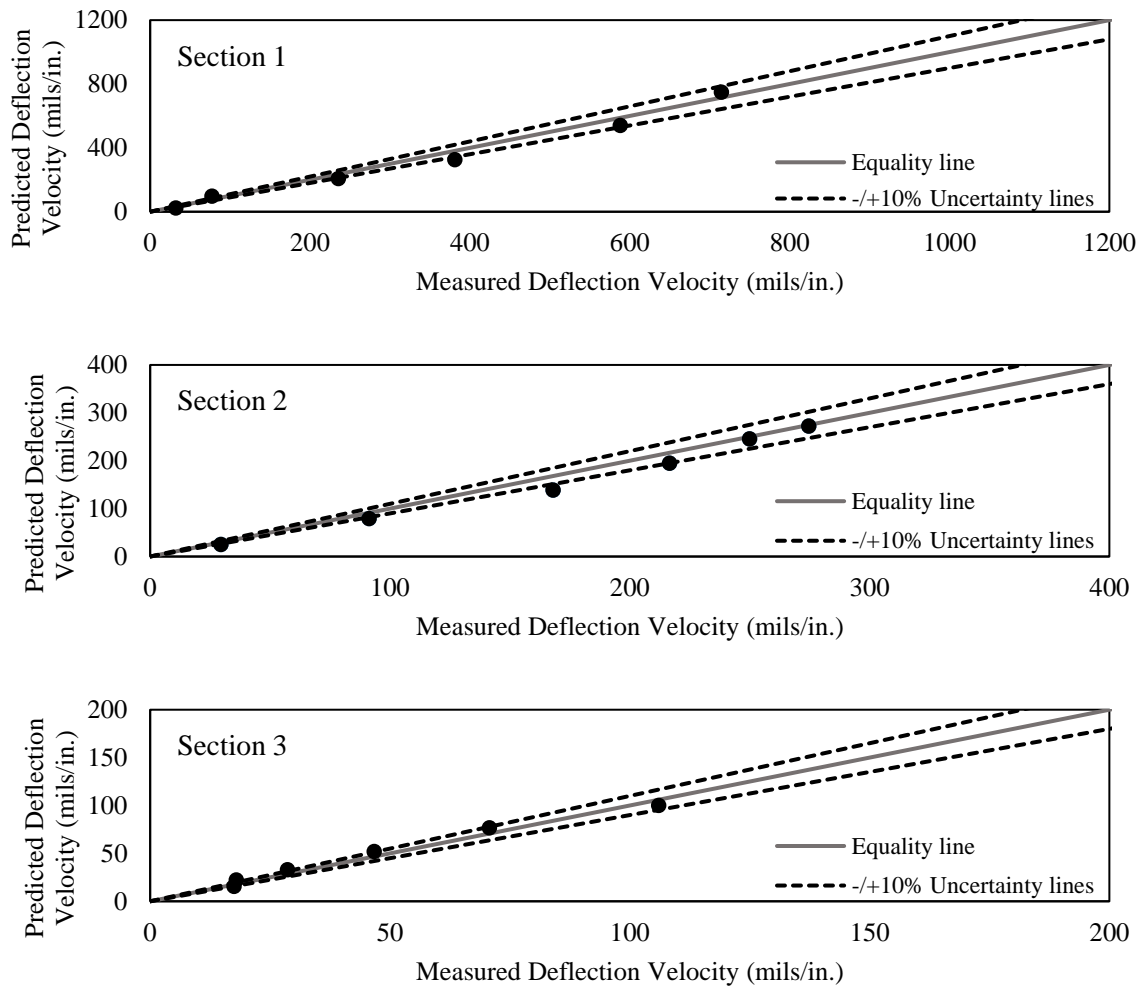


Figure 3.4: Comparison of deflection velocity obtained from finite element simulation of the pavement test sections under TSD and the measured values in the field at 30 mph.

To evaluate the performance of the finite layer approach in modeling the TSD moving load, the 3D-Move program was used to simulate the TSD loading based on the load geometry and pressure distribution from the finite element method. To simulate the TSD loading with rectangular contact area, the aspect ratio of the rectangular footprint was determined based on the tire size, load, and pressure which was consistent with the finite element result. As the input interface of the latest version of the 3D-Move program could not directly generate an input file that could simulate the rectangular and nonuniform contact area, a strategy was needed to develop an algorithm to automatically develop an input file that was compatible with the processor of 3D-Move. For this purpose, a pavement section was simulated under TSD loading with circular contact area and the generated loading input file was rearranged to a format that reflected the rectangular contact area based on the loading distribution resulted in the finite element model (Figure 3.3). The developed loading input file was then used by the software for rectangular area simulations. Figure 3.5 shows the dimensions of the circular and rectangular contact areas considered in the numerical simulations in the 3D-Move analysis tool.

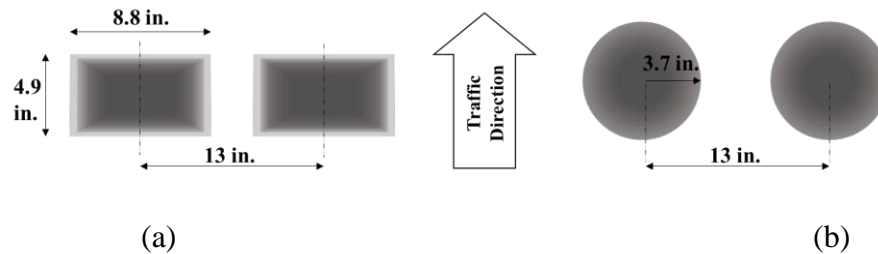


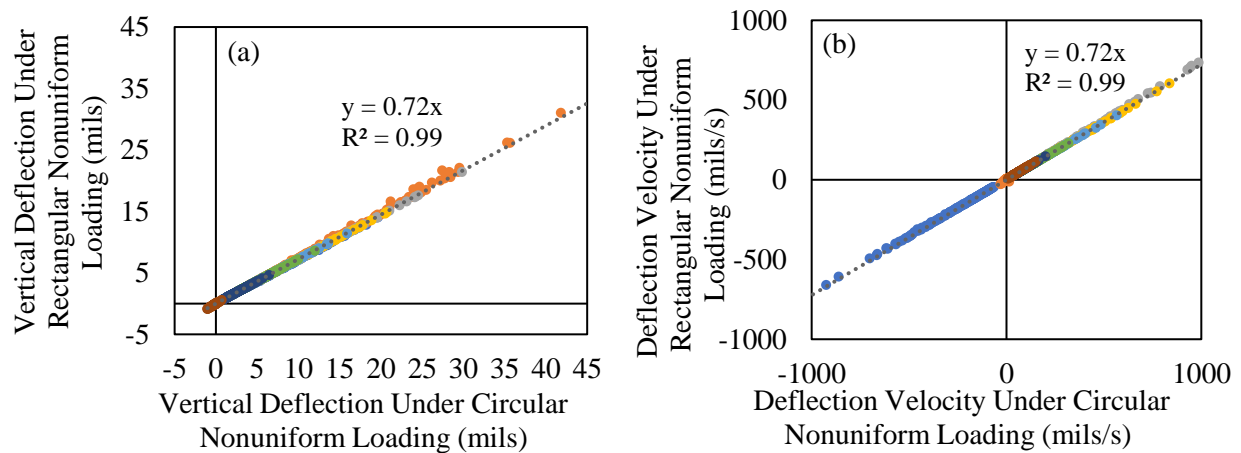
Figure 3.5: TSD tire footprint dimensions considered in 3D-Move models; a) rectangular and b) circular.

Two-hundred three-layer flexible pavement sections were modeled in 3D-Move with the rectangular and circular tire shapes shown in Figure 3.5. The ranges of the uniformly distributed random layer thicknesses and moduli of each pavement layer are listed in Table 3.2. Figure 3.6

compares the deflection and deflection velocities at different TSD sensor locations obtained from the 3D-Move using rectangular and circular contact areas. TSD load with a rectangular contact area caused vertical deflection and deflection velocities of approximately 72% of those occurring under a circular contact area. This indicates that simulating TSD with a circular nonuniform load over-predicts deflections and deflection velocities by about 28%.

Table 3.2: Range of Layer Thicknesses and Material Properties Considered in Numerical Modeling.

Values	Thickness (in.)		Modulus (ksi)		
	Asphalt	Base	Asphalt	Base	Subgrade
Minimum	1	6	300	5	4
Maximum	12	18	700	85	45



TSD Sensors Offset from load (in.): ● -12 ● 0 ● 8 ● 12 ● 18 ● 24 ● 36 ● 60

Figure 3.6: Comparison of deflection parameters induced by TSD with rectangular and circular tire contact area at different sensor positions; (a) vertical deflections and (b) deflection velocities.

### **Time History vs. Instantaneous Pavement Surface Response**

Another characteristic of the simulated models studied was the approach to obtain the pavement surface responses at defined response points in the numerical models. In the literature, the time history response of a single point on the surface was utilized to obtain the variations of the deflection velocity or other parameters along the laser beam length. To obtain the time history of the desired output parameter at each TSD sensor position, time is converted to distance from the load based on the vehicle speed. In another word, the time history concentrates on the variations of a parameter at one sensor while the loading is approaching, reaching on top of the sensor, and moving away from it. This scenario may not reflect the nature of the TSD sensors data acquisition system. TSD captures the data of all laser sensors on the beam almost simultaneously. It means that at the instant that the tire load reaches a point of interest, TSD collects the pavement response at all sensor locations almost at the same time. To capture the instantaneous response profile in 3D-Move, several response points at the TSD sensor locations along the travel path between the two tires must be selected instead of using a single response point. In this situation, the pavement response at all sensor locations was captured at the time step corresponding to the moment that the tire reaches the point of interest identified as zero as shown in Figure 3.7.

Figure 3.7 shows the instantaneous vertical stress profile as calculated after obtaining the response at a particular time of multiple response points along the pavement surface, as well as the time history of a single response point. Several peaks and valleys in the vicinity of the maximum stress are produced which overshoot and undershoot the stress actual values. However, this incident does not happen in the instantaneous surface stress curve where the curve smoothly reaches the peak and then goes down.

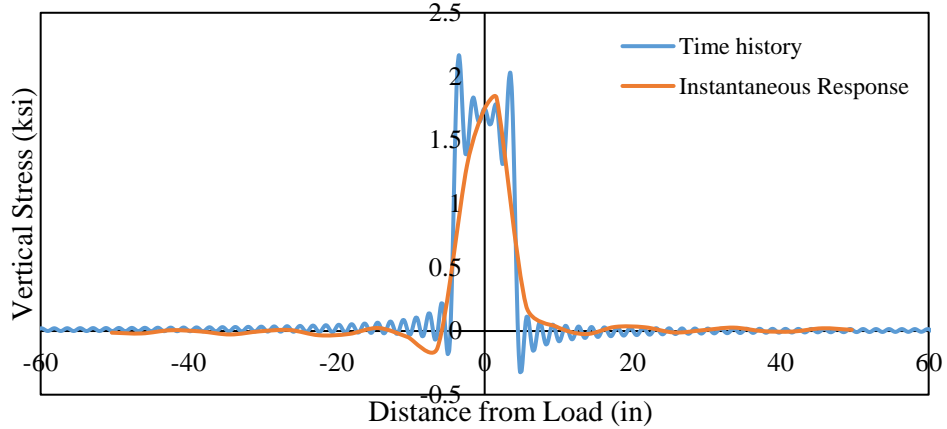


Figure 3.7: Vertical stress variations for time history and instantaneous response conditions.

To corroborate the results from TSD numerical models, the pavement was simulated using the finite element method, and the vertical stresses were calculated at different distances from the moving load along the midline between the two tires. As shown in Figure 3.8, the stress variations with distance in finite element simulation are compatible with that of the instantaneous response method that was used in the 3D-Move simulation indicating that instantaneous responses reflect more realistic stress variations. The low-amplitude sinusoidal waves superimposed on the 3D-Move response have to do with the so-called aliasing of the data associated with the Fourier transform of the data.

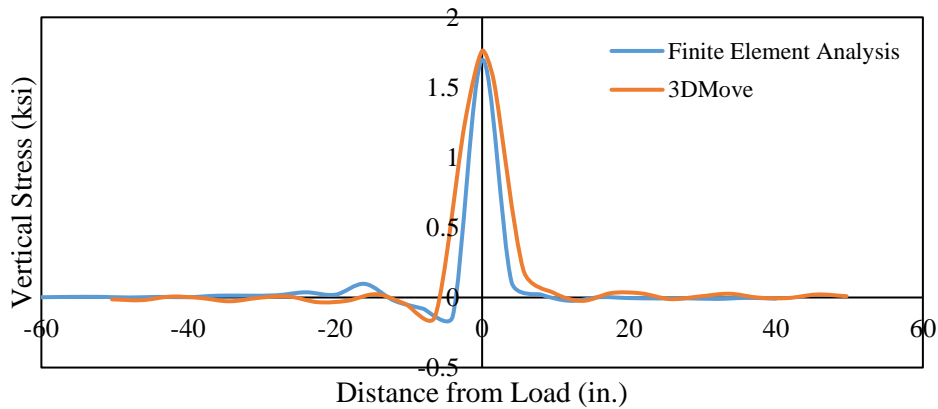


Figure 3.8: Comparison of vertical stress variations from 3D-Move instantaneous response case and finite element simulation.

It is generally known that asphalt pavement failure happens as a result of fatigue cracking and rutting deformation, caused by excessive horizontal tensile strain at the bottom of the asphalt layer and vertical compressive strain on top of the subgrade. As it is necessary to investigate these critical strains in the asphalt pavement design (Ekwulo and Eme 2009), the effect of different response point layouts on the mentioned strains was also explored. Figure 3.9 shows the comparison of the critical strains' variations calculated using the two aforementioned methods. The critical strains consist of the tensile strain at the bottom of the HMA layer (Figure 3.9a) and the compressive strain at top of the subgrade layer (Figure 3.9b). Although the strain values corresponding to the two methods slightly deviate from each other at middle TSD sensors, the trend of the critical strains' variations is quite similar to the instantaneous responses calculated by the 3D-Move program, especially at sensors in the vicinity of the tire load.

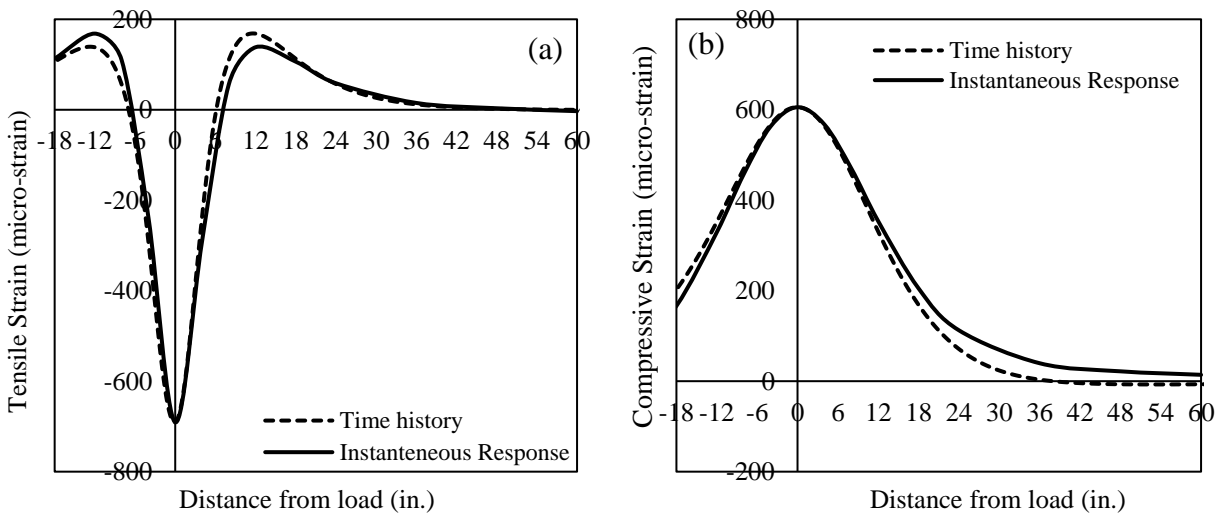


Figure 3.9: Critical strain variations for time history and instantaneous response conditions, a) tensile strain at the bottom of asphalt, and b) compressive strain at top of the subgrade.

Figure 3.10 also shows the instantaneous vertical deflection profile as calculated using the instantaneous response procedure, as well as the time history of a single response point. It appears that the response point layout selection does not significantly affect the trend of deflection variations of the pavement surface. The peak vertical deflections from the two methods are practically the same at the sensors close to the load, but the difference between the two values increases at the sensors with distances of -18 in. to -6 in. and 6 in. to about 48 in. from the tire load.

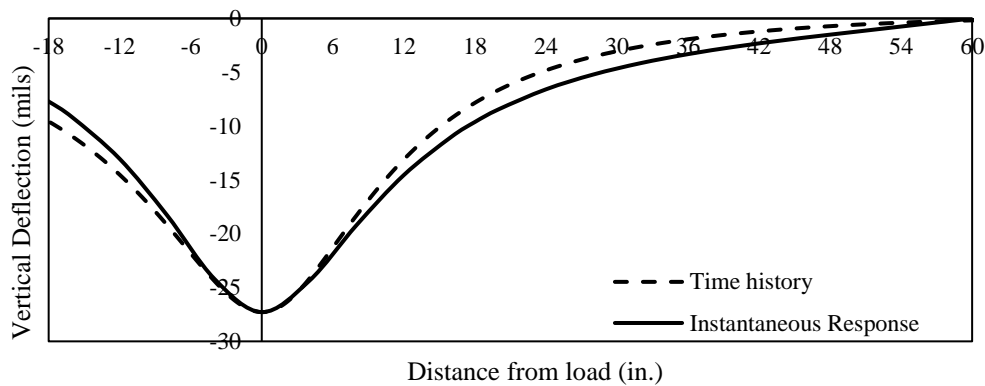


Figure 3.10: Vertical deflection variations for time history and instantaneous response conditions.

In the following analysis, the rectangular nonuniform tire pressure distribution and instantaneous response method were utilized to record the numerical simulation outcomes.

### Numerical Simulation Validation

To assess the performance of the 3D-Move models and substantiate the robustness of the considered simulation approach in terms of the tire contact area shape and the method to obtain the responses, the numerical responses had to be validated with the data from field experiments. The backcalculated layer moduli and the thicknesses of the layers for the three test sections were used as inputs into the TSD 3D-Move models to obtain deflection velocity under the TSD at each

sensor location. As the field TSD data were available at speeds of 30 mph (48 km/hr) and 45 mph (72 km/hr), the simulations were conducted at those two speeds. The calculated parameters were then cross-validated with the experimental data from the field tests.

The measured TSD deflection velocities for the three pavement sections are compared to the predicted numerical responses in **Error! Reference source not found.** The symbols and error bars signify the average deflection velocities and corresponding standard deviations, for the range of TSD deflection velocities measured along the length of the section, respectively. The largest deflection velocity relates to the sensor at 8 in. (215 mm). The deflection velocities gradually decrease and reach the smallest value at 60 in. (1500 mm) away from the load center. The error bars (standard deviations) are larger in Section 3 as this section is stiffest compared to Sections 1 and 2. The numerical and experimental responses agreed with an uncertainty of about  $\pm 10\%$  for all test sections and sensor locations, indicating that models are able to capture field responses adequately. It can also be concluded that the simulation of the TSD with circular nonuniform distribution of the tire pressure could cause more pronounced deviations from the real TSD data obtained in the field since it was shown that the circular contact area overpredicts the responses by 28%.

## Conclusion

This study presents different characteristics of the simulation of the TSD moving load on the pavement surface using the finite layer approach that actually reflects the nature of the TSD performance. Field TSD data and validated finite element model outcomes were used as the reference for comparison and validation of the simulations carried out considering different model properties. One of the numerical model characteristics that was investigated in the current research was the tire contact area and pressure distribution. The footprint of the TSD tire was closer to the

rectangular shape with a nonuniform distribution of pressure rather than a circular uniform pressure distribution. In addition, the results of the 3D-Move simulation of the TSD load on 200 different pavement sections showed that vertical deflections and deflection velocities induced under rectangular contact area were smaller than those of circular contact area by around 28%. Based on the comparison of the simulation results from the rectangular tire contact area and field TSD data, it was observed that the nonuniform rectangular distribution of the tire pressure could model the TSD performance at different speeds with a very promising agreement.

Another characteristic that was studied was the layout of the response points considered in the models at which different parameters were calculated. For this purpose, two approaches were introduced namely time history and instantaneous response methods. In the time history approach, the variations of the response of a single point with time were used to calculate the pavement responses at each TSD sensor location with different distances from the tire load. In the instantaneous response method, which seems closer to the nature of the TSD sensors data collection approach, several response points at the TSD sensor locations along the travel path were selected and the pavement response at each distance from the load was obtained at the instant of tire arriving on top of the sensor at zero. Different important parameters were calculated using the two approaches. The results of the comparison of the time history and instantaneous response methods for tensile strain at the bottom of the asphalt layer, the compressive strain at top of the subgrade layer, and surface vertical deflection showed that the response acquiring method does not significantly affect the responses. However, a considerable difference was observed between the surface vertical stress plots achieved by the two methods. In the time history approach, large peaks in the vicinity of the maximum stress were produced which significantly deviated from the stress actual values. On the other hand, the instantaneous response approach did not result in the

mentioned stress trend and was able to accurately predict the variations of the vertical stress similar to that resulted from the finite element models. The responses of the 200 pavement sections simulated in 3D-Move were obtained based on the instantaneous response method and agreed with the field TSD data with an uncertainty of about  $\pm 10\%$  at all TSD sensor locations.

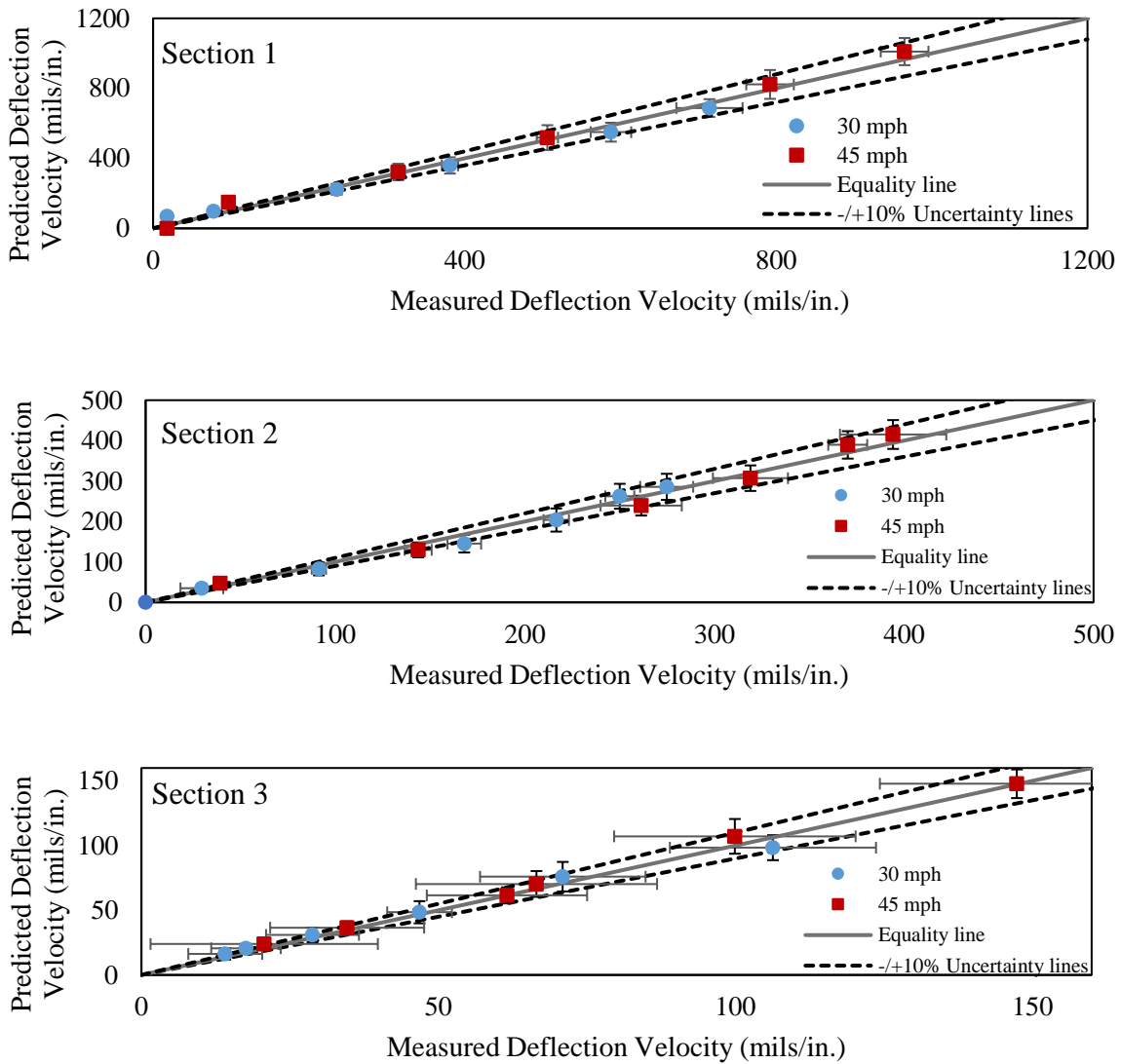


Figure 3.11: Comparison of deflection velocity obtained from 3D-Move simulation of the pavement test sections under TSD and the measured values in the field.

## References

- Abohamer, H., Elseifi, M. A., Zihan, Z. U., Wu, Z., Kebede, N., & Zhang, Z. (2021). Development of an artificial neural network-based procedure for the verification of traffic speed deflectometer measurements. *Transportation research record*, 2675(9), 1076-1088.
- Ekwulo, E. O., & Eme, D. B. (2009). Fatigue and rutting strain analysis of flexible pavements designed using CBR methods. *African Journal of Environmental Science and Technology*, 3(12).
- Elseifi, M., Abdel-Khalek, A. M., & Dasari, K. (2012). Implementation of Rolling Wheel Deflectometer (RWD) in PMS and Pavement Preservation (No. FHWA/11.492). Louisiana Transportation Research Center.
- Elseifi, M. A., & Elbagalati, O. (2017). Assessment of continuous deflection measurement devices in Louisiana-rolling wheel deflectometer: final report 581 (No. FHWA/LA. 17/581). Louisiana Transportation Research Center.
- Elseifi, M. A., Zihan, Z. U., & Icenogle, P. (2019). A Mechanistic Approach to Utilize Traffic Speed Deflectometer (TSD) Measurements into Backcalculation Analysis (No. FHWA/LA. 17/612).
- Ferne, B. W., Langdale, P., Wright, M. A., Fairclough, R., & Sinhal, R. (2013). Developing and implementing traffic-speed network level structural condition pavement surveys. In *Proceedings of the international conferences on the bearing capacity of roads, railways and airfields* (pp. 181-190).

- Flintsch, G., Katicha, S., Bryce, J., Ferne, B., Nell, S., & Diefenderfer, B. (2013). Assessment of continuous pavement deflection measuring technologies (No. SHRP 2 Report S2-R06F-RW-1).
- Hildebrand, G; Rasmussen, S. (2002): Development of a High Speed Deflectograph. (Report 177) Danish Road Institute.
- Katicha, S. W., Flintsch, G. W., & Ferne, B. (2013). Optimal averaging and localized weak spot identification of traffic speed deflectometer measurements. *Transportation research record*, 2367(1), 43-52.
- Katicha, S., Flintsch, G., Shrestha, S., and Thyagarajan, S. (2017). Demonstration of Network Level Structural Evaluation with Traffic Speed Deflectometer: Final Report. FHWA.
- Katicha, S. W., Shrestha, S., Flintsch, G. W., & Diefenderfer, B. K. (2020). *Network Level Pavement Structural Testing With the Traffic Speed Deflectometer* (No. VTRC 21-R4).
- Leiva-Villacorta, F., & Timm, D. (2013). *Falling weight deflectometer loading pulse duration and its effect on predicted pavement responses* (No. 13-2171).
- Nasimifar, S. (2015). *3D-move simulation of TSDDs for pavement characterizations*. University of Nevada, Reno.
- Nasimifar, M., Thyagarajan, S., & Sivaneswaran, N. (2017). Backcalculation of flexible pavement layer moduli from traffic speed deflectometer data. *Transportation Research Record*, 2641(1), 66-74.
- Rada, G.R. and Nazarian, S. (2011). The State-of-the-Technology of Moving Pavement Deflection Testing, Report No. FHWA-HIF-11-013, Federal Highway Administration (FHWA), Washington, DC.

- Rada, G. R., Nazarian, S., Visintine, B. A., Siddharthan, R., & Thyagarajan, S. (2016). Pavement structural evaluation at the network level: final report. Washington, DC: US Federal Highway Administration Report FHWA-HRT-15-074.
- Saremi, S. (2018). Practical models for Interpreting Traffic Speed Deflectometer Data. M.S. Thesis. The University of Texas at El Paso, El Paso, TX.
- Siddharthan, R. V., Yao, J., & Sebaaly, P. E. (1998). Pavement strain from moving dynamic 3 D load distribution. *Journal of Transportation Engineering*, 124(6), 557-566.
- Siddharthan, R. V., Krishnamenon, N., El-Mously, M., & Sebaaly, P. E. (2002). Validation of a pavement response model using full-scale field tests. *International Journal of Pavement Engineering*, 3(2), 85-93.
- Sivaneswaran, N. (2014, September). Network level pavement structural evaluations-a way forward. In *Pavement Evaluation Conference 2014*.
- Steele, D. A., Lee, H., & Beckemeyer, C. A. (2020). Development of the Rolling Wheel Deflectometer (RWD) (No. FHWA-DTFH-61-14-H00019). United States. Federal Highway Administration.
- Stokoe II, K. H., Lee, J. S., Nam, B. H., Lewis, M., Hayes, R., Scullion, T., & Liu, W. (2012). *Developing a Testing Device for Total Pavements Acceptance: Third-Year Report* (No. FHWA/TX-11/0-6005-4).
- Zhang, M., Gong, H., Jia, X., Jiang, X., Feng, N., & Huang, B. (2022). Determining pavement structural number with traffic speed deflectometer measurements. *Transportation Geotechnics*, 35, 100774.

Zihan, Z. U. A. (2019). *Evaluation of Traffic Speed Deflectometer for Pavement Structural Evaluation in Louisiana*. Louisiana State University and Agricultural & Mechanical College.

Zihan, Z. U., Elseifi, M. A., Icenogle, P., Gaspard, K., & Zhang, Z. (2020). Mechanistic-based approach to utilize traffic speed deflectometer measurements in backcalculation analysis. *Transportation research record*, 2674(5), 208-222.

# **CHAPTER 4. IMPACT OF PAVEMENT STIFFNESS ON PERFORMANCE OF TRAFFIC SPEED DEFLECTION MEASUREMENTS**

## **Abstract**

Traffic speed deflection devices have attracted much attention as an innovative tool for assessing the structural capacity of highway networks. However, the sensor and operational limitations of these devices to assess accurately and precisely the pavement structural condition have not been thoroughly established. In this study, the performance of the Traffic Speed Deflectometer (TSD) measurements was evaluated using data from six instrumented pavement sections. The tested sections covered different pavement types such as flexible, composite, and rigid pavements with varying overall stiffness. Based on the comparison between TSD measurements and the data obtained from field-installed instrumentation, TSD could measure the deflection velocity profiles reliably at flexible pavement sections. The level of noise superimposed on the signal of TSD deflection velocities was highly dependent on the pavement type and stiffness.

**KEYWORDS:** Traffic Speed Deflectometer, Accuracy, Precision, Stiffness, Variability.

## **Introduction**

Traffic speed deflection devices (TSDDs) are moving measurement platforms that collect surface deflection measurements at or near traffic speeds up to 400 miles (640 km) per day without disrupting the normal flow of traffic (Elseifi et al. 2011, Flintsch et al. 2013, Steele et al. 2020). Development of TSDDs started in the 1990s, and the first working prototypes were released in the late 1990s/early 2000s (Hildebrand and Rasmussen 2002, Arora et al. 2006). Since then, numerous studies have been performed to assess the performance of different devices and how to best

interpret and use the data collected by the TSDDs for routine pavement structural evaluation for project-level pavement engineering and network-level asset management (Rada and Nazarian 2011, Flintsch et al. 2013, Rada et al. 2016, Elseifi and Elbagalati 2017).

The most popular TSDD is currently the Traffic Speed Deflectometer (TSD) which is in use in more than a dozen countries. These devices span three generations, with the first-generation device limited to four Doppler lasers and the latest third-generation device equipped with as many as 10 Doppler lasers. Several different research groups have evaluated the applicability of TSDs. Rada and Nazarian (2011) reviewed the state-of-the-technology in continuous deflection devices. They concluded that TSD had the potential for network-level applications. They recommend further research to optimize the interval at which measured parameters are averaged that give adequate precision without too much loss of detail. Muller and Roberts (2013) stated that the TSD had the potential to collect measurements of pavement deflection bowls at highway speeds comparable with FWD deflection bowl measurements. Flintsch et al. (2013) identified the TSD as a potential device for network-level structural evaluation in support of maintenance and rehabilitation decision-making. Katicha et al. (2020) reported that the rate of deterioration of the surface condition was affected by the measured structural condition and that TSD could replace the FWD for network-level applications.

The level of accuracy and precision of TSD measurements and the factors affecting these parameters are of great importance. Rada et al. (2016) evaluated TSD on instrumented pavement sections in Minnesota. They stated that although measurements farther from the applied load tended to be less accurate, TSD provided reasonable levels of accuracy for network-level evaluation. Duschlbauer and Lee (2021) installed an array of geophones and accelerometers within several pavement sections to compare TSD and geophone deflection velocities. They observed

some discrepancies that were smaller than the variation between separate passes over the array. They indicated that the effects of different factors on the accuracy of the TSD data still needed to be investigated more thoroughly.

Several factors can affect the TSD deflection measurements. One of the key factors is the pavement characteristics, including the type of pavement, the type of materials used in the layers, and pavement smoothness (International Roughness Index [IRI]). Flintsch et al. (2013) studied the effect of pavement surface on the laser capabilities and discovered that binder-rich surfaces negatively impacted the operation of the TSD Doppler lasers. They also revealed that when measurements were averaged, the standard deviation decreased in proportion to the square root of the number of measurements being averaged. Katicha and Flintsch (2015) concluded that most variations in the TSD measurements could be attributed to the structural condition. Rada et al. (2016) found that the spatial coefficients of variation (COVs) associated with the first four TSD sensors decreased as the FWD central deflection increased for the flexible pavements. The closest sensor to the load exhibited higher COVs than the other sensors on rigid pavements. They also found the accuracy of the TSD and COVs of the measured deflection parameters to be affected by the pavement stiffness but not significantly affected by roughness. Elseifi and Zihan (2018) indicated that higher pavement roughness resulted in a higher COV. Levenberg et al. (2018) stated that the TSD results exhibit a larger spread (higher variability) as compared with the FWD-derived results.

Even though some studies can be found in the literature on the effect of different parameters on the variability of TSD data, these are often limited in scope. The level of accuracy and precision of TSD laser sensors for different pavement types and stiffness is investigated in this study. This study utilized field TSD data collected at every 2 in. (50 mm), which did not appear in almost all

previous studies, to more precisely study the accuracy and variability of TSD sensor measurements in a length of road with constant pavement characteristics. The current study has benefitted from TSD test results and instrumentation data at six different sections with a variety of pavement structures.

### **Objective**

The goal of this study is to evaluate the performance of the deflection velocities collected by TSD Doppler laser sensors by assessing the accuracy and variability of the TSD data acquired at roadway sections. Different pavement types and stiffnesses were covered in this investigation to determine the parameters that impact the performance of the TSD measurements.

### **Methodology**

In the current study, comprehensive experimental data was collected and analyzed to evaluate the accuracy and precision of the TSD measurements and to investigate the effect of pavement stiffness and type on these two concerns. Six pavement sections were instrumented to record their precise responses to TSD runs. The details of the field testing and the approach to assessing the impact of mentioned parameters on TSD-measured data accuracy and precision are provided next. Data collected in the field included TSD data, FWD data, embedded sensors data, and high-speed videos.

### **FIELD DATA COLLECTION**

Field experiments were conducted at the MnROAD facility operated by the Minnesota Department of Transportation, to establish the accuracy and precision of the TSD-measured deflection velocities. The MnROAD facility consists of 45 test sections with live traffic and a closed loop containing 28 sections (<https://www.dot.state.mn.us/mnroad/>). Six pavement test sections were selected to cover different flexible and rigid pavements with different levels of

stiffness. The pavement types, layer thickness, and structural capacity of the six sections are shown in Table 4.1. These test sections covered a wide range of factors affecting the measurement characteristics, including:

- Pavement and surface type,
- Surface layer and total pavement thicknesses, and
- Structural capacity as determined based on measured SCI<sub>12</sub> (the difference between FWD deflections at zero and 12 in. (300 mm) from the center of the load).

Table 4.1: MnROAD Test Sections Properties.

<b>Section</b>	<b>Surface Type</b>	<b>Strength</b>	<b>HMA/ PCC Thickness (in.)</b>	<b>Pavement Thickness (in.)</b>	<b>SCI<sub>12</sub> (mils)</b>
<b>1</b>	HMA	Weak	4.0	20	23.7
<b>2</b>	HMA	Fair	3.5	18.5	13.0
<b>3</b>	HMA	Strong	3.5	19	4.2
<b>4</b>	HMA	Strong	14.8	14.8	4.1
<b>5</b>	PCC	Strong	9.5	13.5	1.7
<b>6</b>	HMA/ PCC	Strong	3.0 HMA/ 6.0 PCC	17	1.4

HMA: Hot Mix Asphalt. PCC: Portland Cement Concrete.

These sections were subjectively classified as Weak, Fair, or Strong for further reference in the paper. Sections 1, 2, and 3 were flexible pavements with thin (<4 in.) asphalt layers and varying overall stiffness. Section 4 was also a flexible pavement but with higher stiffness and a thicker HMA layer than the other flexible pavements. Section 5 was a strong rigid pavement with 9.5 in. (240 mm) of Portland Cement Concrete (PCC) and Section 6 was a composite pavement section comprised of a 3-in. (75 mm) asphalt layer placed over 6 in. (150 mm) of PCC. Both Sections 5 and 6 were considerably stiffer than the rest of the pavement sections.

## Instrumentation

As shown in Figure 4.1, geophones were selected for instrumenting the six MnROAD pavement test sections to measure the surface particle velocity (in TSD terminology deflection velocity) time histories from the TSD transient moving loads. Three geophones were embedded in the outer wheel path of each test section spaced nominally 3 ft (1 m) apart along the center of the wheel path (Figure 4.2). Geophones were deliberately selected since they essentially measure the same parameter as the TSD lasers. The performance of the geophones was verified using FWD test results conducted in each section. For that purpose, one of the FWD sensors was placed directly on top of each embedded sensor. The deflections reported by the FWD were then compared with the corresponding deflections reported by the embedded geophones. The deflections of the FWD and embedded geophones were within about 0.2 mils (5  $\mu\text{m}$ ) of one another. Therefore, embedded geophones were considered reliable in assessing TSD accuracy.

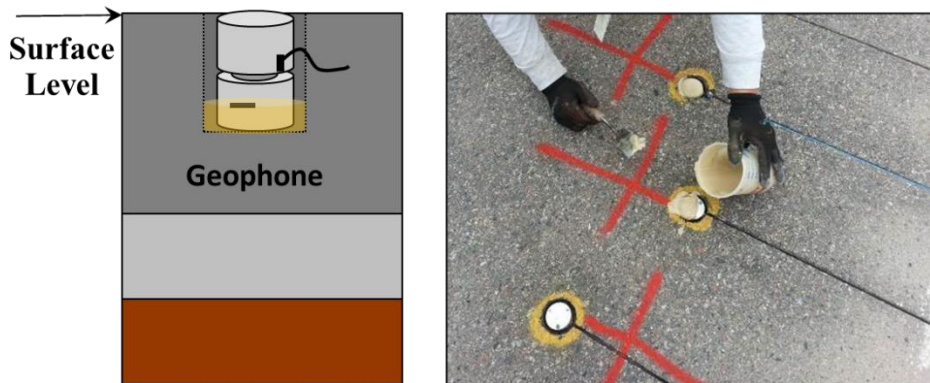


Figure 4.1: Schematic of geophone installed in pavement surface and installing geophone in the field.

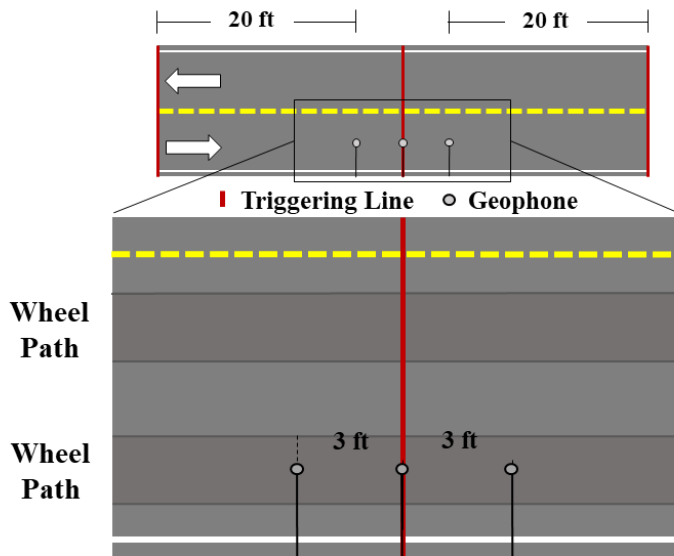


Figure 4.2: Arrangement of the three geophones embedded at each section.

### TSD Tests

At each test section, TSD was operated at different speeds along a length of the pavement that was structurally consistent. The TSD shown in Figure 4.3 was used in this study to collect the deflection velocity profiles under tire loading. The rear axle consisted of a single axle with dual tires spaced 13 in. (330 mm) apart. Tire pressure of 120 psi (830 kPa) and a nominal load of 5200 lbs (2350 kg) per tire were applied by the rear right dual tires. These parameters were verified before actual field testing. The Doppler laser configuration is shown in Figure . Three sensors were mounted behind and eight more sensors were located ahead of the tire at distances shown. The TSD was not equipped with a sensor at the center of the tire load.

At each test section, the TSD data were nominally recorded every 2 in. (50 mm) at different speeds. The data over a distance of 46 ft (14 m), starting 23 ft (7 m) before the middle geophone and ending 23 ft (7 m) ahead of it were extracted for this study. For Sections 1, 2, and 3, five or six runs of the TSD at 30 mph (48 km/hr) and at 45 mph (72 km/hr) mph were conducted. For Sections 4, 5, and 6, five or six passes of TSD were conducted at operating speeds of 30 mph, 45

mph, and 60 mph (48 km/hr, 72 km/hr, and 96 km/hr), respectively. TSD tests were conducted at different speeds to account for any potential impact of the speed on the measurements.



Figure 4.3: Australian Road Research Board (ARRB) TSD truck.

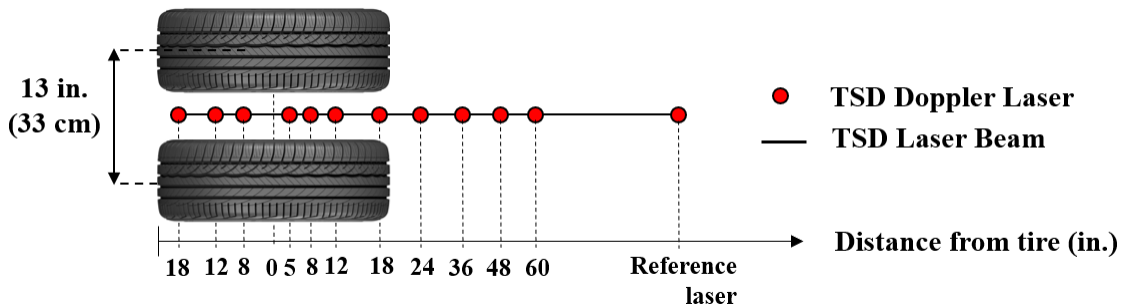


Figure 4.4: TSD instrumented rear axle dual tires with Doppler laser sensor configuration.

In the context of this study, the accuracy was evaluated by comparing the TSD deflection velocities with the corresponding particle velocities from validated geophones embedded in the pavement sections. In each test section, the TSD measurements were compared with geophones' data to assess the level of accuracy of TSD Doppler laser sensors. The deflection parameters measured with the three geophones were averaged and compared with the average deflection parameter values reported from the consecutive TSD passes that were averaged over 2 in. (50 mm).

To perform this comparison properly, the TSD laser beam must pass directly on top of the geophones (i.e., the geophones remain between the dual tires where the laser beam stands). To assure the proper alignment of the tires, a high-speed video camera was mounted in between the TSD tires to record the pavement surface during the TSD operation. Figure 4.5 shows a sample image frame for the best-aligned pass for Section 1, at a speed of 30 mph (48 km/hr). The location of the Doppler laser sensor mounted in the TSD rear axle indicated as a red point within a yellow circle is shown relative to the middle geophone. The same process for finding the best-aligned pass of TSD was followed for all sections. In the image, two accelerometers are also shown on two sides of the geophone which were not utilized in this study. For each test section, the TSD pass with the most accurate alignment among several passes of TSD was identified by reviewing the video frames.



Figure 4.5: Image frame of the best-aligned TSD pass at Section 1 at a speed of 30 mph.

To examine the precision of the TSD data at each pavement test section, the variability-related statistical parameters, i.e., coefficient of variation and standard deviation from each sensor due to repeated runs were calculated at each operational speed. The magnitudes and changes in those parameters were then analyzed to determine the level of precision of the TSD data at different

pavement structures, as well as the effect of different factors such as pavement stiffness, pavement type, and vehicle speed on the TSD data precision.

### Results and Discussion

To analyze the TSD data in terms of accuracy and precision, the TSD data and those from geophones were collected at different vehicle speeds at the six pavement sections. The variations of deflection velocities associated with the embedded geophones and best-aligned TSD pass at 30 mph (48 km/hr) for Section 1 are provided in Figure 4.6. The plot includes the data points showing the mean TSD deflection velocities of each TSD laser sensor collected at every 2 in. along the test section, as well as the curve showing the variation of the average responses obtained by geophones when TSD has passed over them. The error bars also show the standard deviation of the TSD measurements along the test section. The results from the three geophones at the site were within 2% of one another. The TSD and geophone deflection velocities show good agreement.

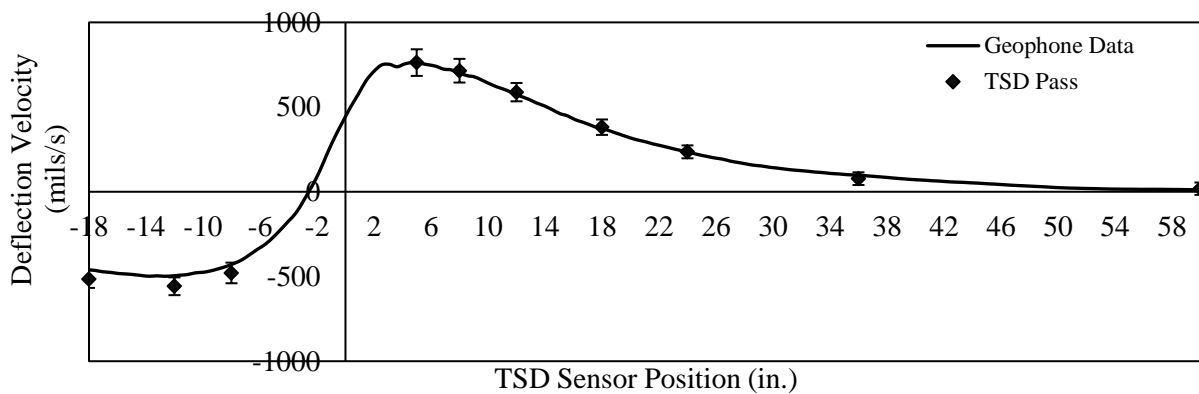


Figure 4.6: TSD collected data vs. geophones obtained data averaged at each TSD sensor position for Section 1 at 30 mph (48 km/hr).

## ACCURACY

The variations of deflection velocities recorded by the installed geophones with those of the TSD sensors using the best-aligned pass at each section as shown in Figure 4.7. Symbols represent the mean deflection velocities corresponding to each TSD sensor along 120 in. (3 m) length of the pavement sections. The standard deviations of the TSD-collected data are shown by vertical error bars. The standard deviations of the geophone data do not appear because they were very small. The mean TSD results are closer to the geophone measurements in Sections 1, 2, and 3 (flexible pavements with thin HMA layers) compared to Sections 4, 5, and 6 (flexible pavement with thick HMA layer, composite pavement, and rigid pavements). For Sections 1, 2, and 3 the mean deflection velocities of the majority of the TSD sensors fall within the  $\pm 20\%$  uncertainty bounds. With an increase in the stiffness of the pavement sections from Sections 1 through 3, the differences between the TSD measurements and the geophones recorded data increase. For the stiffest flexible pavement, composite pavement, and rigid pavement of Sections 4, 5, and 6, the measurements corresponding to the majority of the TSD sensors are positioned outside of the  $\pm 20\%$  uncertainty bounds at all vehicle speeds. In Sections 5 and 6, TSD underestimated the deflection velocities of the pavement surface particles at many TSD sensors. This observation was not made at four flexible pavement sections in which TSD both underestimated and overestimated the pavement responses at different sensor locations. The large vertical error bars for Sections 4, 5, and 6 signify high standard deviations of the TSD deflection velocities for the stiffest flexible and rigid pavements.

The TSD speed also seems to affect the level of accuracy of the deflection velocity measurements. Most of the plots in Figure 4.7 exhibit a greater overall deviation of the TSD measurements from corresponding geophone velocities at higher speeds compared to 30 mph (48

km/hr) speed. In general, TSD seems to collect data that is different from the geophones' data at stiffer pavements and higher operational speeds.

## PRECISION

The raw deflection velocity measurements collected at a speed of 30 mph (48 km/hr) along a length of about 46 ft (14 m) at each test section are shown in **Error! Reference source not found.**4.8. The deflection velocities are smaller for Section 3 than that for Sections 1 and 2 since Section 3 represents the stiffest flexible pavement among them. Sections 4, 5, and 6, which include the stiffer flexible, and rigid pavements, exhibited lower deflection velocities when compared to the first three sections. The changes in plots for the least stiff section (Section 1) to rigid pavement sections with the highest stiffness (Sections 5 and 6) show that with an increase in stiffness of the test sections, more dispersion is observed in data points of different TSD sensors.

Statistical information about the deflection velocities obtained by TSD sensors at different speeds for the data recorded at every 2 in. (50 mm) is shown in **Error! Reference source not found.** for each of the six test sections. The average deflection velocities from each section are shown as bars for different TSD sensors. Error bars represent the  $\pm 1$  standard deviation ( $\sigma$ ) range for the deflection velocities of each sensor. For clarity, the corresponding coefficients of variations are shown on top of each bar to document the variability of the measured data. Different colors of bars are related to different operational speeds at which TSD collected the data.

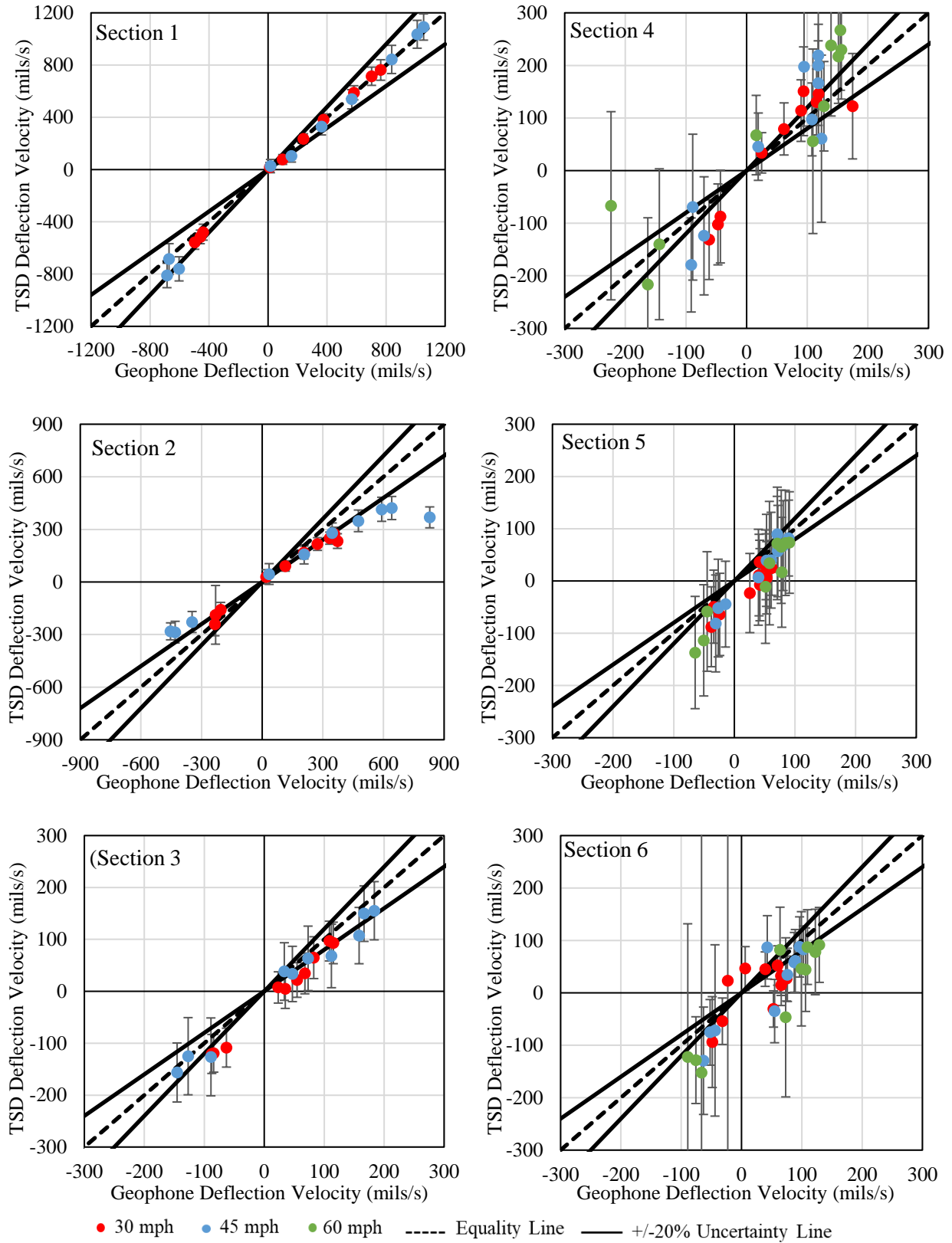


Figure 4.7: Comparison of average TSD deflection velocity and embedded geophone deflection velocity at the best-aligned pass for each section.

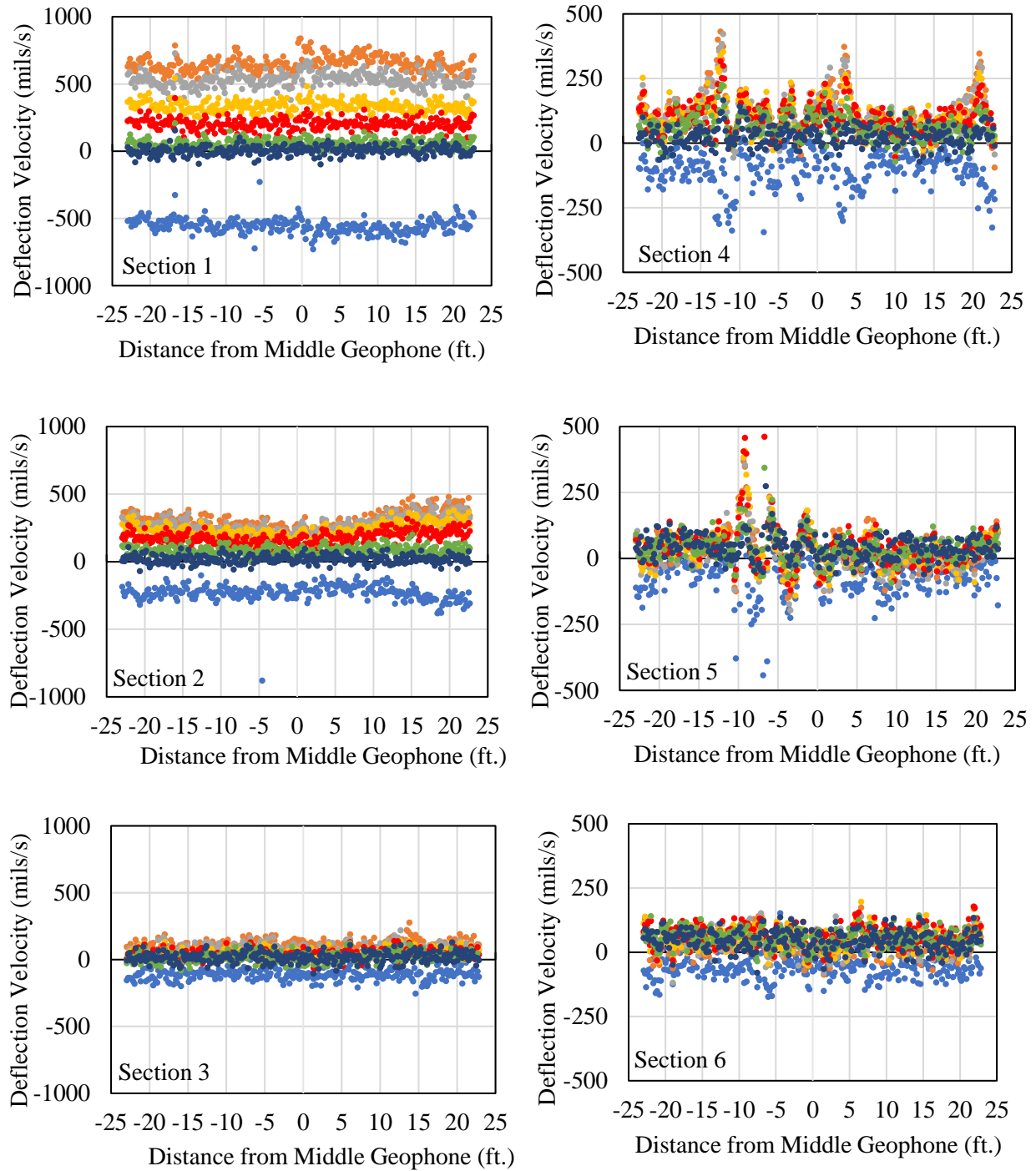


Figure 4.8: TSD deflection measurements in MnROAD test sections.

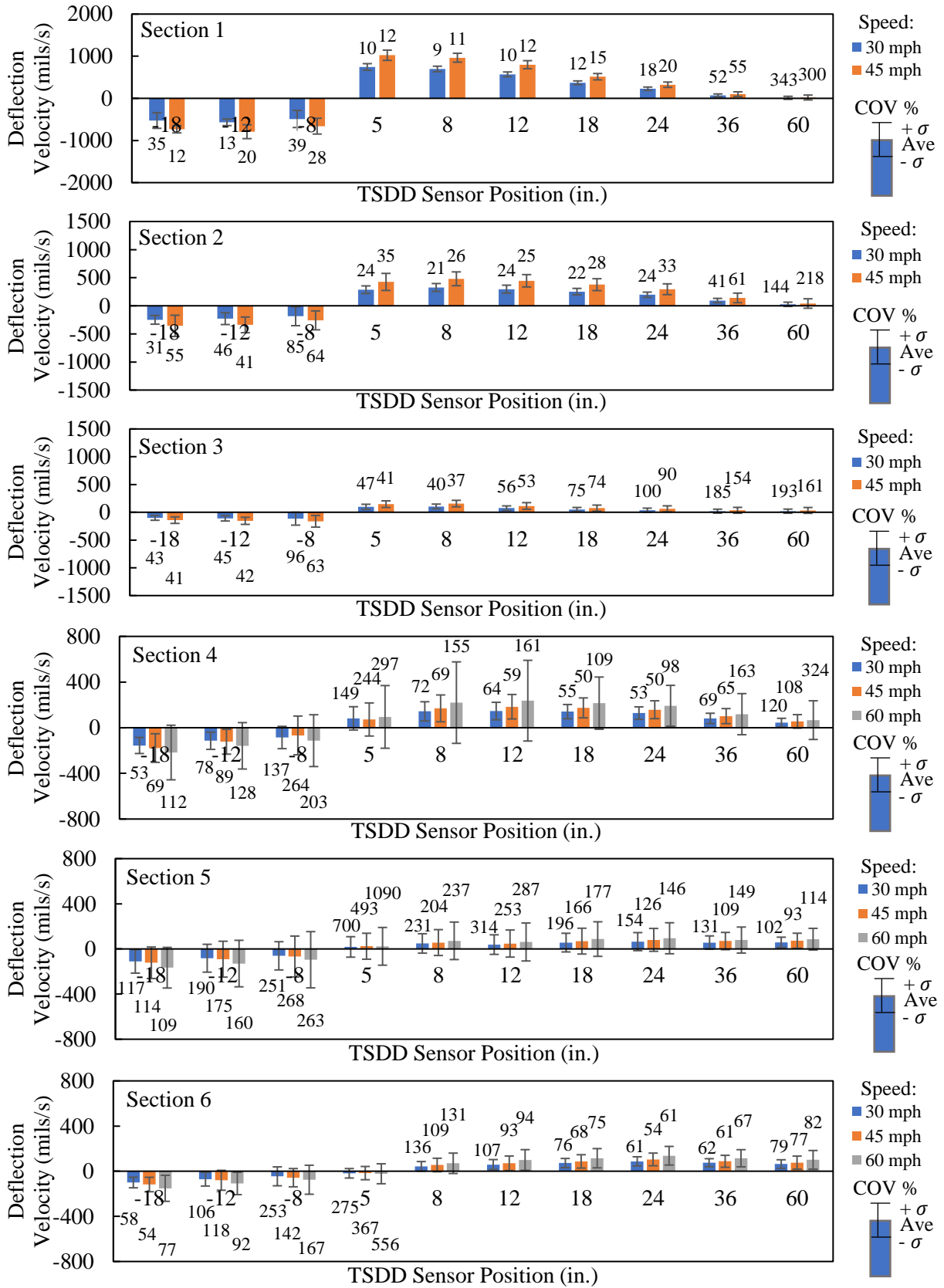


Figure 4.9: Variability of TSD deflection measurements in MnROAD test sections.

The variability of data varies for different sensor locations and test sections. The COV of the measurements for the two farthest sensors exceeded 100% for almost all sites. For these sensors, the deflection velocities are too small to be captured precisely by the sensors. In Sections 1, 2, and 3, the COVs of the sensor measurements decreased as the sensors got closer to the tire load. The COVs for different sensors are larger in Section 3 than in Sections 1 and 2, indicating that higher stiffness resulted in higher variability of the deflection velocities measured by TSD sensors. The speed does not generally seem to affect the measurement in the same way for all sensors. Hence, no trend was observed for the impact of speed in the variability of the TSD data at flexible pavements.

The variability of the deflection velocities in terms of COVs is notably higher for Sections 4, 5, and 6 compared to Sections 1, 2, and 3. The COVs for Sections 4, 5, and 6 exceeded 100% for the majority of the sensors, even those close to the tire load. Overall, the location of the sensor relative to the tire load did not seem to have a specific effect on the TSD measurements variability of Sections 4, 5, and 6 as the COVs did not follow a particular trend when sensors got farther from the loading tires. The change in vehicle speed on the very stiff flexible pavement or rigid pavements impacted the variability of the sensors' data, but the changes did not show a constant trend. A comparison of the statistical parameters of all six test sections indicates that generally, an increase in stiffness in terms of changing pavement type from flexible to rigid or increasing the stiffness in flexible pavements results in higher magnitudes of variability.

The variability of the deflection velocities of all TSD sensors at different speeds for the six test sections is plotted against their corresponding average deflection velocities in Figure 4.10. An inverse relationship is observed between the magnitude and COV of deflection velocities. In other words, the smaller the magnitude of deflection velocity is, the higher the variability will be. Lower

deflection velocities correspond to measurements collected by sensors located farther away from the tire loading or obtained at sections with stiffer pavements. Variability in measurements seems to increase with the vehicle speed as well. The coefficient of variation of less than 20% corresponded to deflection velocities greater than about 200 mils/s (5 mm/s).

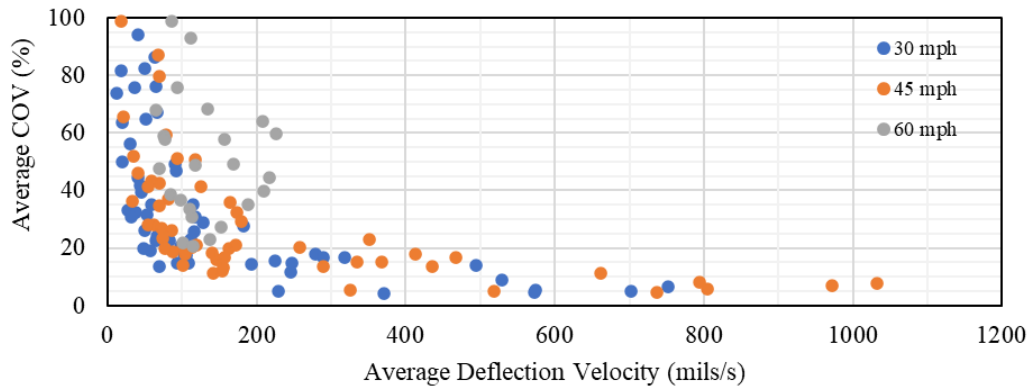


Figure 4.10: Variations of COV with the magnitude of deflection velocity.

To eliminate the effects of vehicle speed on the measurements, the deflection velocities were converted to deflection slopes by dividing the magnitudes of deflection velocity by the corresponding TSD vehicle speed. As shown in Figure 4.11, the variability increases as the deflection slope decrease. To maintain measurements within a 20% variability, the deflection slopes should be greater than 4 mils/ft (0.33 mm/m).

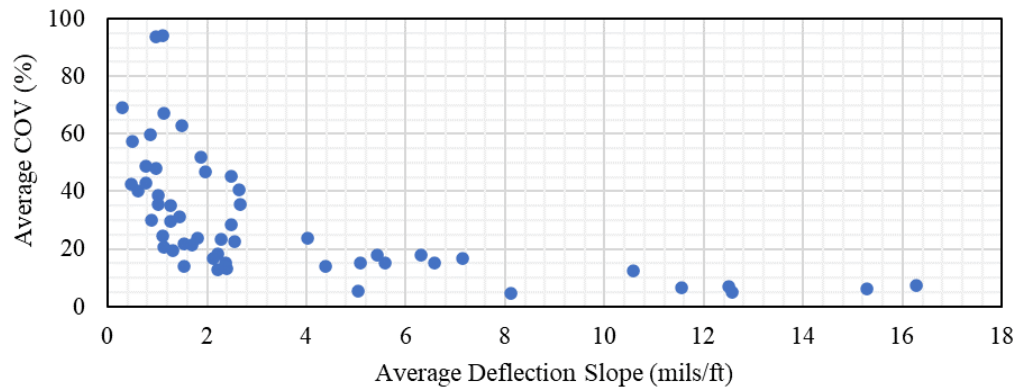


Figure 4.11: Variations of COV with the magnitude of deflection slope.

## Conclusion

In this study, the performance of the deflection velocities collected by TSD Doppler laser sensors was evaluated by assessing the accuracy and variability of the TSD data collected at several pavement sections with different structural properties and at different operational speeds.

The accuracy of the TSD data was evaluated by comparing the TSD deflection velocities with the corresponding data obtained by validated geophones embedded in each pavement section. The best-aligned TSD pass was selected at each vehicle speed based on the high-speed video. At less stiff sections, the mean deflection velocities were within  $\pm 20\%$  of the embedded geophones data for the majority of the TSD sensors. With an increase in the stiffness of the pavement sections, the differences between the TSD measurements and the geophones recorded data increased. For very stiff pavements, the measurements corresponding to the majority of the TSD sensors deviated from the geophones data by more than  $\pm 20\%$ . Also, the overall deviation of the TSD measurements from the geophone velocities was greater at higher speeds compared to the 30 mph (48 km/hr) speed.

The precision of the TSD data was examined by analysis of the variability-related statistical parameters such as COV and standard deviation of each sensor's data due to repeated runs at different operational speeds. The variability of the deflection velocities in terms of COVs was higher in stiffer sections. Stiffer sections correspond to rigid pavements or stiffer flexible pavements. An inverse relationship was observed between the magnitude and COVs of the collected deflection velocities. Variability in measurements seemed to increase with the vehicle speed as well.

## References

- Arora, J., Tandon, V., and Nazarian, S. (2006). Continuous Deflection Testing of Highways at Traffic Speeds, Report No. FHWA/TX-06/0-4380, Texas Department of Transportation, Austin, TX.
- Duschlbauer, D., & Lee, J. (2021, July). Capturing the Moving Deflection Basin Under a Traffic Speed Deflectometer. In Civil Infrastructures Confronting Severe Weathers and Climate Changes Conference (pp. 23-33). Springer, Cham.
- Elseifi, M. A., & Elbagalati, O. (2017). Assessment of continuous deflection measurement devices in Louisiana-rolling wheel deflectometer: final report 581 (No. FHWA/LA. 17/581). Louisiana Transportation Research Center.
- Elseifi, M. A., & Zihan, Z. U. (2018). Assessment of the Traffic Speed Deflectometer in Louisiana for Pavement Structural Evaluation (No. FHWA/LA. 18/590). Louisiana Transportation Research Center.
- Elseifi, M. A., Abdel-Khalek, A., Gaspard, K., Zhang, Z. D., & Ismail, S. (2011). Evaluation of the rolling wheel deflectometer as a structural pavement assessment tool in Louisiana. In Transportation and Development Institute Congress 2011: Integrated Transportation and Development for a Better Tomorrow (pp. 628-637).
- Flintsch, G., Katicha, S., Bryce, J., Ferne, B., Nell, S., & Diefenderfer, B. (2013). Assessment of continuous pavement deflection measuring technologies (No. SHRP 2 Report S2-R06F-RW-1).
- Hildebrand, G; Rasmussen, S. (2002): Development of a High Speed Deflectograph. (Report 177) Danish Road Institute.

- Katicha, S. W., & Flintsch, G. W. (2015). Field demonstration of the traffic speed deflectometer in New York (No. 15-4630).
- Katicha, S. W., Shrestha, S., Flintsch, G. W., & Diefenderfer, B. K. (2020). *Network Level Pavement Structural Testing With the Traffic Speed Deflectometer* (No. VTRC 21-R4).
- Muller, W. B., & Roberts, J. (2013). Revised approach to assessing traffic speed deflectometer data and field validation of deflection bowl predictions. *International journal of pavement engineering*, 14(4), 388-402.
- Rada, G.R. and Nazarian, S. (2011). The State-of-the-Technology of Moving Pavement Deflection Testing, Report No. FHWA-HIF-11-013, Federal Highway Administration (FHWA), Washington, DC.
- Rada, G. R., Nazarian, S., Visintine, B. A., Siddharthan, R., & Thyagarajan, S. (2016). Pavement structural evaluation at the network level: final report. Washington, DC: US Federal Highway Administration Report FHWA-HRT-15-074.
- Steele, D. A., Lee, H., & Beckemeyer, C. A. (2020). Development of the Rolling Wheel Deflectometer (RWD) (No. FHWA-DTFH-61-14-H00019). The United States. Federal Highway Administration.

# CHAPTER 5. QUALITATIVE ASSESSMENT OF TRAFFIC SPEED DEFLECTOMETER DATA COLLECTION PRACTICE

## Abstract

Traffic Speed Deflectometer (TSDs) are being used more frequently for network-level pavement evaluation at traffic speeds. Although it has been established that TSDs can assess pavement conditions at the network and project level, the quality of the obtained data needs to be further evaluated and factors affecting the magnitude and trends of the pavement responses should be more deeply investigated. In this study, TSD field experiments were conducted on several diverse pavement sections under different operational conditions. The effects of parameters such as data collection interval, vehicle operational speed, pavement section structural stiffness, and deflection velocity magnitudes were investigated. Although the vehicle speed did not significantly affect the magnitude of the deflection slopes, it impacted the variability of the obtained raw data. Overall pavement stiffness also directly impacts the quality of the data. Stiffer pavements, including pavements with thick asphalt layer or stabilized base layer and rigid pavements, responded to the moving load with lower deflection velocities and higher variability. Averaging the obtained data over longer intervals also reduced the variability of the deflection parameters.

**KEYWORDS:** Traffic Speed Deflectometer, Data quality assessment, Coefficient of variation, Variability, Averaging intervals.

## Introduction

Due to the demand for network-level pavement structural information to support network-level decision-making, fast development of moving pavement condition evaluation devices has been witnessed in the past few decades. These devices have several advantages over traditional devices such as Falling Weight deflectometer (FWD). Moving devices include Road Deflection

Tester (RDT) developed in Sweden (Andrén 1999), the Traffic Speed Deflectometer (TSD) developed in Denmark (Hildebrand and Rasmussen 2002), the Rolling Wheel Deflectometer (RWD) developed in the United States (Steel et al. 2002), and the Rapid Pavement Tester (RAPTOR) developed in Denmark (Andersen et al. 2017). As TSD is gaining wide acceptance in the U.S., this study is focused on the data obtained from TSD.

Numerous efforts have been made on assessing, analyzing, and interpreting the data collected by the TSD. Rada et al. (2016) studied the dependency of the variability of TSD measurements on its operational speed. They reported that the measured deflection parameters were sensitive to the vehicle speed with the coefficients of variation (COV) of the deflection slopes being about 24% lower at 30 mph (48 km/hr) than at 45 mph (72 km/hr) and were around 38% higher at 60 mph (96 km/hr) than the COVs at 45 mph (72 km/hr). Xiao et al. (2021) confirmed that the effect of the TSD speed on the measurement was significant. However, Kannemeyer et al. (2014) reported that TSD measured accurately the pavement response, even at low speeds (<20 mph, >32 km/hr). Elseifi and Zihan (2018) studied numerically the effect of vehicle speed on surface deflections. They showed the increase in vehicle speed caused a decrease in the majority of the deflections.

In terms of the dependency of TSD measurements on pavement structure, Rada et al. (2016) reported that the COVs from the first four sensors decreased with a decrease in stiffness for the flexible and rigid pavement sections. The COVs of the deflection slopes were found to be relatively higher for the far sensor locations. Zofka et al. (2015), Rada et al. (2016), and Xiao et al. (2021) did not observe a strong correlation between the surface roughness and deflection slopes. However, Elseifi et al. (2012) concluded that there was a significant difference in the coefficient of variation for different roughness categories.

The averaging interval of the recorded deflection parameters has also been assessed for its effects on TSD measurements. In the recent past, the rate of data collection has increased from 1 kHz (one measurement at every 1 in. (28 mm) at 62 mph (100 km/h) vehicle speed) to 250 kHz (one measurement at every 4 mils (0.1mm) at 62 mph (100 km/h) vehicle speed. The data is averaged and reported at intervals ranging from 3.3 ft (1 m) to 330 ft (100 m) with 33 ft (10 m) or 53 ft (16 m) being the most widely used averaging lengths (Katicha et al., 2022). Rada et al. (2016) indicated that averaging of the measurements was a compromise between increasing accuracy and reducing precision of the measurements. If the averaging length is long, the measurements cannot capture the structural variations that occur at a spatial length smaller than the chosen averaging length. There have been many efforts to improve TSDs so that high-quality measurements can be obtained at a 3.3 ft (1 m) averaging interval. Katicha et al. (2013) found that the optimal averaging length depends on the section's structural condition variations. Relatively homogenous sections could have longer averaged lengths while sections with highly variable structural conditions over short distances required shorter averaging lengths.

Flintsch et al. (2012) observed the presence of significant random noise in the raw signals collected at 1 kHz even when averaged across a 0.1-m (4-in.) length. They showed that the “true” deflection profile was suppressed as the averaging length increased from 1 m to 10 m (3.3 ft to 33 ft) and on the weak composite construction even the 10-m average length hid some true deflection variations. They showed that decreasing the sample unit length did not significantly affect the overall trend of the deflection profile or the mean deflection, but it increased the variability over the section length.

## **Objective**

The goal of this study was to assess the impact of different factors on the changes and variability of the data collected by TSD on different pavement sections. The factors investigated in this study include:

- Operational (vehicle speed)
- Structural (pavement type and stiffness)
- Data acquisition system (data averaging intervals)

## **Methodology**

To assess the effect of different parameters on the data collected by TSD, experimental data were obtained in the field. Further statistical analyses were then performed on the changes observed in the measured responses with changes in structural properties, data averaging intervals, and vehicle speed. Data collected in the field included TSD data, embedded sensors' data to validate the accuracy of the TSD measurements, and high-speed videos to check the alignment of the TSD sensors and embedded sensors. In this section, the experimental efforts are described, followed by an explanation of the strategies employed to evaluate the impact of the parameters on the pavement responses subjected to TSD loading.

### **FIELD TSD TESTING**

Field experiments were conducted at the MnROAD facility operated by the Minnesota Department of Transportation. The MnROAD facility consisted of a 3.5-mi (5.6-km) roadway comprising of 45 pavement sections with live traffic and a 2.5-mi (4-km) closed-loop road containing 28 sections. Six test sections were selected for instrumentation and conducting TSD tests as they covered a wide range of factors affecting the measurement characteristics, including:

- Pavement type,
- Surface layer and total pavement thicknesses,
- Structural capacity as determined based on measured SCI<sub>12</sub> (the difference between FWD deflections at zero and 12 in. (300 mm) from the center of the load).

Layer thickness and pavement types of the test sections are shown in Table 5.1. A variety of surface types, i.e., flexible, composite, and rigid pavement, and pavement strengths were considered. Sections were subjectively classified as Weak, Fair, or Strong based on their SCI<sub>12</sub>. Sections 1, 2, and 3 were flexible pavements with varying overall stiffness and thin (less than 4 in., 100 mm) asphalt layers. Section 4 was also a flexible pavement with higher overall stiffness and thicker than the other three flexible pavements. Section 5 was a rigid pavement with 9.5 in. (241 mm) of Portland cement concrete (PCC) and Section 6 was a composite pavement section comprised of a 3-in. (75 mm) asphalt layer placed over 6 in. (150 mm) of PCC. Sections 5 and 6 were considerably stiffer than the other pavement sections.

Table 5.1: MnROAD Pavement Test Sections.

<b>Section</b>	<b>Surface Type</b>	<b>Strength</b>	<b>HMA*/ PCC** Thickness (in.)</b>	<b>Pavement Thickness (in.)</b>	<b>SCI<sub>12</sub> (mils)</b>
<b>1</b>	HMA	Weak	4.0	20	23.7
<b>2</b>	HMA	Fair	3.5	18.5	13
<b>3</b>	HMA	Strong	3.5	19	4.2
<b>4</b>	HMA	Strong	14.8	14.8	4.1
<b>5</b>	PCC	Strong	9.5	13.5	1.7
<b>6</b>	HMA/ PCC	Strong	3.0 HMA/ 6.0 PCC	17	1.4

\*HMA: Hot Mix Asphalt

\*\* PCC: Portland Cement Concrete

The TSD device had an axle load configuration, and Doppler laser configuration, as shown in Figure 5.1. The rear axle that was used to measure the deflection velocities consisted of a single axle with dual tires spaced 13 in. (330 mm) apart. Tire pressure of 120 psi (827 kPa) and a nominal load of 5200 lbs (2350 kg) per tire were measured. Laser sensors were mounted between the two tires with three sensors behind and eight sensors ahead of the tires at different offsets from the load center as shown in the figure.

At each pavement test section, the TSD data were nominally recorded at intervals of 2 in. (50 mm), over a distance of 45 ft (14 m). At Sections 1, 2, and 3, several TSD runs were conducted at 30 mph (48 km/hr) and 45 mph (72 km/hr). Several TSD runs were also carried out at three different speeds of 30 mph (48 km/hr), 45 mph (72 km/hr) mph, and 60 mph (96 km/hr) along Sections 4, 5, and 6. The deflection velocities, which are directly measured by TSD, were recorded at different operational conditions and formed an experimental database for further analysis.

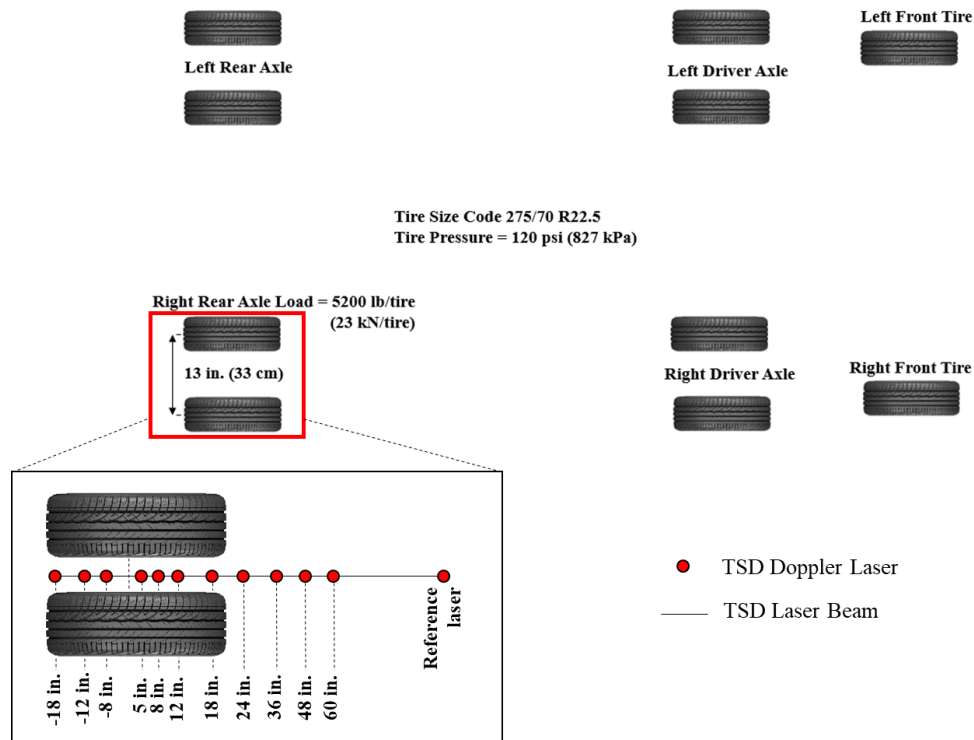


Figure 5.1: TSD axle configuration and loads, and instrumented rear axle with Doppler laser sensor configuration.

## PARAMETRIC ANALYSIS

The effects of different parameters on the data measured by the TSD testing on pavement surface were investigated through statistical analyses of the data under different conditions. To study the impacts of pavement type and stiffness on the TSD data, statistical parameters such as the average, standard deviation, and coefficient of variation were determined for the data collected by each TSD sensor along the six sections. To investigate how the data originally recorded at every 2 in. (50 mm) were compared with the discrete data averaged over every 3.3 ft (1 m). Finally, the TSD measurements at different operational speeds were averaged for each sensor position and compared to analyze the changes in the values of deflection parameters with speed changes.

### Results and Discussion

**Error! Reference source not found.**5.2 shows a sample of the TSD raw deflection velocity measurements collected at a speed of 30 mph (48 km/hr) along a length of about 45 ft (14 m) at each test section., the deflection velocities in Section 3 are smaller than those of Sections 1 and 2 since the pavement of Section 3 is stiffer than Sections 1 and 2. Sections 4, 5, and 6, corresponding to the stiffest flexible pavement, rigid and composite pavements, respectively, exhibited lower deflection velocities when compared to the first three sections. A comparison of the least stiff section (Section 1) to the rigid and composite pavement sections with the highest stiffness (Sections 5 and 6) shows that the data becomes more dispersed with an increase in the stiffness of the pavement.

### EFFECT OF THE PAVEMENT TYPE ON THE VARIABILITY OF THE TSD MEASUREMENTS

Figure 5.3 exhibits the statistical information of the deflection velocities calculated for TSD runs at different speeds along the six test sections for the data recorded at every 2 in. (50 mm). Error bars represent the  $\pm 1$  standard deviation ( $\sigma$ ) range for the deflection parameters. The

corresponding COVs are also shown on top of each bar. The COVs vary significantly for different sensor locations and pavement test sections. The deflection velocities are too small to be captured precisely by the sensors farther from the tire load. For the two farthest sensors, the COVs exceeded 100% at almost all sites. The COVs generally decreased as the sensors got closer to the tire load in Sections 1, 2, and 3. The COVs are also greater in Section 3 than in Section 2 and Section 1. The stiffer pavement which induces smaller pavement responses resulted in higher variability of the deflection velocities. The speed does not generally seem to affect the measurements' standard deviations ( $\sigma$ ) and COVs in the same way for all sensors. Hence, no trend was observed for the impact of the vehicle speed on the variability of the TSD data at flexible pavements.

Sections 4, 5, and 6 experienced notably higher COVs as compared to Sections 1, 2, and 3. The COVs for Sections 4, 5, and 6 exceeded 100% even for sensors closer to the tire load. The location of the sensor relative to the tire did not seem to result in a well-defined trend in variability. The change in vehicle speed in the very stiff flexible or rigid pavements substantially impacted the variability of the sensors' data, but the changes did not show a constant trend. A comparison of the statistical parameters of all six test sections indicates that an increase in pavement stiffness from flexible to rigid or progressive increase in the stiffness in flexible pavements results in higher variability.

The variability of the deflection velocities of all TSD sensors in terms of COV at different speeds for all pavement test sections is plotted against their corresponding average deflection velocities in Figure a. An inverse relationship is observed between the deflection velocities and COVs of deflection velocities. Variability in measurements seems to increase with the vehicle speed as well. The lower deflection velocities corresponded to the measurements made with sensors located farther away from the tire loading or measured at test sections with stiffer

pavements. The COV of less than 20% corresponded to deflection velocities greater than about 600 mils/s (15 mm/s).

The deflection velocities were converted to deflection slopes by dividing the deflection velocities by the corresponding TSD vehicle speed to minimize the effects of vehicle speed on the TSD measurements. As shown in Figure b, the variability increases as the deflection slope decreases. To maintain measurements within a 20% variability, the deflection slopes should be greater than 10 mils/ft (0.8 mm/m).

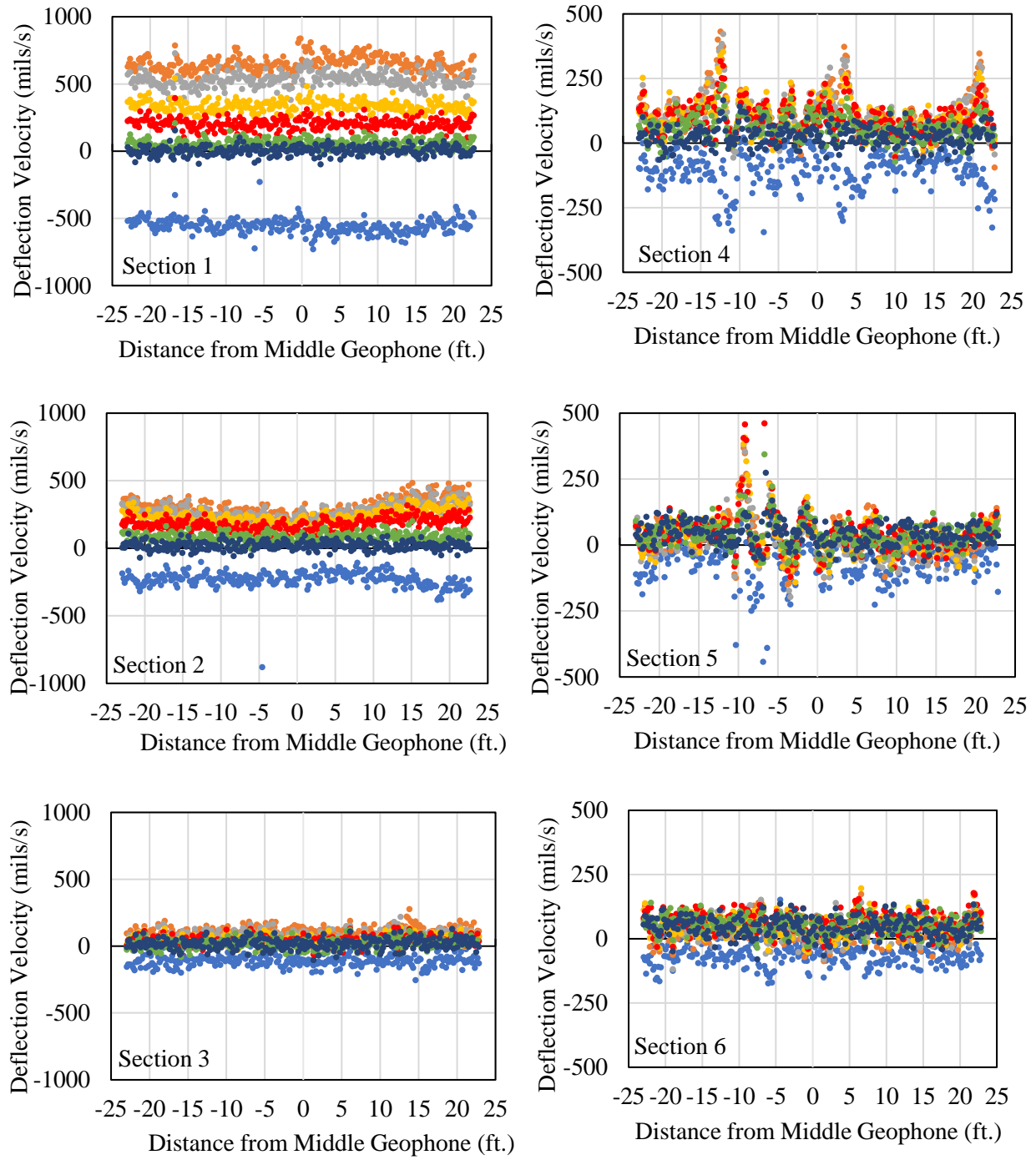


Figure 5.2: TSD deflection measurements in MnROAD test sections.

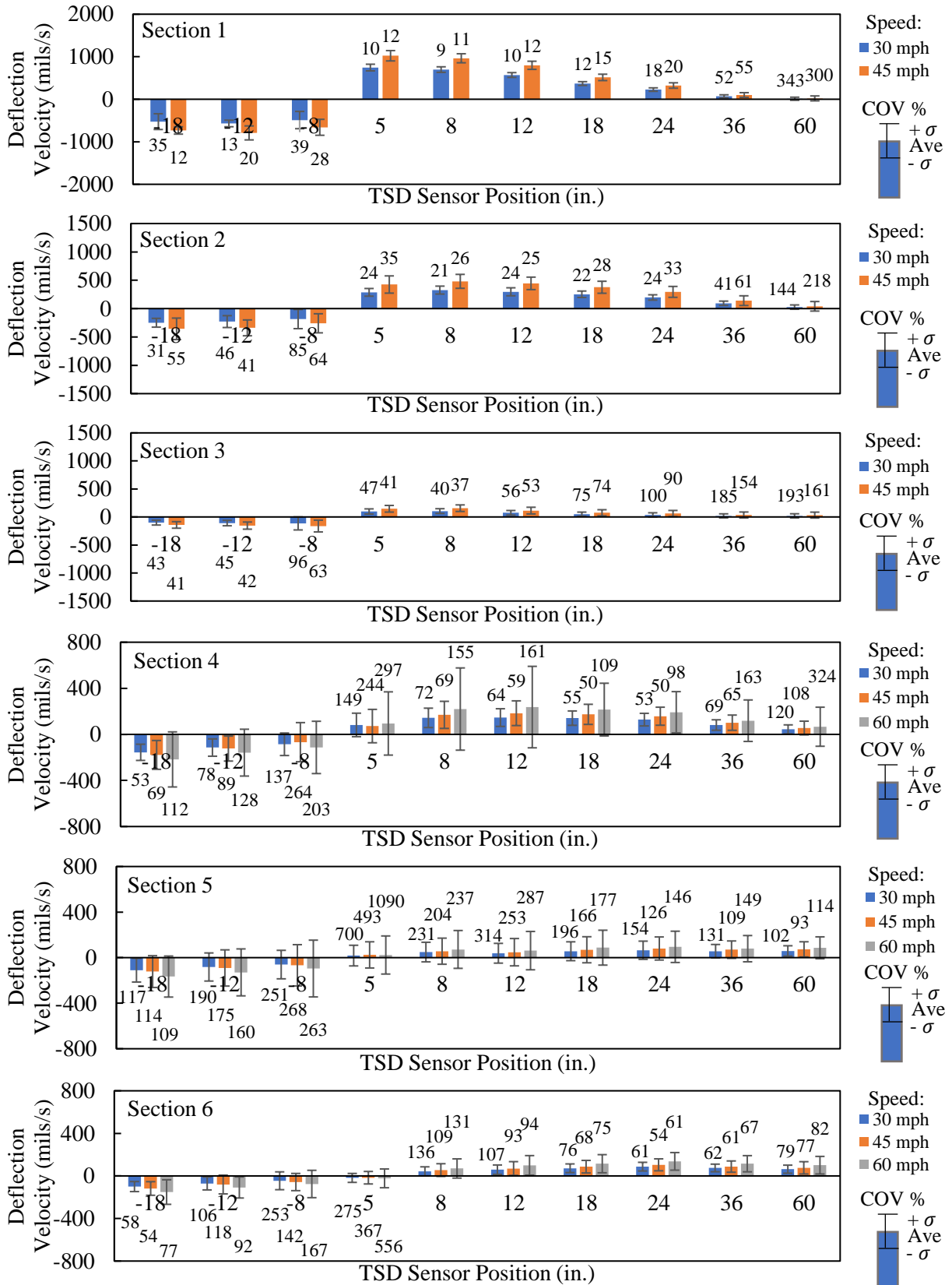


Figure 5.3: Variability of TSD deflection measurements in MnROAD test sections for 2 in. (50 mm) data interval.

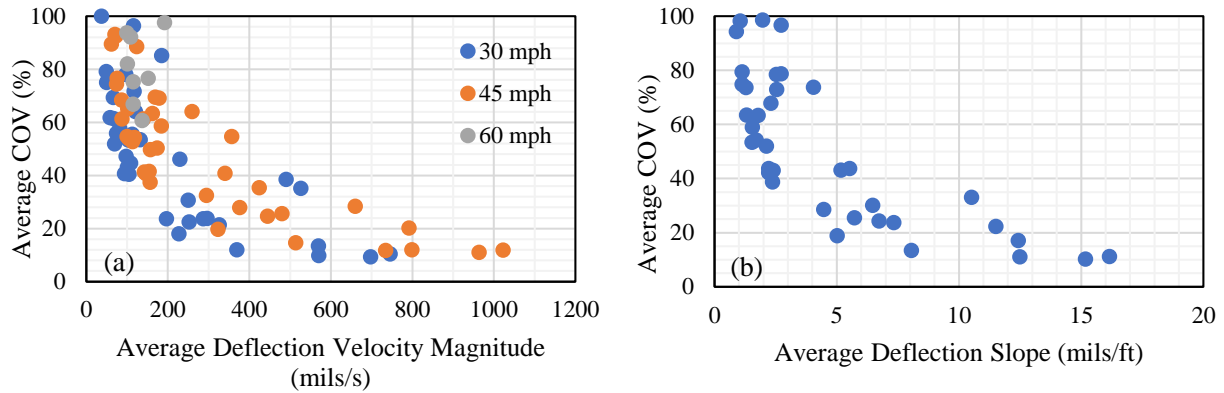


Figure 5.4: Variations of COV with the magnitude of a) TSD deflection velocity and b) TSD deflection slope, for 2 in (50 mm) data interval.

#### EFFECT OF SPATIAL AVERAGING OF DATA (DATA INTERVALS)

To examine the impact of data averaging, the deflection velocities that were originally collected at 2 in. (50 mm) intervals were averaged over intervals of 3.3 ft (1 m) for all TSD sensors. As shown in Figure 5.5, the averaged deflection velocities exhibit less dispersion of data for all test sections and a substantially smaller number of outliers are evident in comparison to deflection velocities with averaging intervals of 2 in. (50 mm). However, the level of noise superimposed on the signal of TSD deflection velocities is still dependent on the pavement type and stiffness.

As shown in Figure 5.6, the COVs of deflection velocities averaged at every 3.3 ft (1 m) decreased significantly when compared to the 2 in. (50 mm) data. The decreases in the COVs of the sensors with larger deflection velocities are more pronounced. Although the difference in the COVs of the flexible pavements and the stiffer rigid or composite pavements reduced with averaging the data for every 3.3 ft (1 m), still notably higher variability was observed in Sections 4, 5, and 6 compared to Sections 1, 2 and 3. Additionally, while averaging data generally decreased the variability of the measurements, the COVs of the data obtained in Sections 4, 5, and 6 at many

sensors still exceeded 50%. The impact of change in vehicle speed on the variability of the sensors' data decreased with an increase in data interval to 3.3 ft (1 m) for all test sections. However, the changes in the COVs of the sensors' data at a particular section did not show a constant trend with change in speed.

Similar to 2 in. (50 mm) interval data, the farther sensors' data had higher COVs for the 3.3 ft (1 m) interval data in flexible pavements of Section 1, 2, and 3, while in stiffer pavements of Section 4, 5 and 6 the data of the sensors closer to the tire load exhibited larger COVs compared to the farther ones. The increase in stiffness from Section 1 to 3 or from the first three flexible pavements to the stiffer pavements of Sections 4, 5, and 6 still increased the variability of the sensors data. A comparison of the statistical parameters of all six test sections indicates that still an increase in pavement overall stiffness results in higher variability for 3.3-ft (1-m) data.

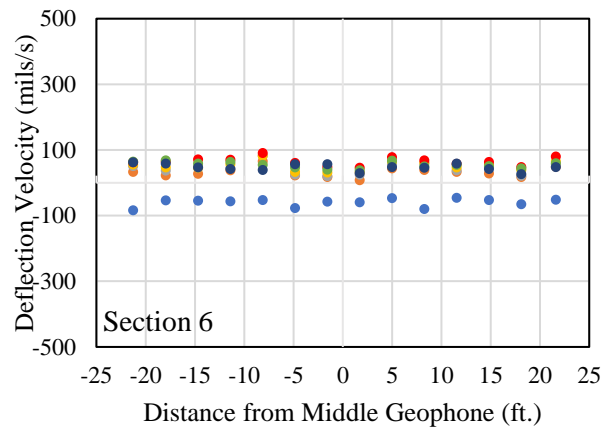
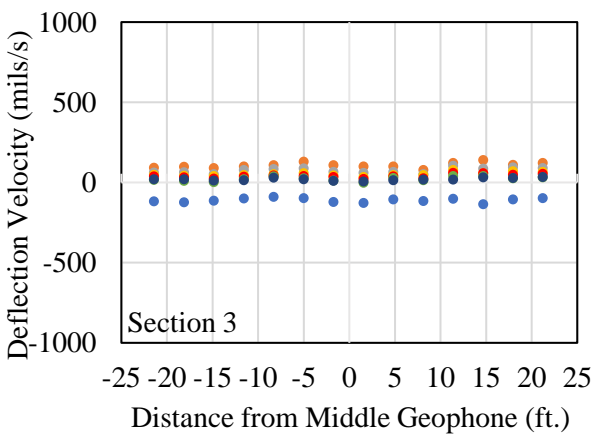
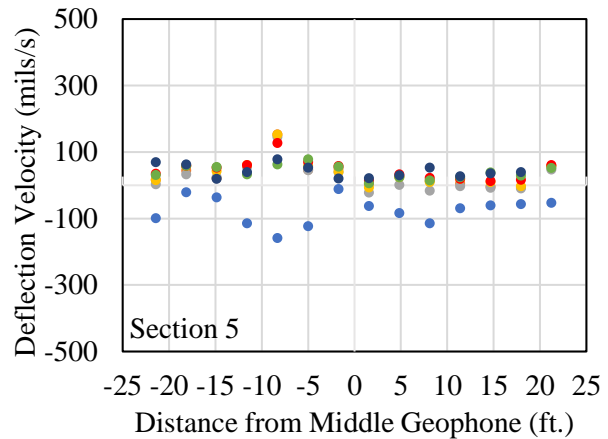
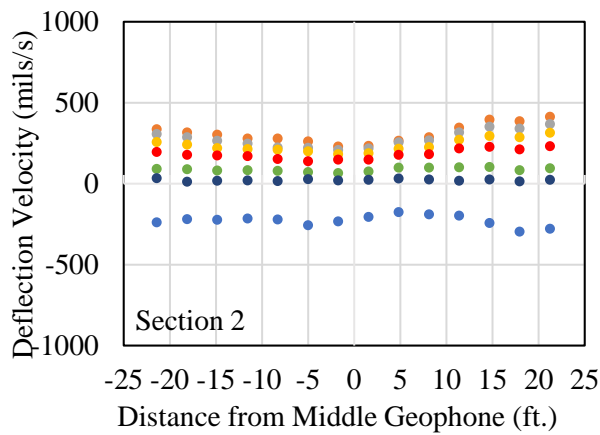
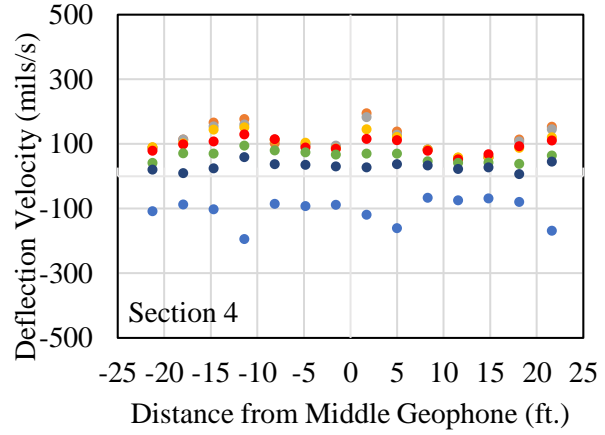
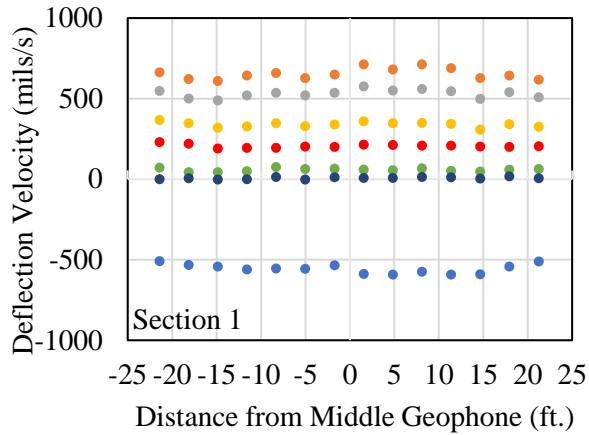


Figure 5.5: TSD deflection measurements in Low Volume Road and Main-Line sections for 3.3 ft (1 m) data interval.

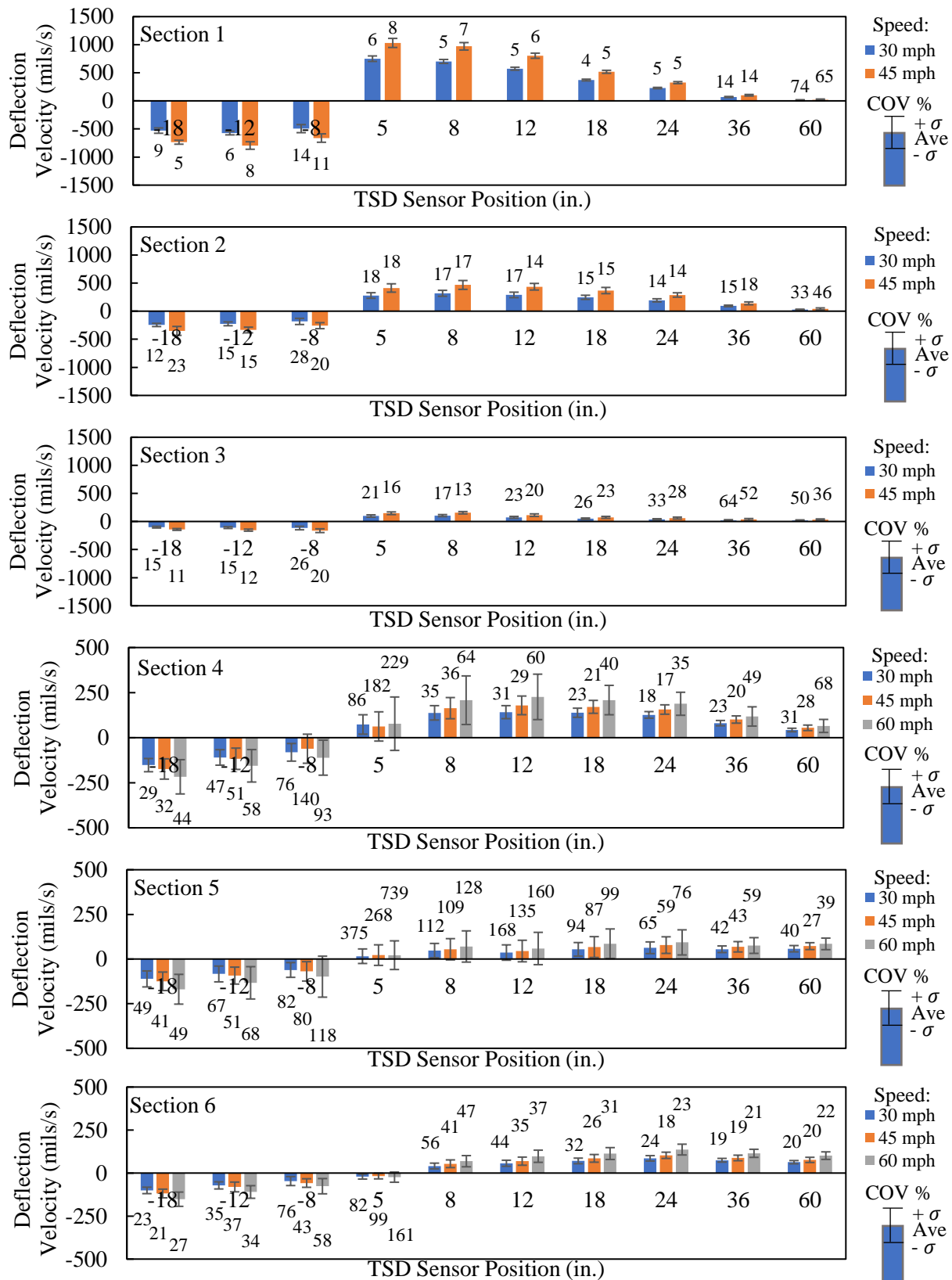


Figure 5.6: Variability of TSD deflection measurements in MnROAD test sections for 3.3 ft (1 m) data interval.

The variability of the deflection velocities in terms of average COV of all TSD sensors at different speeds for all test sections is plotted against their corresponding average deflection velocities for 3.3 ft (1 m) data in Figure 5.7.a. The COV increases with a decrease in deflection velocity in a manner similar to the data reported at 2 in. (5 mm) intervals in Figure 5.6.a. Again, the overall variability seems to increase with the increase in vehicle speed. In this case, COVs of less than 20% are generally observed for deflection velocities greater than about 200 mils/s (5 mm/s) which is remarkably smaller compared to the same value when dealing with 2 in (5 mm) data, 600 mils/s (15 mm/s).

As shown in Figure 5.7.b, the variability of the deflection slopes increases as the deflection slope decreases. To maintain measurements within a COV of 20%, the deflection slopes should be greater than 4 mils/ft (0.3 mm/m) which again is less in comparison with that of the data with intervals of 2 in. (5 mm).

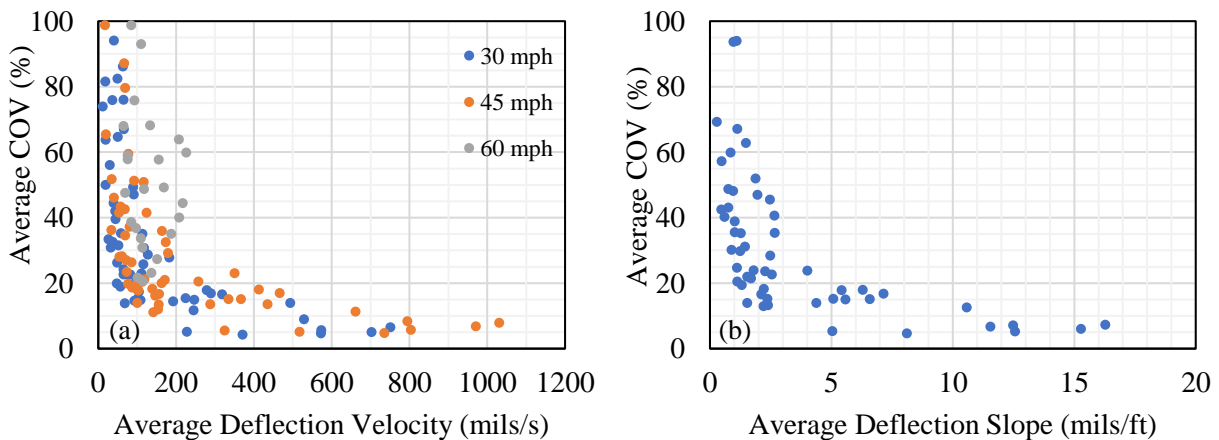


Figure 5.7: Variations of COV with the magnitude of a) TSD deflection velocity and b) TSD deflection slope, for 3.3 ft (1 m) data interval.

## EFFECT OF VEHICLE SPEED ON THE TDS DATA

To evaluate the effects of the device operating speed on the pavement responses, the average deflection slopes corresponding to 45 mph and 60 mph (72 km/hr and 96 km/hr) at each TSD sensor location are plotted against the corresponding average deflection slopes of 30 mph (48 km/hr) in Figure 5.8. The best-fitted line exhibits a slope of 0.99 which means that in the ranges of speed studied the viscoelasticity of the materials is not apparent.

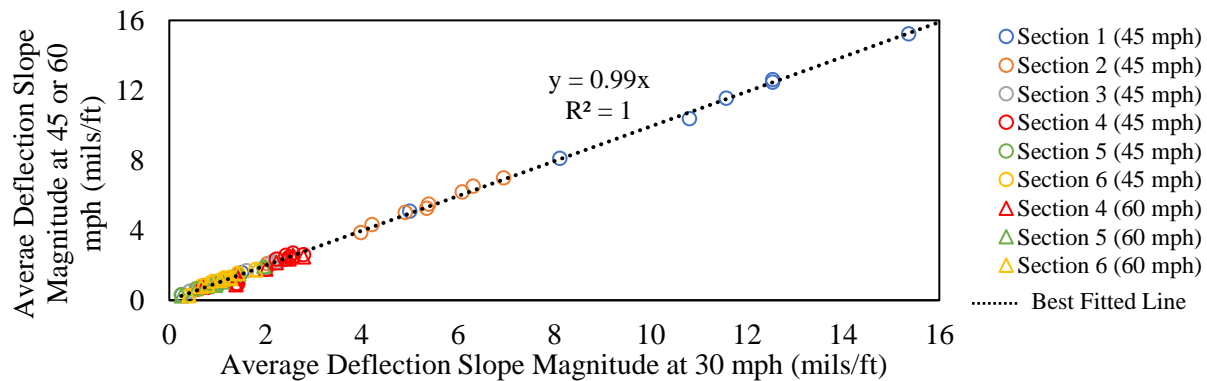


Figure 5.8: Deflection slopes obtained by TSD at different operating speeds vs. deflection slopes at 30 mph (48 km/hr).

### Conclusion

In this study, the impact of different factors such as operating speed, pavement structural condition, and intervals of data averaging on the variability of the data collected by TSD was investigated. For this purpose, experimental data collected at six pavement test sections in the MnROAD facility was used. The test sections covered a wide range of structural properties and different pavement types. The analysis of the effect of the pavement type on the variability of the TSD measurements showed that the higher pavement stiffness which led to smaller pavement responses resulted in higher variability of the deflection velocities measured by the TSD sensors. Compared to less stiff sections (Sections 1 through 3), the sections with rigid pavements or stiffest

flexible pavements (Sections 4 through 6) experienced notably higher COVs where they exceeded 100% for almost all TSD sensors. The magnitude of the collected deflection velocities and corresponding COVs exhibited an inverse relationship. The COV of less than 20% corresponded to deflection velocities and deflection slopes greater than about 600 mils/s (15 mm/s) and 10 mils/ft (0.8 mm/m), respectively. The lower deflection velocities corresponded to the measurements made with sensors located farther away from the tire loading or measured at test sections with stiffer pavements.

To analyze the effect of the spatial data averaging on the collected TSD data, deflection velocities were averaged at every 3.3 ft (1 m). The averaged deflection velocities showed significantly smaller COVs compared to the 2 in. (50 mm) data. The decreases in the COVs of the sensors with larger deflection velocities were more pronounced. Although a notable decrease in the COVs was observed with data averaging, the increase in stiffness of the pavements still increased the variability of the sensors data. For the data averaged at every 3.3 ft (1 m), COVs of less than 20% were generally observed for deflection velocities and deflection slopes greater than about 200 mils/s (5 mm/s) and 4 mils/ft (0.3 mm/m), respectively. These limits were remarkably smaller compared to the same value when dealing with 2 in (5 mm) data,

To evaluate the effects of the vehicle speed on the pavement responses, the average deflection slopes corresponding to 45 mph (72 km/hr) and 60 mph (96 km/hr) at each TSD sensor were compared with average deflection slopes of 30 mph (48 km/hr). The results showed that the change of speed from 30 mph (48 km/hr) to 45 mph (72 km/hr) and 60 mph (96 km/hr) did not have a notable impact on the average deflection slopes while seems to increase the COVs associated with average deflection velocities.

## References

- Andersen, S., Levenberg, E., & Andersen, M. B. (2017). Inferring pavement layer properties from a moving measurement platform. In 10th International Conference on the Bearing Capacity of Roads, Railways and Airfields (pp. 675-682). Taylor & Francis.
- Andr n, P. (1999, January). High-speed rolling deflectometer data evaluation. In Nondestructive Evaluation of Aging Aircraft, Airports, and Aerospace Hardware III (Vol. 3586, pp. 137-147). International Society for Optics and Photonics.
- Elseifi, M., Abdel-Khalek, A. M., & Dasari, K. (2012). Implementation of Rolling Wheel Deflectometer (RWD) in PMS and Pavement Preservation (No. FHWA/11.492). Louisiana Transportation Research Center.
- Elseifi, M. A., & Zihan, Z. U. (2018). Assessment of the Traffic Speed Deflectometer in Louisiana for Pavement Structural Evaluation (No. FHWA/LA. 18/590). Louisiana Transportation Research Center.
- Flintsch, G. W., Ferne, B., Diefenderfer, B., Katicha, S., Bryce, J., & Nell, S. (2012). Evaluation of traffic-speed deflectometers. *Transportation research record*, 2304(1), 37-46.
- Hildebrand, G; Rasmussen, S. (2002): Development of a High Speed Deflectograph. (Report 177) Danish Road Institute.
- Kannemeyer, L., Lategan, W., and McKellar, A. (2014). Verification of Traffic Speed Deflectometer Measurements using Instrumented Pavements in South Africa. *Pavement Evaluation 2014*, Blacksburg, VA.

- Katicha, S. W., Flintsch, G. W., & Ferne, B. (2013). Optimal averaging and localized weak spot identification of traffic speed deflectometer measurements. *Transportation research record*, 2367(1), 43-52.
- Katicha, S., Flintsch, G., & Diefenderfer, B. (2022). Ten Years of Traffic Speed Deflectometer Research in the United States: A Review. *Transportation Research Record*, 03611981221094579.
- Rada, G. R., Nazarian, S., Visintine, B. A., Siddharthan, R., & Thyagarajan, S. (2016). Pavement structural evaluation at the network level: final report. Washington, DC: US Federal Highway Administration Report FHWA-HRT-15-074.
- Steele, D., Hall, J., Stubstad, R., Peekna, A., & Walker, R. (2002). Development of a high-speed rolling wheel deflectometer. In Pavement Evaluation Conference, 2002, Roanoke, Virginia, USA.
- Xiao, F., Xiang, Q., Hou, X., & Amirkhanian, S. N. (2021). Utilization of traffic speed deflectometer for pavement structural evaluations. *Measurement*, 178, 109326.
- Zofka, A., Graczyk, M., & Rafa, J. (2015). Qualitative evaluation of stochastic factors affecting the Traffic Speed Deflectometer results. In *Transportation Research Board 94th Annual Meeting Washington DC*.

# CHAPTER 6. PRACTICAL PROCESS FOR VERIFICATION OF TRAFFIC SPEED DEFLECTOMETER MEASUREMENTS

## Abstract

The limitations of the Falling Weight Deflectometer (FWD) as a stationary device to obtain pavement responses have led to the development of traffic speed deflection devices (TSDDs) that can measure pavement responses at traffic speeds. Recent research studies have shown the usefulness and applicability of TSDDs in support of the network-level pavement management process of the highway network. There is a strong need to develop a practical procedure to verify the results of the TSDDs and ensure the accuracy and precision of the measurements in a rigorous, yet timely manner. One logical method of verifying the TSDDs' measurements can be through comparison with widely accepted FWD measurements. Because of the fundamental differences in FWD and TSDD measurements, practical relationships are needed to relate the two sets of data. This paper presents relationships for the verification and interpretation of the Traffic Speed Deflectometer (TSD) data. To achieve this goal, Artificial Neural Network (ANN) models for different pavement types and properties, and vehicle speeds were developed to relate TSD and FWD results. To establish the ANN models, an extensive database comprising different flexible pavement sections was developed using the pavement responses obtained from a series of numerical simulation models. Field experiment results were then compared with the corresponding ANN-estimated values to verify the TSD measurements. The results showed that the TSD deflection measurements were within a level of uncertainty of about 20% of the ANN estimated values.

**KEYWORDS:** Traffic Speed Deflection Device, Falling Weight Deflectometer, Pavement Response, Artificial Neural Network.

## Introduction

State Highway Agencies (SHAs) have traditionally relied on pavement surface conditions (e.g., roughness and distress) to characterize the overall condition of their pavement network and assess their maintenance and rehabilitation (M&R) needs. Ignoring the structural condition can cause less than optimal treatment selection at the network level since the correlation between the surface condition and the structural condition is weak (Flora 2009, Bryce et al. 2012). Incorporating the structural and surface conditions into the pavement management decision-making process can lead to better-informed and more cost-effective decisions (Ferne et al. 2013, Zaghoul et al. 1998, Steele 2015).

Several SHAs have used Falling Weight Deflectometer (FWD) measurements to enhance their network-level pavement management processes (Flintsch and McGhee 2009, Katicha et al. 2013). The limitations of the FWD for the network-level structural condition assessment have led to several studies focused on investigating the feasibility of using TSDDs for that purpose (Rada and Nazarian 2011, Stokoe et al. 2012, Elseifi et al. 2012, Flintsch et al. 2013, Rada et al. 2016, Katicha et al. 2017 and Katicha et al. 2020).

TSDDs are moving measurement platforms that collect surface deflections near traffic speeds and can cover up to 400 miles/day (650 km/day) without disrupting the normal flow of traffic (Elseifi et al. 2011, Flintsch et al. 2013, Steele et al. 2020). Numerous studies have assessed the performance of TSDDs, and how to best interpret and use the data collected by them for routine pavement structural evaluation for project-level pavement engineering and network-level asset management (Rada and Nazarian 2011, Flintsch et al. 2013, Rada et al. 2016, Elseifi and Elbagalati 2017).

One popular TSDD, the Traffic Speed Deflectometer (TSD), is a device that has been used worldwide. The TSD applies a load to the pavement via the trailer's rear axle dual wheel assembly as schematically depicted in Figure 6.1, while Doppler laser sensors capture the deflection-velocity profile of the pavement surface.

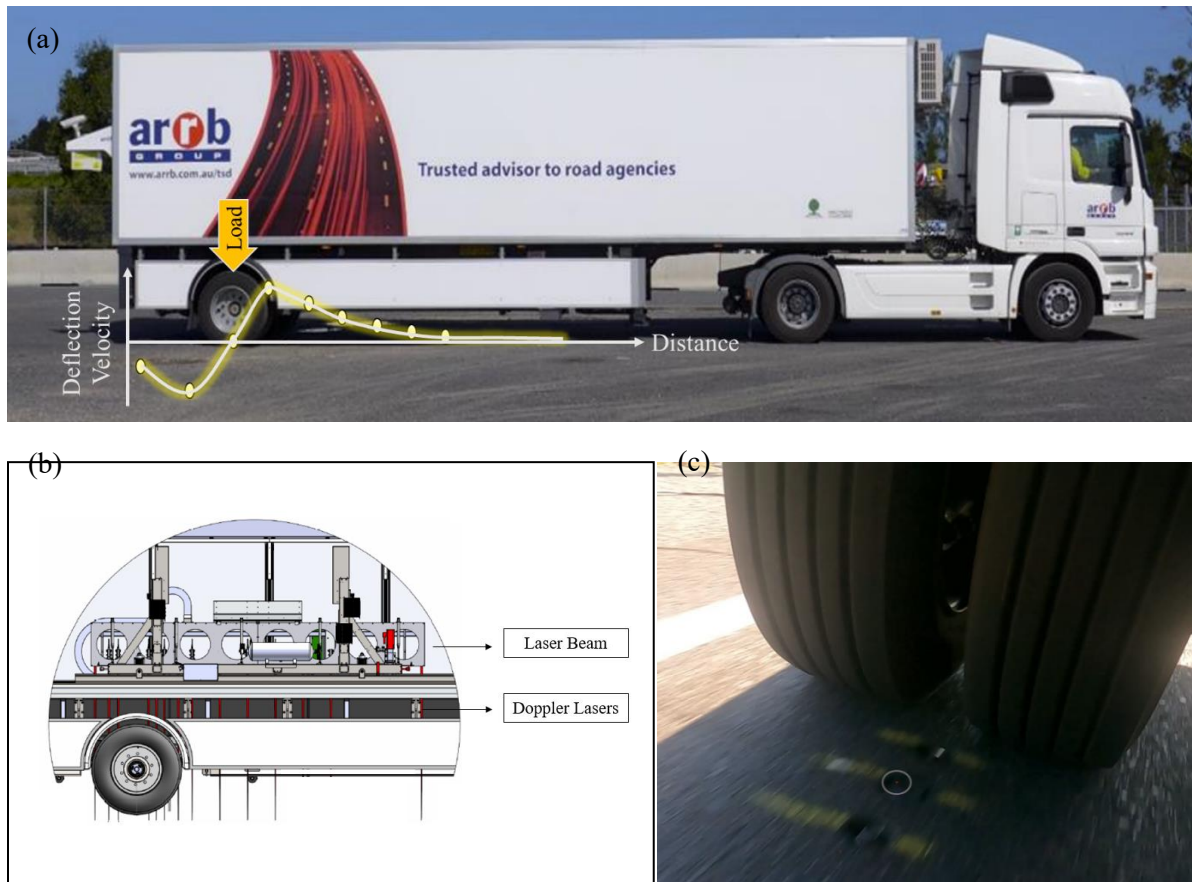


Figure 6.1: TSD load and laser configuration, (a) Schematic of loading by rear axle right dual tires and deflection velocity curve provided by lasers (Hasanuzzaman and Ives 2016), (b) laser beam between the dual tires and Doppler lasers (Katicha et al. 2017), and (c) Doppler laser reflection on pavement surface.

Several research efforts have shown the usefulness and applicability of TSDs for evaluating pavement structural conditions (Rada and Nazarian 2011, Flintsch et al. 2013, Rada et al. 2016,

Elseifi and Elbagalati 2017). Aside from the calibration of the TSD following the manufacturer's process, no accepted or convenient procedure for the verification and validation of TSD measurements exists. The most rigorous way to achieve this is via embedding sensors into pavements to directly compare the output of the TSD with the response of embedded sensors (Rada et al. 2016). One less rigorous but pragmatic method of verifying the TSDs' measurements can be through comparison with widely accepted FWD measurements. The underlying differences between TSD and FWD in terms of the type of loading, load contact area, pavement response measurement technology, and the method to estimate pavement deflections, should be rigorously considered in this comparison.

FWD records the vertical deflection bowl at several discrete locations due to an impact on its loading plate placed on the pavement surface, while TSD reports the surface deflection velocity at several discrete points as it moves over the pavement section. Because of the stationary and discrete nature of the FWD data against the dynamic nature of the TSD data, the number of the surveyed points along a length of a pavement by FWD and TSD and their specific locations can be different. Since the responses measured by the two devices are not the same, it would be difficult to obtain a "straightforward universal" relationship between TSD and FWD measurements (Saremi 2018). Hence, a method is needed to post-process the FWD data obtained in the field in a way that can be comparable to TSD measurements. For this purpose, the development of relationships between the two devices' primary measurements or post-processed parameters is required to calculate TSD's equivalent response to the experimental FWD's measurement. The equivalent TSD response can then be compared to the measured TSD deflection-velocity profile to verify the TSD measurements.

Many studies have attempted to determine correlations between the two devices' measurements. Katicha et al. (2014) converted the TSD and FWD measurements to the Structural Curvature Index (SCI) and the Base Damage Index (BDI). They concluded that the relationships between the calculated SCI and BDI from the two devices were reasonably close to the line of equality, with a significant variation and a bias in those relationships. Different studies have developed relationships from numerical simulation to estimate FWD deflections from TSD measurements utilizing genetic programming based on a symbolic regression approach (Saremi 2018) or mathematical models (Chai et al. 2016). Based on data from 16 flexible pavements, Elbagalati et al. (2018) developed an ANN model to estimate FWD deflection basins from TSD deflections. Zihan et al. (2020) also utilized ANN to calculate FWD deflections from layer moduli, thicknesses, and TSD measurements. Using 162 pavement sections, Abohamer et al. (2021) developed an ANN model to estimate FWD deflections, which was trained using TSD deflections and some deflection-based indices from pavement sections in Louisiana. Although the model estimated FWD with an  $R^2$  of 0.99, it needed the conversion of TSD-obtained data (deflection velocity) to vertical deflections which are not trivial (Saremi 2018).

To address the limitations of the previous studies, in this study, data from field test sections was used to validate the numerical models developed. A comprehensive database simulated with the validated models was also deployed to establish the relationships between FWD and TSD responses, which serve as the basis for the verification of TSD measurements in this research. Although many structural factors such as pavement layer moduli, thickness, and other relevant structural characteristics, have an impact on the pavement responses from TSD or FWD, it is not always feasible to obtain all desired structural parameters in real practice. Hence, the number of input parameters used in ANN models should be optimized and representative parameters should

be selected to develop an efficient yet robust model to estimate the TSD responses. As the layer moduli are mostly unknown in roadways, especially at the network level, the ANN models proposed in this study were developed in such a manner that eliminates the need to incorporate this parameter in the analysis algorithm. Another major enhancement of the ANN models developed in the current study is that the deflection velocities directly measured by TSDs at different laser positions are used in the models, and hence, there is no need to convert the raw data recorded by TSD to a secondary parameter or to calculate the deflection-based indices.

### **Objective**

The objective of this research is to devise a robust and rapid verification procedure for TSD measurements by comparing the TSD deflection-based measurements with those obtained from FWD. The proposed approach is based on both numerical simulation and field-testing efforts to cross-validate the analysis results. To achieve such a purpose, models using machine-learning techniques were developed to establish FWD-TSD relationships. In particular, this study made use of ANN to develop models to relate the measurements of the two NDT devices while overcoming the complications posed by the distinct nature of the measurements.

### **Methodology**

Figure 6.2 illustrates the flowchart of the methodology for the development of the verification procedure of TSD measurements devised in this study. The approach consisted of three major components: (1) field data collection, (2) numerical simulation modeling and validation, and (3) the development of ANN models to establish the FWD-TSD relationships. Multiple pavement test sections with varying structural properties were designated for test conduction. At each section, FWD tests were conducted at various points to obtain the vertical deflection basins induced under FWD plate loading. Several runs of TSD tests were also conducted at the same

pavement sections at different speeds, i.e., 30 mph, and 45 mph (48 km/hr, and 72 km/hr, respectively) to obtain the deflection velocity profiles of the pavement surface at 2 in. (50 mm) intervals.

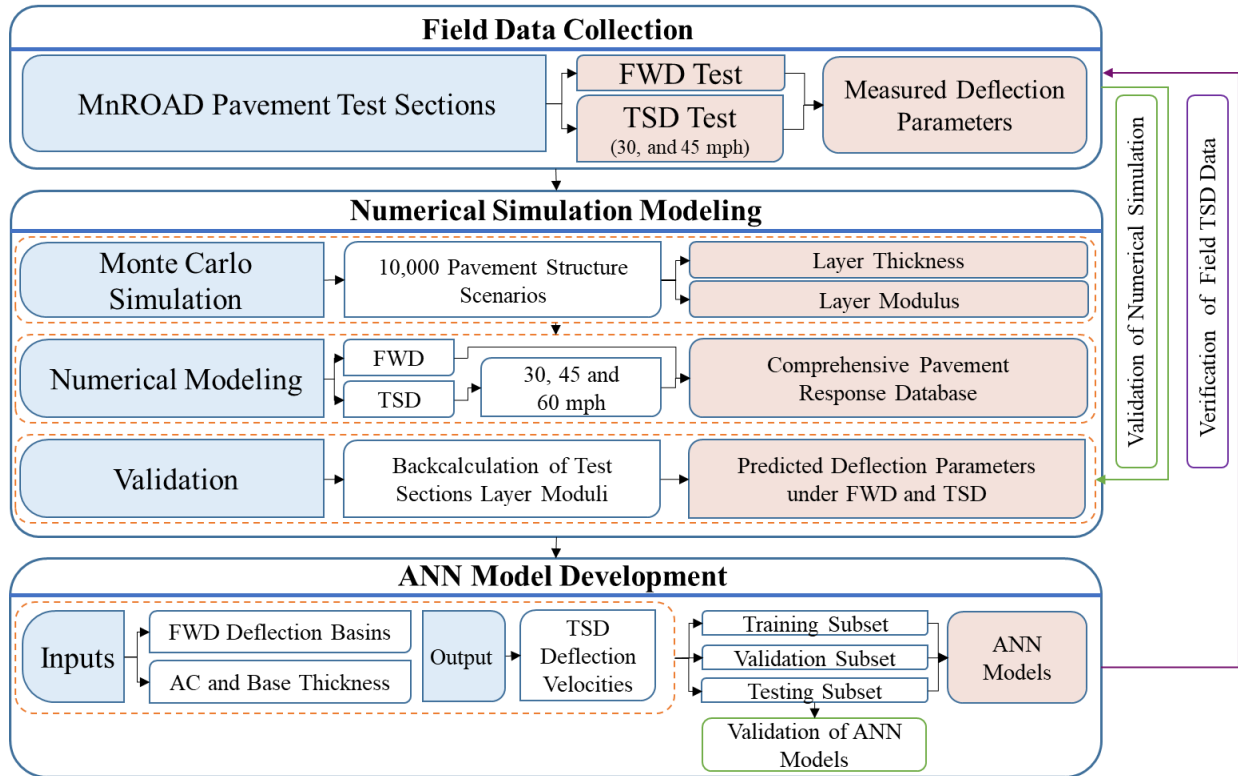


Figure 6.2: Flowchart of research methodology.

To begin the numerical simulations, 10,000 random pavement structures with varying uniformly distributed thicknesses and layer moduli were generated using the Monte-Carlo simulation (MCS) technique to cover a wide variety of structural properties. A comprehensive database of pavement responses under FWD load and different speeds of TSD was built to establish FWD-TSD relationships. To build confidence in the results of the numerical models, the estimated test sections' results were cross-validated with the deflection parameters measured by FWD and TSD tests in the field. For this purpose, test sections' layer information, i.e., layer thicknesses from the construction maps and backcalculated layer moduli based on FWD deflection

basins in the field, was used to simulate the test sections under FWD and TSD loading, and the numerical responses were compared with the experimental data from tests conducted at MnROAD sections.

The comprehensive pavement response database developed in the previous stage was utilized to establish ANN models to convert FWD deflections to the corresponding TSD measurements. This means that ANN models developed in this study can estimate TSD deflection velocities corresponding to the FWD deflection basins and layer thicknesses. The ANN-estimated deflection velocities of the TSD sensors can then be compared to the TSD data collected in the field to verify them. Ultimately, the TSD data obtained at the MnROAD test sections were verified by the proposed ANN models.

#### **FIELD DATA COLLECTION**

A series of field experiments were carried out at the MnROAD facility operated by the Minnesota Department of Transportation. This facility was selected since it provided a multitude of test sections with different structural characteristics in one location. Three pavement test sections with different strength parameters were selected to account for the potential effect of the pavement properties on the measurements. The relevant information on the layer thickness and structural capacity of the three pavement sections is provided in Table 6.1. Structural capacity was determined based on the measured  $SCI_{12}$  (the difference between FWD deflections at zero and 12 in. (300 mm) from the center of the load) and subjectively classified as Weak, Fair, or Strong.

Table 6.1: MnROAD Pavement Test Sections.

<b>Pavement Section</b>	<b>Strength</b>	<b>Asphalt Thickness (in.)</b>	<b>Base Layer Thickness (in.)</b>	<b>SCI<sub>12</sub> (mils)</b>
<b>1</b>	Weak	4.0	16	23.7
<b>2</b>	Fair	3.5	15	13.0
<b>3</b>	Strong	3.5	12	4.2

Each test section was instrumented with geophones to record the pavement response time history under the moving load of TSD. At each test section, in addition to FWD tests, several runs of TSD at operational speeds of 30 mph (48 km/hr) and 45 mph (72 km/hr) were conducted to account for the potential effects of vehicle speed on the measurements. FWD tests were conducted at a nominal load of 10 kips (45 kN) on a 6 in. (152 mm) diameter plate that exerted nominally a 90 psi (550 kPa) pressure to the surface. At each test section, FWD tests were conducted every 3.3 ft (1 m) at up to 13 locations. The TSD data were nominally recorded at every 3.3 ft (1 m) over a distance of 40 ft (12 m).

Figure 6.3 shows a sample plot of the deflection velocity values associated with the embedded geophones and a TSD pass at 45 mph for Section 1. The plot includes the data points showing the average of the TSD deflection velocities of each TSD laser sensor collected at every 3.3 ft (1 m) along the test section, as well as the curve showing the variation of the average responses obtained by geophones when TSD has passed over them. The error bars also show the standard deviation of the TSD measurements along the test section. The TSD and geophone deflection velocities are in good agreement. However, the average deflection velocities associated with the TSD sensors at 5 in. to 12 in. from tire load have more deviation from the geophone data compared to other TSD sensors.

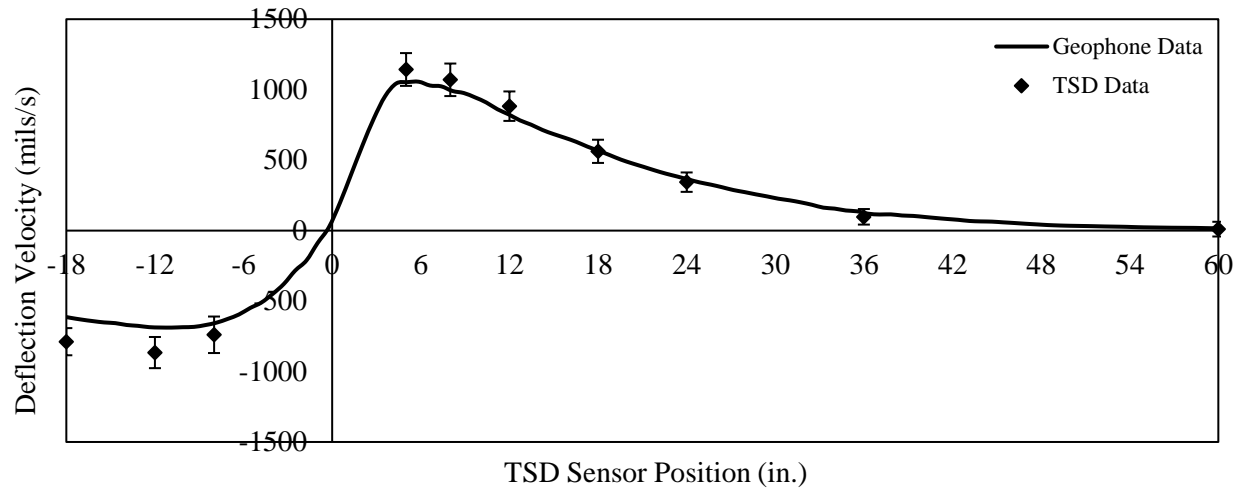


Figure 6.3: TSD collected data vs. geophones obtained data averaged at each TSD sensor position for Section 1 at 45 mph (72 km/hr).

The TSD and FWD measurements were further incorporated into the analysis algorithm devised in this study to (1) validate the numerical simulation results obtained from a finite layer software (3D-Move analysis software by the University of Nevada, Reno (UNR)), and (2) ensure that the TSD data measured in the field are in agreement with the values calculated using the verified ANN models.

#### NUMERICAL SIMULATION MODELING

Since assembling an extensive field-testing database that can lead to FWD-TSD relationships is not practical, numerical simulation techniques were used to develop the required database. Assembling the comprehensive numerical modeling database started with randomly generating pavement sections with various layer thicknesses and moduli, using MCS techniques. These pavement structural properties were generated based upon a uniform distribution function defined in MATLAB with the set forth limits associated with each parameter, as indicated in Table 6.2. The pavement structure was regarded as a flexible pavement consisting of an asphalt concrete

(AC) layer over an unbound aggregate base constructed over subgrade soil. These pavement properties were used as inputs in the numerical simulation models of 3D-Move software. The pavement responses, including the FWD deflection basin and TSD deflection velocity profile, were compiled into the database. 10,000 pavement scenarios were included in the developed database to simulate the FWD loading conditions. Furthermore, three different operational speeds for TSD, i.e., 30 mph, 45 mph, and 60 mph (48 km/hr, 72 km/hr, and 96 kph, respectively) were considered in the numerical simulation matrix, yielding a total of 30,000 numerical permutations (i.e., 10,000 cases at each TSD speed).

Table 6.2: Range of Layer Thicknesses and Material Properties for Numerical Modeling.

<b>Pavement Type</b>	<b>Values</b>	<b>AC Thickness (in.)</b>	<b>Base Thickness (in.)</b>	<b>AC Modulus (ksi)</b>	<b>Base Modulus (ksi)</b>	<b>Subgrade Modulus (ksi)</b>
Flexible Pavement on Unbound Aggregate Base	Minimum	1	6	300	5	4
	Maximum	12	18	700	85	45

### **FWD and TSD Simulation**

The FWD device was simulated as a circular plate applying a 10,000 lb. (45 kN) load that exerted a 90 psi (550 kPa) contact pressure on the pavement surface similar to the FWD utilized in the field. The FWD vertical deflections at sensor locations with the same distance from plate loading as the TSD sensors were obtained from the numerical simulations. Prominent features attributed to the TSD device, i.e., loading configuration, and sensor arrangement, closely resembled the only TSD available in the US at the time of this study for a more realistic simulation.

Figure 6.4 schematically shows the rear axle right dual tires spaced 13 in. (330 mm) apart, coupled with the Doppler laser sensors configuration considered in the numerical simulation phase of this study. Nominal tire pressure of 120 psi (827 kPa) with a load of 5200 lbs (2350 kg) per tire was simulated. The TSD truck housed three sensors behind the tire and eight sensors ahead of the tire at different distances from the center of the two tires. Hence, to replicate the laser sensor arrangements of the TSD truck, the corresponding response points were evaluated, and the respective pavement responses (deflection velocity at each TSD sensor location) were extracted from the numerical analysis.

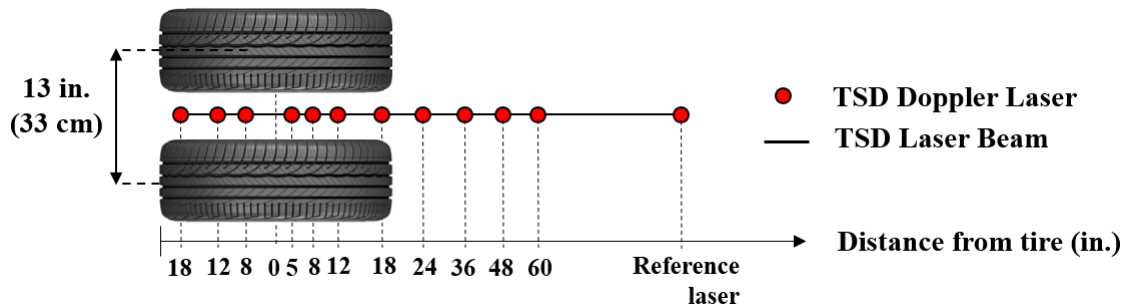


Figure 6.4: TSD axle configuration and instrumented rear axle with Doppler laser sensor configuration.

### Approach to Validate Numerical Simulations

The next step of the analysis pertained to the validation of the numerical simulation models. Figure 6.5 schematically shows the flowchart for validation of the numerical models based on the field data. The moduli of AC, base and subgrade layers were backcalculated using the FWD deflection basins at each test section. The backcalculated layer moduli, as well as the layer thicknesses, were input into 3D-Move software to obtain surface deflection under FWD and deflection velocity under TSD at each sensor location. Ultimately, the FWD and TSD deflection

parameters estimated by 3D-Move models were compared with those recorded by field experiments to validate the numerical models.

### ANN MODELS DEVELOPMENT

ANN models were developed to estimate the TSD responses equivalent to FWD measurements. The TSD responses estimated from the ANN models were in turn compared with the experimental data obtained from TSD tests to verify the data measured in the field. The architecture of the ANN models employed in this study is shown in Figure 6.6. The inputs to the ANN models were the thicknesses of AC and base layers, as well as the FWD-measured deflections at different sensor locations from loading. The outputs comprised of TSD deflection velocities at the same sensor locations as FWD. As the moduli of the layers are not normally available or hard to obtain, they were excluded from the machine learning algorithm to eliminate the need for the tedious and uncertain FWD backcalculation process or core sampling.

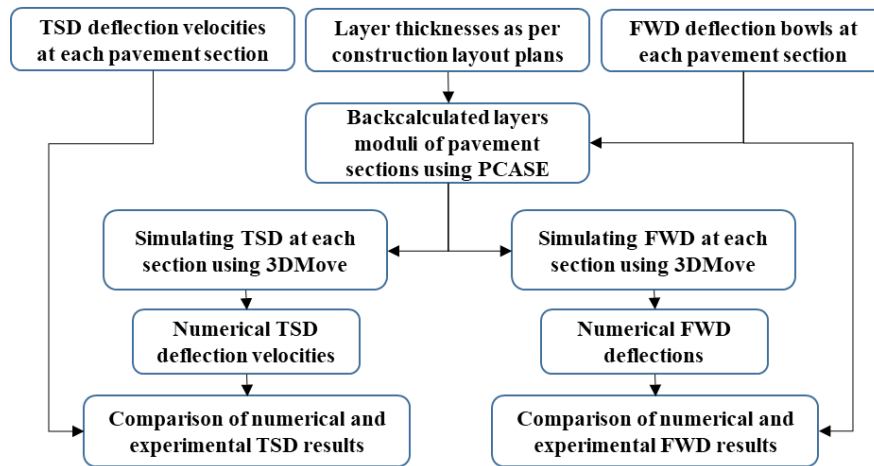
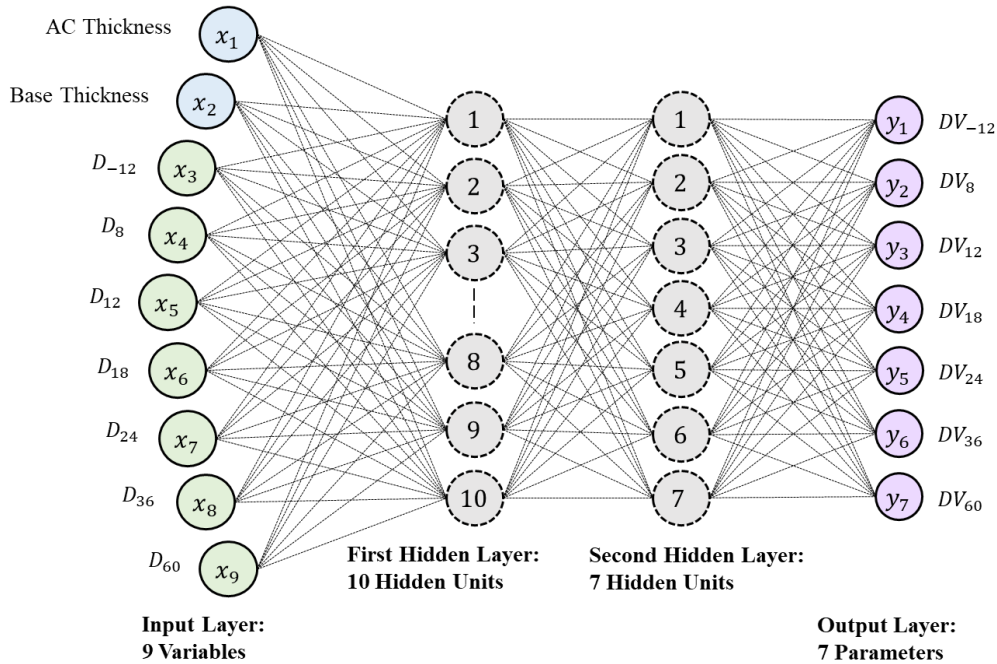


Figure 6.5: Flowchart for 3D-Move models validation.



$D_i$ : FWD measured deflection at the sensor located at  $i$  in. from the load.

$DV_i$ : TSD estimated deflection velocity at the sensor located at  $i$  in. from the load.

Figure 6.6: Architecture of multi-layer ANN model used to relate FWD and TSD data.

A multilayered feed-forward ANN with a Levenberg-Marquardt algorithm (Madsen et al. 2004) was used. The input layer included nine neurons, while the output layer consisted of seven neurons. All ANN models included two hidden layers with ten and seven neurons each. The ANN model was formulated using 10,000 deflection velocity basins. The data were divided into three subsets: 70%, 15%, and 15% for training, validation, and testing, respectively. These percentages were adopted since they resulted in the best performance of the proposed model. The pavement structures in different subsets of training, validation, and testing were selected randomly. To avoid overfitting, the training of the developed ANN model was terminated when the validation error leveled. ANN models were built for three distinct speeds of 30 mph, 45 mph and 60 mph (48 km/hr, 72 km/hr, and 96 km/hr, respectively).

In order to validate the ANN models, the ANN-estimated deflection velocities of the testing subset were plotted against the corresponding numerical TSD deflection velocities. Figure 6.7 shows a sample comparison plot for the ANN model developed for 30 mph (48 km/hr) speed. The ANN-estimated results agreed very well with the numerical responses of the TSD as the slope of the best-fit line through data points was close to one with  $R^2$  and Standard Error of Estimate (SEE) of around 0.99 and 0.1 mils/s (0.0025 mm/s), respectively. The same results were observed for ANN models of other speeds. Overall, the models were able to estimate the numerical TSD responses with  $R^2$  values close to unity and a maximum SEE of less than 1 mils/s (39 mm/s). This indicates that the ANN models could estimate the corresponding numerical TSD deflection parameters well since the uncertainty of the ANN models is several times less than the uncertainty of the TSD measurements.

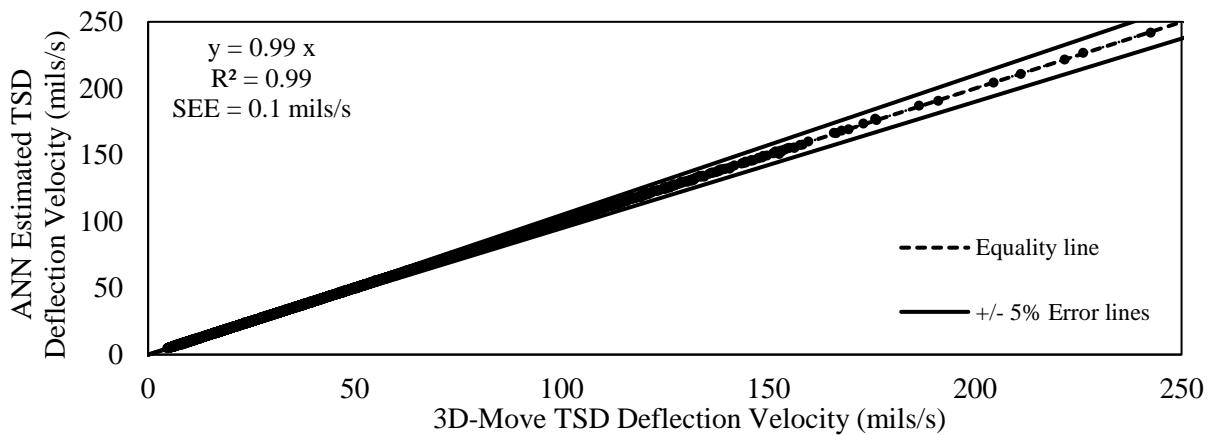


Figure 6.7: ANN estimated VS. numerical analysis calculated TSD deflection velocities for vehicle speed of 30 mph (48 km/hr).

## Results and Discussion

### VALIDATION OF NUMERICAL SIMULATIONS

The numerically estimated and measured FWD deflections for the three pavement sections after the backcalculation process are compared in Figure 6.8. The horizontal uncertainty bars at each data point refer to the standard deviation of the data obtained by FWD at 13 points along each test section. Therefore, the deflections calculated by simulating the pavement sections using backcalculated layer modulus also exhibit standard deviations shown as vertical uncertainty bars. Each data point refers to the deflections at sensor locations of 8 in., 12 in., 18 in., 24 in., 36 in., and 60 in. (215 mm, 300 mm, 450 mm, 600 mm, 900 mm, and 1500 mm) from loading. The data point with the largest deflection value relates to the sensor closest to the load center and increase in sensor offset leads to decrease in the magnitude of the FWD deflections. The numerical results agree well with the field FWD data, as the differences between the estimated and measured deflections are typically within the  $\pm 10\%$  uncertainty lines for all test sections. The backcalculated layer moduli were further used in the validation of numerical models of the three sections.

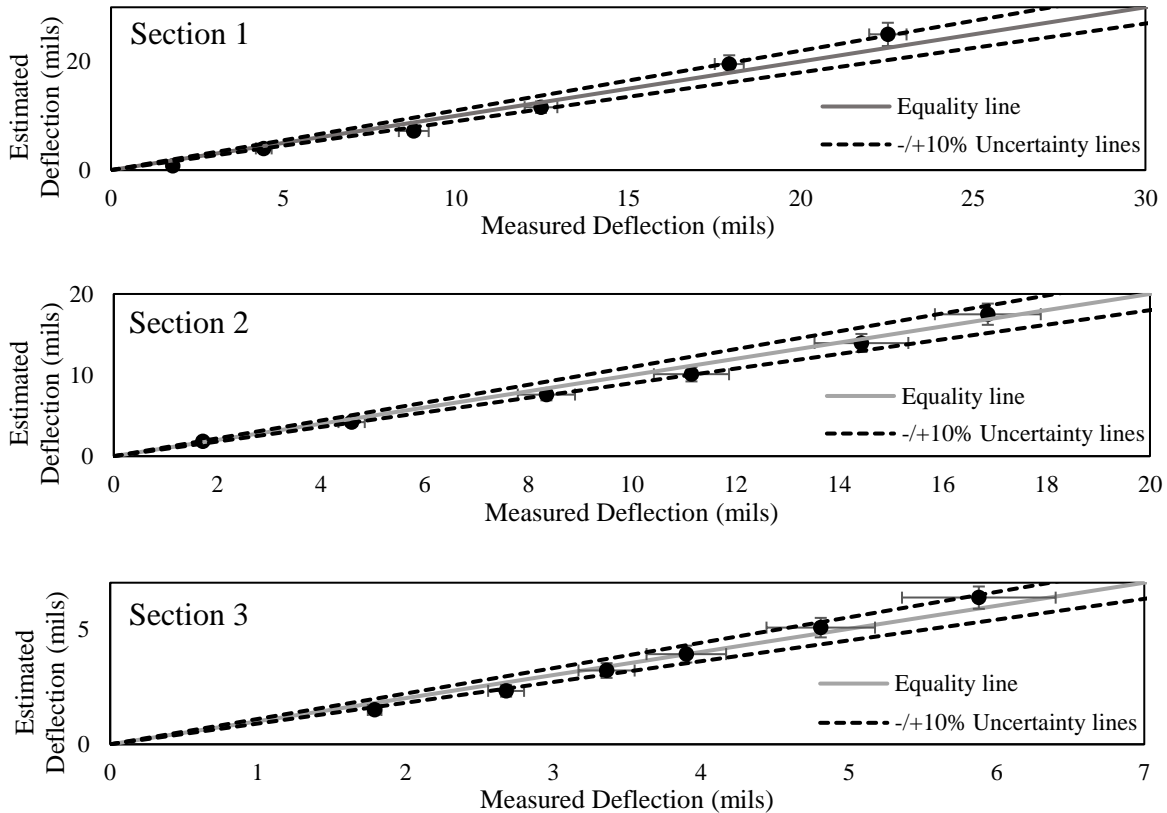


Figure 6.8: Estimated vs. measured FWD deflections at three MnROAD test sections.

Figure 6.9 provides sample results attributed to the comparison of the 3D-Move -estimated and measured TSD deflection velocities for the three pavement test sections **Error! Reference source not found.** The data points and error bars signify the average deflection velocities, and their standard deviations, for the range of TSD deflection velocities measured along the length of the section, respectively. Data points refer to average deflection velocities at sensor locations of 8 in., 12 in., 18 in., 24 in., 36 in., and 60 in. (215 mm, 300 mm, 450 mm, 600 mm, 900 mm, and 1500 mm) from tire loading. The largest deflection velocity relates to the sensor at 8 in. and for sensors placed farther away, the deflection velocities gradually decrease. The numerical models on average estimated the results from the field experiments within an uncertainty of about 10% for all test sections. Ultimately, the numerical and experimental responses agreed with an uncertainty

of about  $\pm 10\%$  for all pavement sections and sensor locations, indicating that models were able to capture field responses adequately. The numerical models developed were capable of realistically predicting the pavement responses imposed by FWD and TSD loading mechanisms, and hence, could make provisions for the development of a comprehensive database required to establish ANN models.

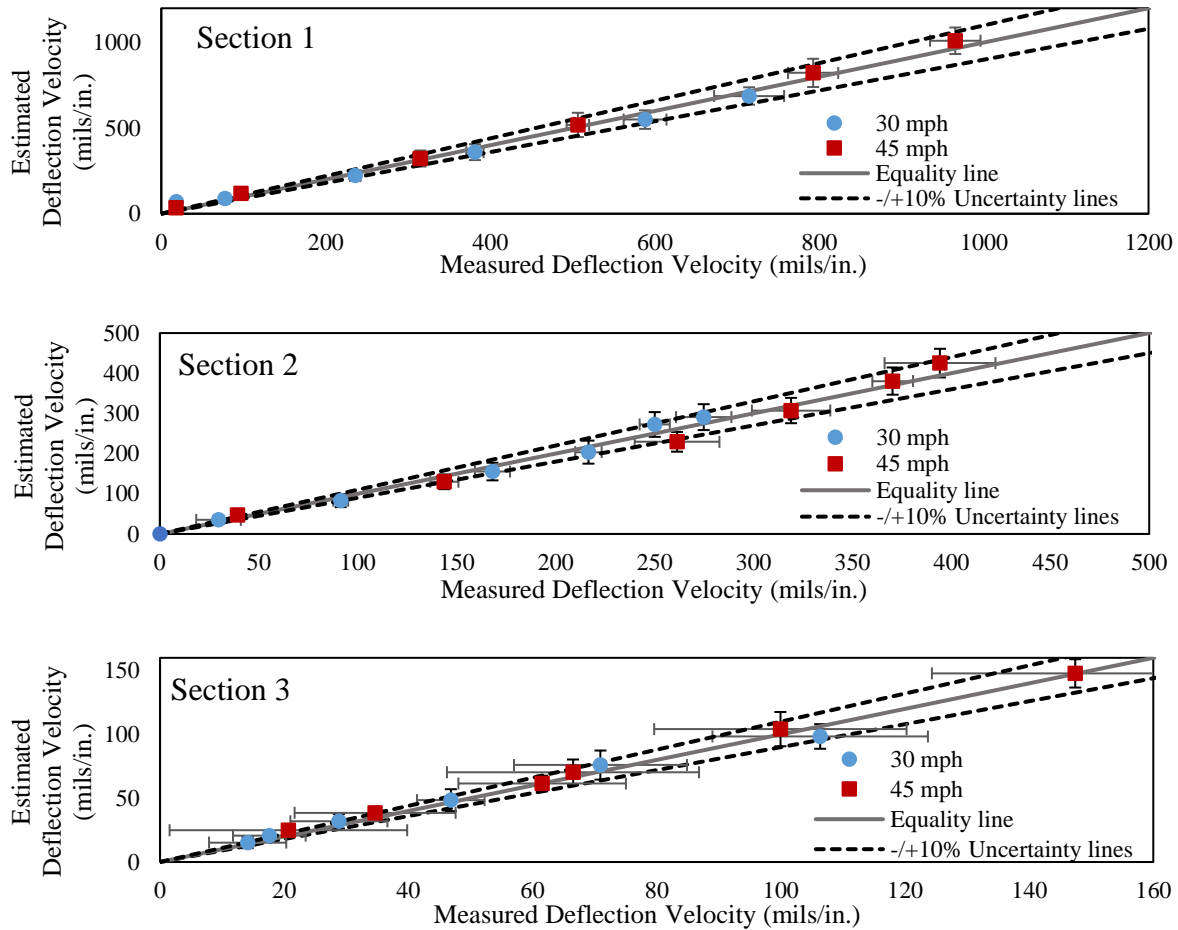


Figure 6.9: Estimated vs. measured TSD deflection velocity at three MnROAD test sections.

### VERIFICATION OF FIELD TSD DATA

To verify TSD measurements, the collected data by TSD sensors were compared with the ANN-estimated deflection velocities. The cross plots of the ANN-estimated against field TSD parameters at 30 mph (48 km/hr) and 45 mph (72 km/hr) for three pavement sections are shown in

Figure . The error bars represent the standard deviations of the results. The measured TSD deflection velocities are within  $\pm 20\%$  of the ANN-estimated TSD deflection parameters in most sensors. At the two closest sensors to the tire load (i.e., at 8 in., 200 mm and 12 in., 300 mm) from the load center, the differences between the average ANN-estimated and experimental TSD deflection velocity magnitudes are more than 20%, but the standard deviation bars have reached the range within the  $\pm 20\%$  uncertainty bounds.

As stated in the validation of the numerical models' section, the numerical models were adequately validated based on the results of the comparison of the ANN estimated pavement responses under TSD with those obtained in the field. Therefore, the comprehensive database developed by numerical simulations using 3D-Move was credible to feed the neural network models in order to train and test them. In addition, the ANN models proposed to relate the FWD responses and thicknesses of the asphalt and base layers to TSD deflection velocities were tested. The ANN models could estimate the TSD responses with  $R^2$  of close to unity and SEE which is significantly less than the uncertainties of the TSD measurements. Hence, the ANN models are valid to be used as the tool for verification of the TSD device measurements. On the other, based on the instrumentation data collected under the TSD pass, the sensors located at up to around 12 in. from tire load experienced more deviations from the geophones data. This fact is similar to what the ANN results show in Figure 6.10. The TSD overestimated the deflection velocities at sensors located at 8 in. and 12 in. from the load. Moreover, the change in speed from 30 mph (48 km/hr) to 45 mph (72 km/hr) has not significantly affected the deviations of the data points from the  $\pm 20\%$  uncertainty bounds. The plausible reason could be either the calibration issues of the sensors or the interaction between the tires and the sensors. This matter required further investigation.

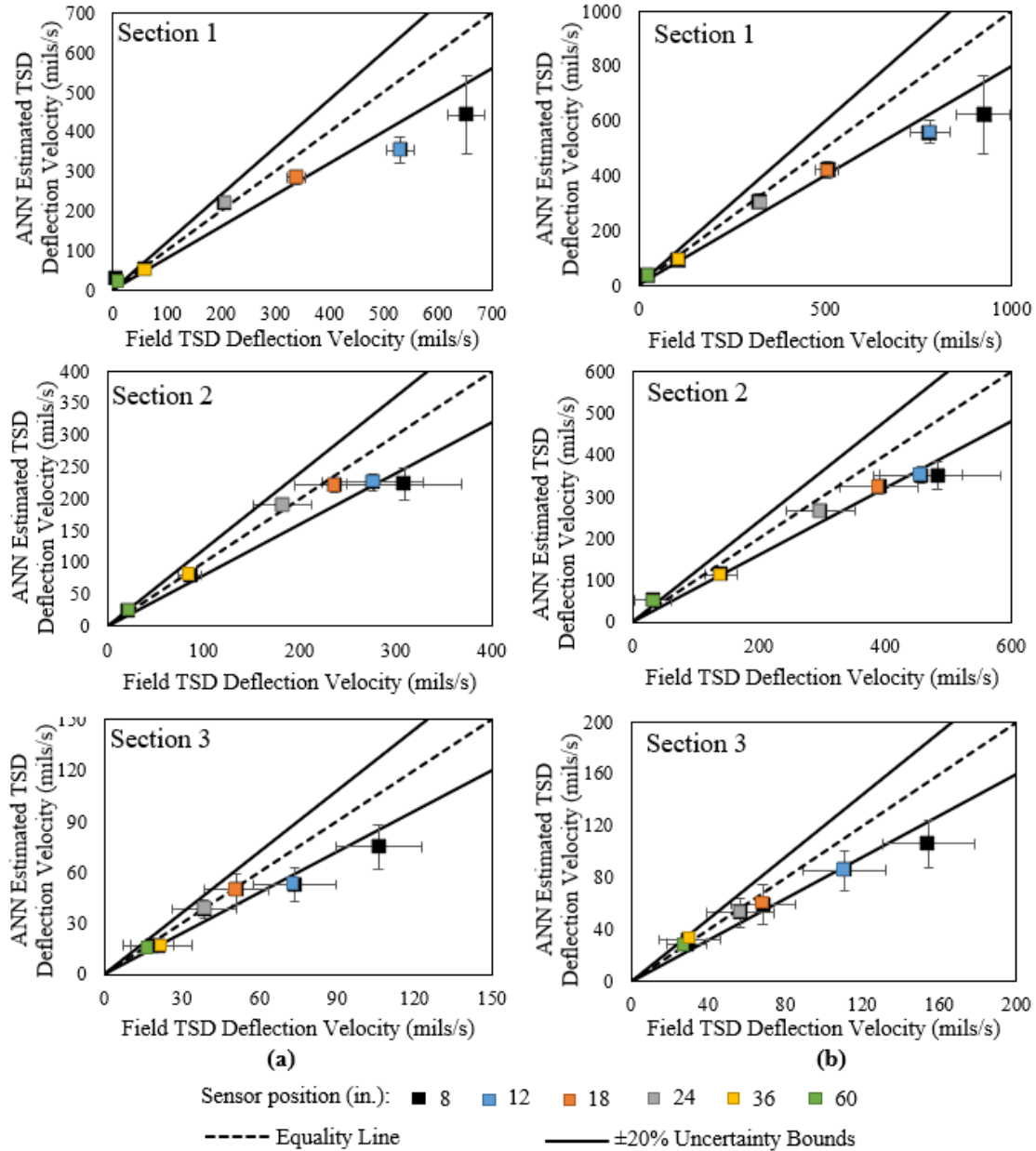


Figure 6.10: ANN estimated vs. measured TSD deflection velocity at three MnROAD test sections at speed of a) 30 mph, and b) 45 mph.

### Conclusion

Even though the best approach to verifying the measurements of the TSD is direct field instrumentation, this study presents a practical procedure for the verification of the TSD measurements using FWD data. Extensive field tests, coupled with advanced numerical simulation

and machine learning techniques, were deployed in this study to devise a sound approach to ensure the accuracy and precision of the TSD measurements in a rigorous, yet timely manner. Field experiments were carried out at three representative pavement sections. A comprehensive database of pavement responses under FWD load and different speeds of TSD was also established using a series of numerical simulation models in 3D-Move software. The Monte Carlo simulation technique was used to randomly generate pavement structures with varying thicknesses and layer moduli to cover a wide variety of structural properties. Comparison of numerical simulation results with field data cross-validated the developed numerical models for realistic calculation of the pavement responses induced under FWD and TSD loading mechanisms, as the numerical and experimental responses agreed with an uncertainty of about  $\pm 10\%$  for all pavement sections.

Furthermore, machine-learning techniques were used to relate the measurements of the FWD and TSD devices, based on the validated numerical simulation results. A series of ANN models for different pavement types and properties and vehicle speeds were developed in this study to establish practical FWD-TSD relationships while overcoming the complications posed by the distinct nature of the measurements. The ANN architecture was developed in such a manner to relate the FWD responses and thicknesses of the asphalt and base layers (as the input parameters) to TSD deflection velocity (as the output parameter). Evaluation of the ANN models using the testing subset of the assembled database revealed that the ANN models developed in this study could estimate the TSD responses with  $R^2$  of close to unity and standard error of estimates that were several times less than the uncertainty in the measured deflection velocities. Hence, they are appropriate for the verification of the TSD measurements. The ANN-estimated deflection velocities were ultimately compared with the experimental data collected by TSD sensors to verify the data measured in the field. The field-measured TSD deflection velocities were found to be

within  $\pm 20\%$  of the ANN-estimated TSD deflection parameters at almost all sensors. The inclusion of data from various test speeds in the analysis showed that the change in speed from 30 mph (48 km/hr) to 45 mph (72 km/hr) has not significantly affected the response of the TSD.

### References

- Abohamer, H., Elseifi, M. A., Zihan, Z. U., Wu, Z., Kebede, N., & Zhang, Z. (2021). Development of an artificial neural network-based procedure for the verification of traffic speed deflectometer measurements. *Transportation research record*, 2675(9), 1076-1088.
- Arora, J., Tandon, V., and Nazarian, S. (2006). Continuous Deflection Testing of Highways at Traffic Speeds, Report No. FHWA/TX-06/0-4380, Texas Department of Transportation, Austin, TX.
- Bryce, J., Katicha, S., Flintsch, G. W., & Ferne, B. (2012). Analyzing repeatability of continuous deflectometer measurements, Transportation Research Board Meeting (paper No. 12-1732).
- Chai, G., Manoharan, S., Golding, A., Kelly, G., & Chowdhury, S. (2016). Evaluation of the Traffic Speed Deflectometer data using simplified deflection model. *Transportation Research Procedia*, 14, 3031-3039.
- Elbagalati, O., Mousa, M., Elseifi, M. A., Gaspard, K., & Zhang, Z. (2018). Development of a methodology to backcalculate pavement layer moduli using the traffic speed deflectometer. *Canadian Journal of Civil Engineering*, 45(5), 377-385.
- Elseifi, M., Abdel-Khalek, A. M., & Dasari, K. (2012). Implementation of Rolling Wheel Deflectometer (RWD) in PMS and Pavement Preservation (No. FHWA/11.492). Louisiana Transportation Research Center.

- Elseifi, M. A., & Elbagalati, O. (2017). Assessment of continuous deflection measurement devices in Louisiana-rolling wheel deflectometer: final report 581 (No. FHWA/LA. 17/581). Louisiana Transportation Research Center.
- Elseifi, M. A., Abdel-Khalek, A., Gaspard, K., Zhang, Z. D., & Ismail, S. (2011). Evaluation of the rolling wheel deflectometer as a structural pavement assessment tool in Louisiana. In Transportation and Development Institute Congress 2011: Integrated Transportation and Development for a Better Tomorrow (pp. 628-637).
- Ferne, B. W., Langdale, P., Wright, M. A., Fairclough, R., & Sinhal, R. (2013). Developing and implementing traffic-speed network level structural condition pavement surveys. In *Proceedings of the international conferences on the bearing capacity of roads, railways and airfields* (pp. 181-190).
- Flintsch, G., & McGhee, K. (2009). Managing the quality of pavement data collection. *Transportation Research Board of the National Academies, Washington, DC*.
- Flintsch, G., Katicha, S., Bryce, J., Ferne, B., Nell, S., & Diefenderfer, B. (2013). Assessment of continuous pavement deflection measuring technologies (No. SHRP 2 Report S2-R06F-RW-1).
- Flora, W. F. (2009). *Development of a structural index for pavement management: An exploratory analysis*. Purdue University.
- Hasanuzzaman, H. T., & Ives, M. P. (2016, November). NSW Roads and Maritime's experience with traffic speed deflectometer technology. In ARRB Conference, 27th, 2016, Melbourne, Victoria, Australia.

- Hildebrand, G; Rasmussen, S. (2002): Development of a High Speed Deflectograph. (Report 177) Danish Road Institute.
- Katicha, S. W., Flintsch, G. W., & Ferne, B. (2013). Optimal averaging and localized weak spot identification of traffic speed deflectometer measurements. *Transportation research record*, 2367(1), 43-52.
- Katicha, S. W., Flintsch, G. W., Ferne, B., & Bryce, J. (2014). Limits of agreement method for comparing TSD and FWD measurements. *International Journal of Pavement Engineering*, 15(6), 532-541.
- Katicha, S., Flintsch, G., Shrestha, S., and Thyagarajan, S. (2017). Demonstration of Network Level Structural Evaluation with Traffic Speed Deflectometer: Final Report. FHWA.
- Katicha, S. W., Shrestha, S., Flintsch, G. W., & Diefenderfer, B. K. (2020). *Network Level Pavement Structural Testing With the Traffic Speed Deflectometer* (No. VTRC 21-R4).
- Madsen, K., Nielsen, H. B., & Tingleff, O. (2004). Methods for non-linear least squares problems. Technical Report. Informatics and Mathematical Modeling, Technical University of Denmark.
- Rada, G.R. and Nazarian, S. (2011). The State-of-the-Technology of Moving Pavement Deflection Testing, Report No. FHWA-HIF-11-013, Federal Highway Administration (FHWA), Washington, DC.
- Rada, G. R., Nazarian, S., Visintine, B. A., Siddharthan, R., & Thyagarajan, S. (2016). Pavement structural evaluation at the network level: final report. Washington, DC: US Federal Highway Administration Report FHWA-HRT-15-074.

- Saremi, S. (2018). Practical models for Interpreting Traffic Speed Deflectometer Data. M.S. Thesis. The University of Texas at El Paso, El Paso, TX.
- Steele, D. A., Beckemeyer, C. A., & Van, T. P. (2015, June). Optimizing Highway Funds by Integrating RWD Data into Pavement Management Decision Making. In 9th International Conference on Managing Pavement Assets.
- Steele, D. A., Lee, H., & Beckemeyer, C. A. (2020). Development of the Rolling Wheel Deflectometer (RWD) (No. FHWA-DTFH-61-14-H00019). United States. Federal Highway Administration.
- Stokoe II, K. H., Lee, J. S., Nam, B. H., Lewis, M., Hayes, R., Scullion, T., & Liu, W. (2012). *Developing a Testing Device for Total Pavements Acceptance: Third-Year Report* (No. FHWA/TX-11/0-6005-4).
- Zaghloul, S., He, Z., Vitillo, N., & Brian Kerr, J. (1998). Project scoping using falling weight deflectometer testing: New Jersey experience. *Transportation Research Record*, 1643(1), 34-43.
- Zihan, Z. U., Elseifi, M. A., Icenogle, P., Gaspard, K., & Zhang, Z. (2020). Mechanistic-based approach to utilize traffic speed deflectometer measurements in backcalculation analysis. *Transportation research record*, 2674(5), 208-222.

# CHAPTER 7. CONCLUSIONS AND RECOMMENDATIONS FOR FUTURE WORK

## Summary

The goal of this study was to develop a practical verification procedure for the TSD measurements. To that end, first, the numerical simulation of the TSD moving load on different pavement sections was validated before it was used in the TSD verification approach. The effects of different structural and operational parameters on the variations of the TSD measurements and their accuracy and precision were then investigated. Finally, a procedure for verifying TSD data with FWD deflection measurements using machine learning techniques was proposed. The research presented in this dissertation has led to multiple findings. Some of the main contributions of this research are:

- Presenting different characteristics of the TSD simulation using the finite layer approach.
- Providing results of extensive field TSD tests used as the reference for validation of the simulations and developed ANN models.
- Evaluating the accuracy of the measurements by comparing the TSD deflection velocities with the embedded sensors data at each pavement section.
- Assessing precision of the TSD data collected at structurally different pavement sections by analysis of the variability-related statistical parameters of each TSD sensor's data due to repeated runs at different operational speeds.
- Investigating the impact of TSD operating speed, pavement structural condition, TSD measurements magnitude, and intervals of data averaging on the variability of the TSD data.

- Presenting a robust and practical procedure for the verification of the TSD measurements employing the analysis of field tests results coupled with advanced numerical simulation and machine learning techniques.
- Evaluating the ANN models using the testing subset of the assembled database and verifying the verification procedure utilizing experimental data collected by TSD sensors.

### **Conclusions**

The following conclusions present the major findings of this study for helping achieve the goal of this research:

- **NUMERICAL SIMULATION OF TRAFFIC SPEED DEFLECTOMETER TESTING**
  - Significant effort was required to modify the 3D-Move to be applicable to this study.
  - The footprint of the TSD tire was closer to the rectangular shape with a nonuniform distribution of pressure.
  - Vertical deflections and deflection velocities induced under rectangular contact area were smaller than those of circular contact area.
  - The nonuniform rectangular distribution of the tire pressure could capture the TSD responses at different speeds with a very promising agreement.
  - Substituting the time history of the numerical simulation responses with instantaneous responses did not significantly affect the values and trend of the tensile strain at the bottom of the asphalt layer, the compressive strain at top of the subgrade layer, and surface vertical deflection.

- Substituting the time history of the numerical simulation responses with instantaneous responses had a considerable effect on the surface vertical stress variations with distance from the load.
- The 3D-Move models developed using nonuniform pressure distribution on rectangular tire contact area and instantaneous response method was validated with the field TSD data.
- **IMPACT OF PAVEMENT STIFFNESS ON PERFORMANCE OF TRAFFIC SPEED DEFLECTION MEASUREMENTS**
  - The average deflection velocities agreed better with the installed geophones data for less stiff sections.
  - The differences between the TSD measurements and the geophone-recorded data increased as the stiffness of the pavement sections increased.
  - Increase in TSD operational speed resulted in a slightly larger overall deviation of the TSD measurements from the geophone velocities.
  - The TSD data became less precise as the pavement structure became stiffer.
  - The magnitude of the TSD collected data and corresponding COVs from repeated runs exhibited an inverse relationship.
- **QUALITATIVE ASSESSMENT OF TRAFFIC SPEED DEFLECTOMETER DATA COLLECTION**
  - COVs were higher for the smaller deflection velocities corresponding to the measurements made with sensors located farther away from the tire loading or measured at test sections with stiffer pavements.
  - Averaging data collected at every 2 in. (50 mm) for 3.3 ft (1 m) intervals significantly decreased COVs of the TSD deflection velocities.

- Increasing vehicle speed from 30 mph (48 km/hr) to 45 mph (72 km/hr) and 60 mph (96 km/hr) did not have a notable impact on the average deflection slopes while seems to increase the COVs associated with average deflection velocities.
- **PRACTICAL PROCESS FOR VERIFICATION OF TRAFFIC SPEED DEFLECTOMETER MEASUREMENTS**
  - A robust process for verification of the TSD measurements was developed based on validated ANN models which estimate TSD deflection velocities from layer thicknesses and corresponding FWD deflection bowls.
  - The experimental data collected by TSD sensors was verified using ANN-estimated deflection velocities.

### **Recommendations for Future Studies**

Although the current study showed promising results, full implementation of the proposed frameworks requires further research endeavor. The following recommendations for future work can enhance the process:

- Collecting more field data associated with different weather or structural conditions is strongly recommended. This will be a solid basis for further validation and calibration of the theoretical frameworks proposed in this dissertation.
- Artificial neural network models were developed in this study to serve as the basis of the verification procedure. Other analysis approaches such as different machine learning techniques are also recommended to be investigated.

- The numerical simulation database provided in this study shows desirable coverage of different pavement properties. It can even be improved by considering a wider range of material properties and pavement layer layouts.
- FWD-TSD relationships are recommended to be developed based on the numerical analysis of the pavement sections considering the viscoelastic behavior of the asphalt layer material.

## VITA

Mahsa Beizaei completed graduate work at the Ferdowsi University of Mashhad in soil mechanics and foundation engineering in 2016. Besides completing her master's studies, she began working as a civil engineer with Ravak Construction Co. to gain practical skills. She also has been lecturer of several academic courses related to geotechnical engineering, pavement engineering, and transportation engineering at graduate level. In January 2019, she joined the doctoral program in Civil Engineering at the University of Texas at El Paso. Obtaining a GPA of 4/4, she has been honored to be awarded the Anita Mochen Loya Scholarship for two consecutive semesters in 2019. During her PhD studies, she has been actively involved in research project funded by NCHRP emphasizing on transportation infrastructures and non-destructive testing of the roadways. Mahsa Beizaei is a Standing Member of the TRB-AKP40 Technical Committee on Pavement Structural Testing and Evaluation, and an active research member of the Center for Transportation Infrastructure Systems and the Transportation Leadership Council. She has been privileged to serve as a teacher assistant and co-instructor to deliver undergraduate and graduate courses. She has contributed to several scholarly publications; including project technical reports, conference proceedings, and journal articles published by ASCE, Springer, and NCHRP. She is an active peer reviewer for several prestigious journals.

Email: [mbeizaei@miners.utep.edu](mailto:mbeizaei@miners.utep.edu)